Weissel, J., Peirce, J., Taylor, E., Alt, J., et al., 1991
Proceedings of the Ocean Drilling Program, Scientific Results, Vol. 121

15. LATE NEOGENE PALEOCEANOGRAPHY AND PALEOCLIMATOLOGY OF THE NORTHEAST INDIAN OCEAN (SITE 758)[1]

John W. Farrell[2] and Thomas R. Janecek[3]

ABSTRACT

The evolution of oceanic and climatic conditions the northeast Indian Ocean during the last 7 m.y. is revealed in the sediments from Site 758. We present detailed and continuous records of $\delta^{18}O$ and $\delta^{13}C$ from planktonic foraminifers, weight percent calcium carbonate, weight percent coarse fraction, magnetic susceptibility, and geomagnetic reversals. Sample spacing of the records ranges from 3 to 10 cm and is equivalent to an average time interval of 2000 to 6000 yr. Despite the fact that core recovery ranged between 100% and 105%, recovery gaps as large as 2.7 m occurred at nearly every break between advanced hydraulic piston cores. Approximately 12% of the late Neogene sequence was not recovered in each of the two holes drilled at Site 758. To circumvent the discontinuity introduced by the gaps, a composite depth section was constructed from multiple cores taken from offset holes at Site 758. The resulting composite depth section extends continuously from 0 to 116 mbsf, from the Holocene to the upper Miocene.

A detailed chronostratigraphy is based on geomagnetic reversals which extend from the Brunhes Chron to Chron 6, and on $\delta^{18}O$ stages 1 through 105, which span from 0 to 2.5 Ma. The $\delta^{18}O$ record is dominated by a ~40-k.y. cycle in the late Pliocene and early Pleistocene, and is followed by a change to a ~100-k.y. cycle in the late Pleistocene. The mid-Pleistocene transition between these two modes of variability occurs between $\delta^{18}O$ stages 25 and 22 (between 860 and 800 Ka). Thirteen major volcanic ash horizons from the Indonesian arc are observed throughout the sedimentary section and are dated by their relative position within the geomagnetic reversals and the $\delta^{18}O$ chronostratigraphy.

Since 5 Ma, there has been a long-term decline in weight percent $CaCO_3$ and $CaCO_3$ mass accumulation rates, and an associated rise in non-$CaCO_3$ mass accumulation rates. We attribute these changes to a decrease in $CaCO_3$ productivity and an increase in terrigenous sedimentation through enhanced riverine input. Such input may be linked to rapid tectonic uplift of the Himalayas and the Tibetan Plateau via mechanisms such as the intensification of the monsoonal rains, increased fluvial erosion, and regional glaciation. The long-term increase in percent coarse fraction since 5 Ma suggests a gradual increase in $CaCO_3$ preservation. Higher frequency fluctuations in $CaCO_3$ preservation are superimposed on the long-term trend and are related to climate fluctuations. The abrupt drop (~50%) in $CaCO_3$ accumulation at 3.4 Ma signals a dramatic decrease in $CaCO_3$ production that occurred over much of the Indian Ocean.

INTRODUCTION

One of the principal objectives of Ocean Drilling Program (ODP) Leg 121 was to recover a complete late Neogene sediment sequence to address fundamental questions regarding the paleoenvironment of the northeastern Indian Ocean. A continuous record of predominantly undisturbed late Neogene sediments, with moderate to high accumulation rates, is provided by the multiple advanced hydraulic piston cores (APC) from three offset holes at Site 758, atop the northern end of the Ninetyeast Ridge (Fig. 1). The geomagnetic reversal record from this site is excellent. All major magnetic events from the Brunhes Chron through Chron 6 are present, and reversal boundaries are sharp and well-defined (Shipboard Scientific Party, 1989).

The sedimentary records from Site 758 provide a rare opportunity for the simultaneous evaluation of (1) the oceanic and climatic evolution of the northeast Indian Ocean; (2) the periodic nature of climate change attributed to the Milankovitch mechanism; (3) the effects of tectonic uplift of the Himalayas and the Tibetan Plateau; and (4) the history of volcanic activity in the nearby Indonesian arc. To address these objectives, a database of long, continuous, and detailed paleoenvironmental indices must be constructed and synthesized. Our focus in this study is to generate and provide preliminary analysis of weight percent (wt%) $CaCO_3$ and wt% coarse fraction records spanning the last 5.2 m.y., and $\delta^{13}C$ and $\delta^{18}O$ records from planktonic foraminifers extending from 0 to 2.5 Ma. $CaCO_3$ is examined because it is the dominant component and because it provides information about biological productivity in the surface ocean and $CaCO_3$ dissolution on the seafloor. Percent coarse fraction is an independent index of $CaCO_3$ preservation. The stable isotope record provides a chronostratigraphy and information about fluctuations in ice volume, surface water temperature, and salinity. Because preliminary investigation suggests that the sedimentary concentrations of biogenic opal and organic carbon (D. Murray, pers. comm., 1990) are low at Site 758, the terrigenous percentage of the sediment can be approximated as 100 − wt% $CaCO_3$. This estimate is slightly higher than the true percentage of terrigenous sediments. The volcanic ash at Site 758 provides a tephrochronology of Indonesian arc volcanism. A complete description of the ash layers referred to in this study by alphabetic nomenclature (e.g. "ash A"), is presented by Dehn et al. (this volume). The records generated in this study are examined in the context of geomagnetic reversal and magnetic susceptibility (MS) records of the last 7.3 m.y. By constructing a composite depth section from Holes 758A and 758B, which splices across recovery gaps, it is possible to produce an undisturbed, continuous sedimentary section that extends from 0 to 116 meters below seafloor (mbsf) which is equivalent in time to the past 7.3 m.y.

The sediment at Site 758 is primarily biogenic pelagic $CaCO_3$, but terrigenous silts and clays and volcanic tephra are also important components. The modern eolian contribution to the eastern equatorial Indian Ocean is negligible, as shown by the low concentration of soil (mineral) aerosol particles in the marine atmos-

[1]Weissel, J., Peirce, J., Taylor, E., Alt, J., et al., 1991. *Proc. ODP, Sci. Results*, 121: College Station, TX (Ocean Drilling Program).

[2]Department of Geological Sciences, Brown University, Providence, RI 02912-1846, U.S.A.

[3]Ocean Drilling Program, Texas A&M University, 1000 Discovery Drive, College Station TX 77845, U.S.A.

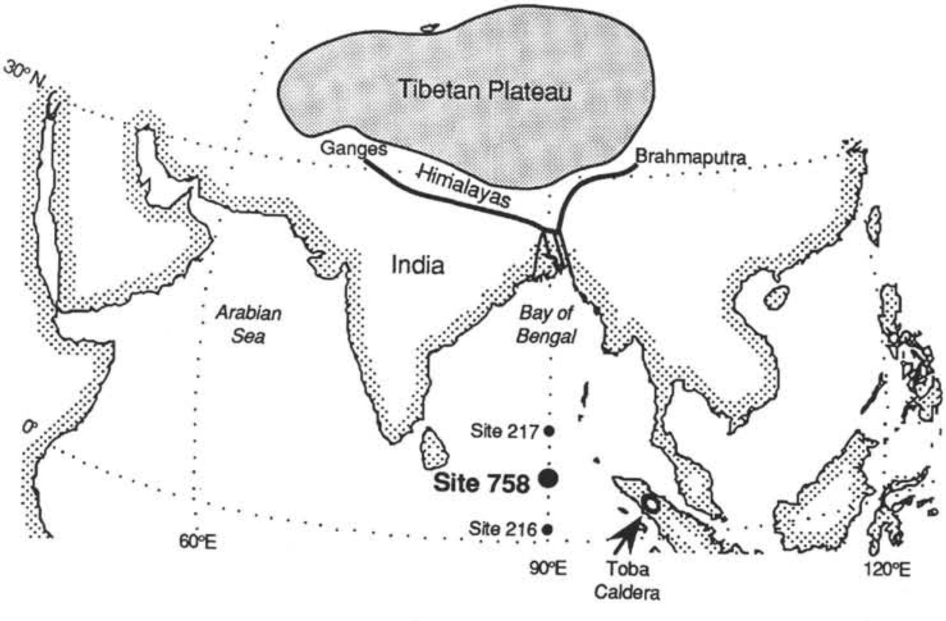

Figure 1. Location of Site 758. Also shown are DSDP Sites 216 and 217.

phere (Prospero, 1981). Rivers contribute most of the terrigenous sediment, which is predominantly allochthonous Si-Fe smectites and illites (Bouquillon et al., 1989). The Ganges and the Brahmaputra rivers drain the Himalayas and the Indian subcontinent and contribute 1.7×10^9 tons of sediment to the ocean per year (Milliman and Meade, 1983), more than any other river system in the world. These sediments have built the Bengal Fan, one of the world's largest fans. Coarse-grained materials are confined to the fan but the finer silts and clays are transported to Site 758 which lies about 1000 m above the Bengal Fan. Silt and clay are most likely transported by turbidity currents and within nepheloid layers (Kolla et al., 1976; Stow et al., 1990).

DATA AND METHODS

Site 758 (5°23′N, 90°21′E; 2925 m water depth) is on the southeast side of a large en echelon block of the Ninetyeast Ridge approximately halfway between Deep Sea Drilling Project (DSDP) Sites 216 and 217 (Fig. 1). For Site 758, we report here late Neogene records of wt% $CaCO_3$, wt% coarse fraction (>150 µm), and planktonic foraminifer $\delta^{13}C$ and $\delta^{18}O$. Specifically, a total of 922 10-cm^3 samples were analyzed at 10-cm intervals in Cores 121-758A-1H through 121-758A-8H (00.01 to 73.55 mbsf) and at 10-cm intervals in various sections within Hole 758B. These records are compared to shipboard wt% $CaCO_3$ data and to records of the whole-core volume MS and geomagnetic reversals. All records are displayed as a composite depth section (see below) based primarily on samples from Hole 758A and secondarily on samples from Hole 758B.

Sample Preparation

All samples were subsampled, retaining approximately 1 cm^3 for wt% $CaCO_3$ analysis. The remainder of the sample was freeze-dried, weighed, diggregated in tap water, wet-sieved through a 150-µm sieve, and dried at 50°C. Percent coarse fraction is the weight percentage of the sample >150 µm. The fine fraction (<150 µm) was allowed to settle for 24 hr, the water siphoned off to within about 1 cm of the sediment-water interface, and the fine residue dried, weighed, and saved for future studies. The coarse fraction (>150 µm) was divided into two aliquots, one for faunal analysis and the other for stable isotope analysis. Seven samples (identified in Appendix F) consisting primarily of volcanic ash were subsampled and analyzed for wt% $CaCO_3$ only, the remainder was not processed further.

Wt% $CaCO_3$ Analysis

The wt% $CaCO_3$ of the bulk dry sediment was determined on the Brown University $CaCO_3$ system. This is a modified version of the Jones and Kaiteris (1983) gasometric technique with a differential pressure gauge used in place of a vacuum gauge and with carbonate reactions measured at atmospheric pressure. Replicate analyses of both samples and standards give an analytical precision better than 1% by weight.

To determine whether the results of shipboard wt% $CaCO_3$ analyses were similar to those obtained in this study, such that the two databases could be combined without offset in future studies, we analyzed aliquots of 38 shipboard samples that had been measured for both wt% $CaCO_3$ and physical properties. Shipboard wt% $CaCO_3$ analyses were made on a Coulometrics 5010 Coulometer coupled with the 5030 Carbonate Carbon apparatus described elsewhere (Peirce, Weissel, et al. 1989). Our analyses of the shipboard samples show that the results of the two laboratories are nearly identical (Appendix A, Fig. 2). On average, the shipboard wt% $CaCO_3$ data are only 1% greater than our data. Because this difference is well within the combined analytical precision of the two laboratories, no adjustments to either database are required before merging the two.

Stable Isotope Analysis

The $\delta^{13}C$ and $\delta^{18}O$ of planktonic foraminifers were measured in the Brown University Benedum Stable Isotope Laboratory on 6 to 15 individuals of Globigerinoides sacculifera, predominantly without sacs, and picked from the 300- to 355-mm size range. The restricted size range and preference of specimens without sacs minimizes the noise from ontogenetic variation on the isotopic composition (Berger et al., 1978; Curry and Matthews, 1981). Since we observed no large difference in the isotopic composition of G. sacculifera with sacs vs. those without, all were included when calculating the mean isotopic value for a given sample depth.

Picked foraminifer samples were cleaned ultrasonically for about 10 s to remove adhering fine-grained material. Dry samples were transferred into stainless steel boats filled with ethyl alcohol.

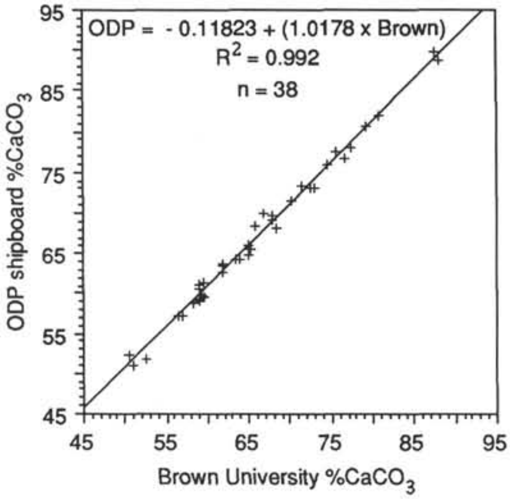

Figure 2. Comparison of wt% $CaCO_3$ data from the Brown University and the ODP shipboard laboratories. Although ODP values average 1% greater than those from Brown, the difference is insignificant given the combined precision of the two laboratories.

The alcohol facilitates the transfer to the boats and prevents sample loss. The samples were crushed with a glass pestle to prevent sample loss and to enhance the reaction with the acid. The boats were placed in a drying oven at 75°C for at least one hr. Dry samples were roasted in vacuo at 300°C for 1 hr to remove possible organic contaminants. The samples were then either analyzed or returned to the drying oven. In the extraction line, each $CaCO_3$ sample was reacted with phosphoric acid at 90°C for 14 min. During this reaction, water and carbon dioxide were extracted by continuous trapping with liquid nitrogen. The carbon dioxide was analyzed on a fully automated online VG Sira 24 Micromass mass spectrometer. Isotopic composition is expressed as a deviation per mil from the Pee Dee belemnite (PDB) standard (Craig, 1957).

The Benedum Stable Isotope Laboratory's mass spectrometry reference gas (BIG-5) is calibrated to PDB by analysis of National Bureau of Standards (NBS) 19 and 20. The Benedum Laboratory values for NBS-19 are –2.09‰ ($\delta^{18}O$) and 1.88‰ ($\delta^{13}C$), which compares to values reported by the NBS (I. L. Barnes, pers. comm., 1985) of –2.19‰ ($\delta^{18}O$) and 1.92‰ ($\delta^{13}C$). The Benedum Laboratory values for NBS-20 are –4.20‰ ($\delta^{18}O$) and –1.04‰ ($\delta^{13}C$), which compares to NBS values of –4.14‰ ($\delta^{18}O$) and – 1.06‰ ($\delta^{13}C$) (I. L. Barnes, pers. comm., 1985).

Analytical precision (1 σ), indicated by the first acceptable analysis of the in-house working carbonate standard (BP-4) before each analytical session (36 days), is ±0.07‰ for oxygen and ±0.05‰ for carbon. Analytical precision (1 σ) based on 359 duplicate analyses, almost always run on separate days, is ±0.09‰ for oxygen and ±0.08‰ for carbon.

Dry-Bulk Density Estimates

Dry-bulk density values, which are required to calculate mass accumulation rates (MAR), were estimated from shipboard data. The data consists of wet-bulk density estimates from gamma-ray attenuation (GRAPE) data measured at an average interval of 1.8 cm, and discrete wet-bulk density (WBD) and dry-bulk density (DBD) values (table 18, pp. 425–426 in Pierce, Weissel, et al., 1989) measured at an average interval of 80 cm in the APC cores from Holes 758A and 758B. The GRAPE WBD estimates from Hole 758A were smoothed with a 3-point Gaussian filter and were sampled at depths corresponding to the discrete WBD and DBD measurements using a linear interpolation between adjacent measurements. A linear regression of the resulting GRAPE WBD and the discrete WBD,

$$\text{discrete WBD} = 0.077 + (0.924 \cdot \text{GRAPE WBD}),$$
$$r^2 = 0.87,\ n = 130,$$

was used to transform GRAPE values into discrete WBD estimates. The transformed WBD estimates were then converted to DBD estimates by the linear regression of the discrete WBD against the discrete DBD:

$$\text{discrete DBD} = -1.570 + (1.541 \cdot \text{discrete WBD}),$$
$$r^2 = 0.98,\ n = 130.$$

With these relationships established, the smoothed GRAPE values were sampled at depths corresponding to samples used in our study by linear interpolation. Where GRAPE data were not available for intervals in Hole 758A (as for section 7 and core-catcher samples from every core), the GRAPE data from the equivalent section (based on the correlation of MS records) from Hole 758B were substituted. The dry-bulk density estimates (in units of grams of dry sediment per wet volume, in cm^3) are listed in Appendixes B and C.

Mass Accumulation Rates

MAR is the mass of a sedimentary material preserved per unit area and unit of time, commonly expressed in units of grams, per square centimeter, per 1000 yr ($g/cm^2/k.y.$). MAR can be thought of as either the flux of material onto a substrate, or the flux across the water/sediment interface. We calculated the MAR of $CaCO_3$ from the linear sedimentation rate (LSR, in m/m.y.), the DBD (in g/cm^3), and the wt% $CaCO_3$. $CaCO_3$ MAR was calculated as:

$$CaCO_3\ \text{MAR}\ (g/cm^2/k.y.) = [\text{LSR}\ (m/m.y.) \cdot \text{DBD}\ (g/cm^3) \cdot \text{wt\%}\ CaCO_3] / 1000.$$

It is worth stressing that MAR estimates are only as accurate and detailed as the chronostratigraphy upon which they are based. This stems from the fact that the magnitude of the variations in $CaCO_3$ MAR at Site 758 are strongly controlled by LSR changes, and less so by changes in wt% $CaCO_3$ and DBD. In absolute values, the variations in LSR are almost always greater than those in wt% $CaCO_3$ and DBD. A detailed chronostratigraphy from an $\delta^{18}O$ record will enable us to determine LSR changes, and thus $CaCO_3$ MAR changes on the order of 10^4 yr. A chronostratigraphy based on linear interpolation between age estimates separated by a long time interval, such as between the sediment/water interface and the Brunhes/Matuyama geomagnetic reversal, cannot resolve high-frequency fluctuations in LSR. As a result, $CaCO_3$ MAR variations based on a low-resolution chronostratigraphy are controlled by variations in wt% $CaCO_3$ and DBD, which do not necessarily reveal the dynamics of oceanographic change at high frequencies.

Magnetic Susceptibility and Declination Data

Shipboard MS provides the fundamental lithostratigraphy for this study. The MS data shown in Figure 3 (back pocket) were measured at 3- to 5-cm intervals. Measurements of whole-core low-field MS are rapid, simple, and nondestructive. MS is gaining recognition as an invaluable lithostratigraphy in a variety of sedimentary regimes (see Robinson, 1990, for an excellent review of MS methodology and application). MS is primarily a measure of the concentration (per unit volume) of magnetizable material such as the ferromagnetic minerals and paramagnetic materials including clays (smectite, in particular). In the absence of complicating factors, such as suboxic diagenesis and rust flakes in the core pipes, MS variations in pelagic sediments primarily reflect the ratio of biogenic to lithogenic components (Thompson and Oldfield, 1986; Robinson, 1990; deMenocal and Bloemendal, 1990). A significant exception to this generalization is mafic volcanic ash. At Site 758, the ferromagnetic minerals, such as titanomagnetite, in some ash layers are easily identified by the extremely high ($\sim 100 \cdot 10^{-6}$ cgs) MS values. The MS values in ash-free sediments from Site 758 range between 0 and $\sim 20 \cdot 10^{-6}$ cgs. The high-resolution MS records are used in this study (1) to construct detailed lithostratigraphic correlations among the holes; (2) to identify sediments disturbed by the coring process; (3) to determine coring gaps of unrecovered sediment; (4) to identify volcanic ash layers; and (5) to construct a composite depth section for the past 7.3 m.y. Future work will help establish the degree to which the MS data can be used to interpret paleoceanographic and paleoclimatic conditions at Site 758. MS values corresponding to the sample depths in our composite record are listed in Appendix F. These values were obtained by linear interpolation of adjacent shipboard MS values.

Magnetic declination data and the interpreted geomagnetic reversal stratigraphy are shown along with the raw shipboard MS data in Figure 3 (back pocket). The magnetic reversal record is the primary chronostratigraphy for this study. The natural remanent magnetization of whole-round sections of all APC cores from Holes 758A and 758B was measured at 10-cm (and occasionally 5-cm) intervals using the shipboard cryogenic magnetometer (Pierce, Weissel, et al., 1989). The resulting declination-based magnetostratigraphies are of exceptionally high quality. The magnetic reversal boundaries are generally sharp and well-defined. All chrons and subchrons (except perhaps the two Reunion Subchrons) from the Brunhes Chron to Chron 6 were recovered in Hole 758A and/or Hole 758B.

COMPOSITE DEPTH SECTION

Because our objectives include detailed examination of a high-resolution sedimentary section and, eventually, time-series analysis, continuity of the records from Site 758 is critical. With considerable effort, we have constructed a continuous depth section for Site 758 and ensured its continuity with several independent stratigraphies.

At Site 758, three holes were drilled within 26 m of each other to recover the late Neogene sedimentary sequence. The cores from Holes 758A and 758B were drilled at staggered depths in order to overlap core breaks. Although APC core recovery was excellent, ranging from 100% to 105%, interhole correlation of the high-resolution MS and other stratigraphies shows sediment recovery gaps as large as 2.7 m at nearly every core break (Fig. 3, back pocket) (table 12, pp. 416–417, in Shipboard Scientific Party, 1989). An average of 1 m of sediment is missing between each successive APC core in Holes 758A and 758B. This suggests that 12% of the APC-cored sequence was not recovered in each hole. This percentage translates into about 13 m of unrecovered sediment in the top 110 mbsf. Similar occurrences of missing sediment at APC core breaks have been reported for several DSDP/ODP legs, including Leg 94 (Ruddiman et al., 1987; Ruddiman et al., 1989; Raymo et al., 1989), Leg 111 (Alexandrovich and Hays, 1989), Leg 115 (Robinson, 1990), and Leg 117 (deMenocal and Bloemendal, 1991; Murray and Prell, 1991). Precise identification of the sediment gaps, unaccounted for by the normal process of sub-bottom depth assignment, would have been impossible had Site 758 not been double-cored and measured for magnetic susceptibility.

Analysis of the sedimentary sequence at Site 758 was complicated by these gaps. To circumvent this problem, a composite section for Site 758 was constructed by splicing the missing sedimentary intervals at the core breaks in Hole 758A with the equivalent intervals from Hole 758B. Identification of equivalent intervals was based on interhole correlation of MS and geomagnetic reversals. These intervals were independently verified by stratigraphic correlation of wt% $CaCO_3$, wt% coarse fraction, and $\delta^{18}O$ records where possible. An example is shown in Figure 4. The splices are accurate to within 3 to 10 cm (the respective sample spacing of the MS and other stratigraphies), which is equivalent to an average time interval of 2 to 6 k.y. Sub-bottom depths were calculated for the composite section by assigning the sediment-water interface a depth of 0.00 m and progressively adding the length of each successive Hole 758A interval and Hole 758B splice down through the sedimentary sequence (Table 1). The addition of the splices results in composite depths which grow progressively deeper than the depths assigned by the nominal ODP method, which does not recognize, and therefore account for, the gaps. For example, Section 121-758A-11H-7, at 65 cm, has a composite depth of 116.19 mbsf, which is 13.74 m greater than the ODP depth of 102.45 mbsf. This implies that shipboard sub-bottom depths are too shallow (e.g., ~14 m at the bottom of Core 121-758A-11H, more than the length of an entire drill pipe). The apparent discrepancy between shipboard sub-bottom depths and those assigned here could be resolved if distinct lithostratigraphic markers in the recovered cores are correlated to the downhole logging results. Preliminary attempts to correlate the cores to the logs have proven unsuccessful. This is attributed to the fact that the top 42 m of Hole 758A were logged through the drill string such that the distinct ash layers in the cores could not be identified in the logs. Improvements in the resolution of logging tools will undoubtedly aid in future attempts to correlate cores and logs.

Why is sediment missing at the core breaks and why is it missing if core recovery exceeded 100%? In a review of sediment disturbance due to the coring process, Ruddiman et al. (1987) examined several ways in which "under-recovery" of sediment can occur. The most likely explanation for the gaps between cores at Site 758 involves sediment loss, accompanied by expansion and/or stretching of sediment. Sediment loss may occur in the drill hole due to ship heave. APC-coring is not heave-compensated. Heave of the ship, even in calm seas, can easily move the drill string up and down by a meter or two. Downheaval of the drill string between the times when cores are taken would disturb or displace an interval of the sedimentary sequence. If this occurred, the top of the interval recovered by the subsequent core would be deeper in the sedimentary sequence than anticipated. The uppermost sediments intended for recovery would have been pushed aside and not recovered. Since under-recovery occurred at almost every core break, it would appear that downheaval and sediment displacement occurred before every core was taken. However, it seems unlikely that the ship consistently heaved downward before each APC core was taken. The chances of upheaval just prior to APC-coring are just as likely as downheaval.

Upheaval of the ship just before shooting the APC would result in the retrieval of a short sedimentary section with an interval of water at the top. The uppermost sediments in such a core could be disturbed by sloshing of the water during core retrieval or they could absorb the water resulting in core expansion and a decrease in bulk density. This may explain why low GRAPE values are

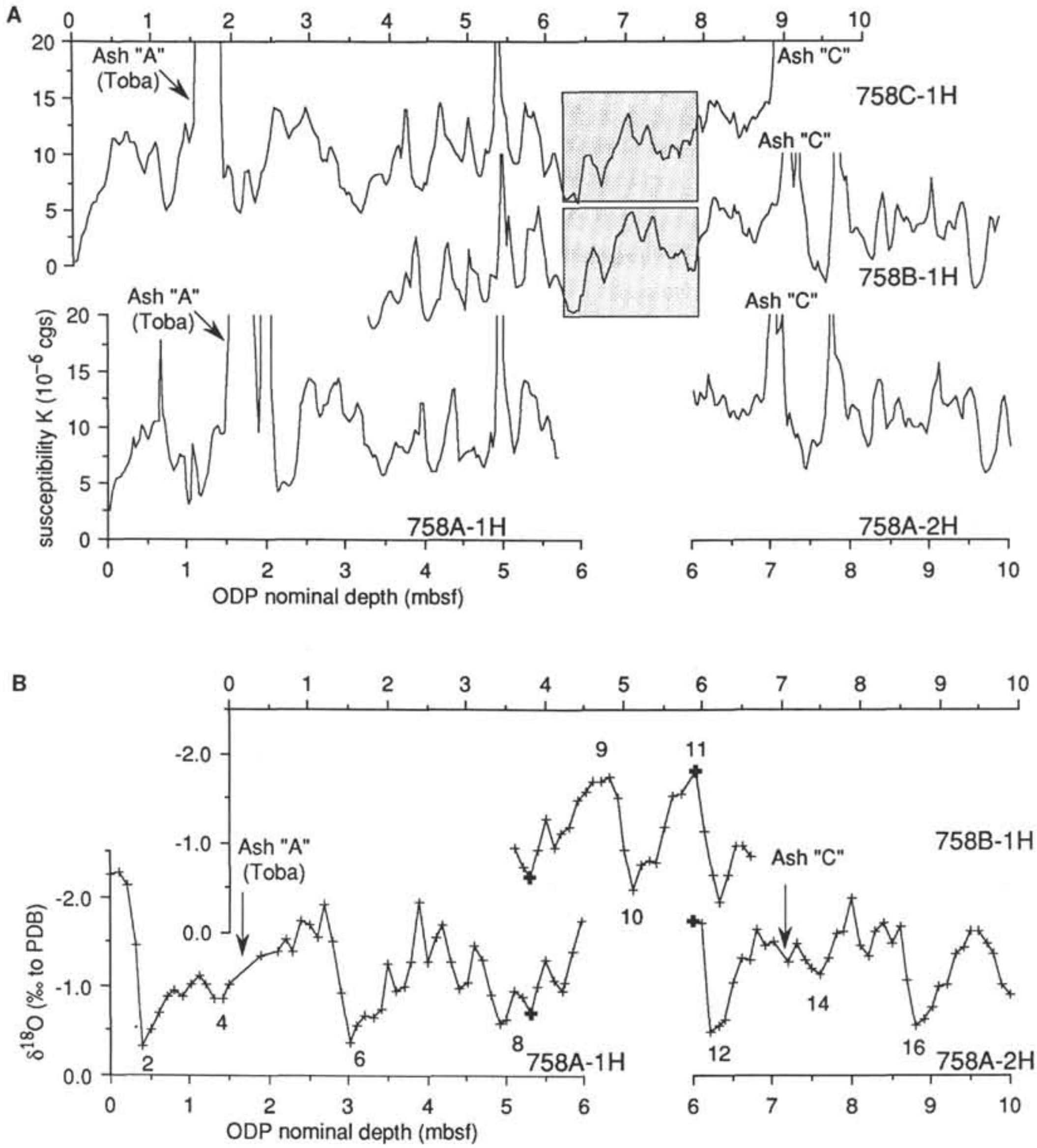

Figure 4. Example of a recovery gap and splices based on magnetic susceptibility and $\delta^{18}O$ records. **A.** High-resolution (3-cm interval) magnetic susceptibility records show a recovery gap at the break between Cores 121-758A-1H and 121-758A-2H and a core splice (shaded region) from both Cores 121-758B-1H and 121-758C-1H to fill the approximately 1.36-m gap. **B.** Core splice from Core 121-758B-1H demonstrates that half of interglacial $\delta^{18}O$ stages 9 and 11 and the entire glacial stage 10 (nearly 100 k.y.) were lost in the break between Cores 121-758A-1H and 121-758A-2H despite core recovery of between 102% to 104%. Heavy crosses identify the tie points used to splice between holes in the construction of the composite depth section.

often observed at the tops of cores. Nevertheless, under-recovery due to upheaval seems unlikely because the core tops of almost every APC core from Site 758 appear pristine, and because the GRAPE values in the tops of cores from Site 758 were not anomalously low.

Lateral drift of the ship may also result in under-recovery (Ruddiman et al., 1987). Drift toward the positioning beacon would bury the drill pipe down into the sediment prior to APC coring. The sediments intended for recovery would be displaced by the drill string and the core actually retrieved would be from a sub-bottom depth interval deeper than expected. The dynamic positioning system of the *JOIDES Resolution* is much improved over that of the *Glomar Challenger*. Nevertheless, some drift occurs and it may contribute to under-recovery. Dynamic positioning of the *Resolution* apparently keeps the ship at a surface location within 2% of the water depth. If this is true, then in 2925 m of water (the depth of Site 758) 0.6 m of sediment at Site 758 could have been displaced by one drift of the ship toward the beacon. Drift toward the beacon during the shooting of all 22 APC cores at Site 758 is highly unlikely. Drift away from the beacon would result in recovery of less than 100%.

Expansion and stretching of the sedimentary section can occur in several ways. A minor amount of sediment expansion may result from the decrease in hydrostatic pressure during retrieval of the core from the seafloor to the sea surface. The relatively high silt and clay content of the sediments (15% to 45%) may have

Table 1. Composite depth section for Site 758.

Hole	Core, section, interval (cm) Top	Bottom	ODP Depth (mbsf) Top	Bottom	Composite depth (m) Top	Bottom
758A	1H-1, 1	1H-4, 81	.00	5.31	.00	5.31
758B	1H-3, 81	1H-4, 141	3.81	5.91	5.32	7.42
758A	2H-1, 01	2H-CC, 1	6.01	15.78	7.43	17.20
758B	2H-5, 21	2H-5, 71	15.71	16.21	17.21	17.71
758A	3H-1, 21	3H-7, 61	15.81	25.21	17.72	27.12
758B	3H-3, 141	3H-5, 81	23.31	25.71	27.13	29.53
758A	4H-1, 01	4H-7, 71	25.21	34.91	29.54	39.24
758B	4H-5, 101	4H-6, 41	35.41	36.31	39.25	40.15
758A	5H-1, 21	5H-7, 51	35.01	44.31	40.16	49.46
758B	5H-4, 131	5H-6, 91	43.81	46.41	49.47	52.07
758A	6H-1, 31	6H-7, 71	44.71	54.11	52.08	61.48
758B	6H-4, 61	6H-5, 81	52.81	54.51	61.49	63.19
758A	7H-1, 01	7H-7, 61	54.01	63.61	63.20	72.80
758B	7H-4, 121	7H-5, 91	63.01	64.21	72.81	74.01
758A	8H-1, 01	8H-7, 41	63.71	73.11	74.02	83.42
758B	8H-5, 11	8H-5, 81	73.11	73.81	83.43	84.13
758A	9H-1, 11	9H-7, 63	73.51	83.03	84.14	93.66
758B	9H-4, 138	9H-6, 90	82.58	85.10	93.67	96.19
758A	10H-1, 84	10H-7, 63	83.94	92.73	96.20	104.99
758B	10H-4, 78	10H-5, 96	91.58	93.26	105.00	106.68
758A	11H-1, 15	11H-7, 65	92.95	102.45	106.60	116.19

contributed to sediment expansion. The sediments did not contain gas which would have led to sediment expansion. No propane was found, ethane was observed in only one sample, and the concentration of methane never exceeded 9 ppm (Shipboard Scientific Party, 1989). Shipboard handling of the core may be responsible for stretching the sediments. During the extraction of the core from the core barrel and during the transfer of the core from the rig floor to the catwalk, the core liner and the sedimentary section within may stretch. The stretching could produce a sedimentary section that is longer than the section which was cored *in situ*, i.e., at the seafloor. Post-coring expansion/stretching from one or more of these processes probably accounts for core recovery exceeding 100% and helps explain some portion of the sub-bottom depth discrepancy between the composite depth section and the standard ODP section.

In summary, a composite depth section was constructed for Site 758 because the detailed lithostratigraphy from MS documents sediment recovery gaps between nearly every APC core in Holes 758A and 758B. The exact cause of the gaps remains unclear but is definitely related to the drilling process. At present, the best explanation for the gaps is downheaval of the ship, which displaces a portion of the sedimentary section, and post-coring expansion/stretching of the sedimentary section which results in core recovery that exceeds 100%.

TIME SCALE AND SEDIMENTATION RATES

The primary chronostratigraphy for this study is provided by the 25 chron and subchron boundaries in the geomagnetic reversal record of the past 7 m.y. at Site 758. The magnetic reversals are assigned the ages of Berggren et al. (1985). The magnetic reversals in the composite depth section (Table 2) were taken directly from the particular interval in Hole 758A or splice from Hole 758B used to construct the composite. Linear sedimentation rates were calculated for each interval between paleomagnetic datums and are listed in Table 2. Instantaneous sedimentation rates were calculated for each sample in the Site 758 composite record (Appendix F). The average sedimentation rate over the entire composite section is 1.6 cm/k.y. This rate is equivalent to an average sample spacing of 2 k.y. in the shipboard MS database and a spacing of 6 k.y. in our wt% $CaCO_3$, wt% coarse fraction, and stable isotope database.

Table 2. Depths and ages of chron and subchron boundaries and linear sedimentation rates in the Site 758 composite depth section.

Hole	Composite depth (m)	Age (Ma)	Time zone	Linear sedimentation rate (cm/k.y.)
758A	0.00	0.00	(core top)	
758A	12.17	0.73	Brunhes/Matuyama	1.67
758A	15.57	0.91	Jaramillo (upper)	1.89
758A	16.77	0.98	Jaramillo (lower)	1.71
758B	28.07	1.66	Olduvai (upper)	1.66
758A	30.33	1.88	Olduvai (lower)	1.03
758A	38.53	2.47	Matuyama/Gauss	1.39
758A	44.65	2.92	Kaena (upper)	1.36
758A	45.65	2.99	Kaena (lower)	1.43
758A	47.05	3.08	Mammoth (upper)	1.56
758A	48.10	3.18	Mammoth (lower)	1.05
758B	51.31	3.40	Gauss/Gilbert	1.46
758B	61.63	3.88	Cochiti (upper)	2.15
758A	63.24	3.97	Cochiti (lower)	1.79
758A	65.39	4.10	Nunivak (upper)	1.65
758A	67.84	4.24	Nunivak (lower)	1.75
758A	70.69	4.40	Sidufjall (upper)	1.78
758A	72.24	4.47	Sidufjall (lower)	2.21
758B	73.00	4.57	Thvera (upper)	0.76
758A	77.11	4.77	Thvera (lower)	2.06
758A	86.98	5.35	Gilbert/Chron 5	1.70
758A	91.08	5.53	Chron 5 event 1 (upper)	2.28
758A	93.28	5.68	Chron 5 event 1 (lower)	1.47
758A	96.61	5.89	Chron 5/Chron 6	1.59
758A	102.41	6.37	Chron 6 event 1 (upper)	1.21
758A	104.31	6.50	Chron 6 event 1 (lower)	1.46

Note: Ages are from Berggren et al. (1985).

Sedimentation rates over last 7.3 m.y. can be divided into four general intervals: (1) 6.50 to 5.89 Ma, (2) 5.89 to 3.40 Ma, (3) 3.40 to 1.66 Ma, and (4) 1.66 to 0.00 Ma. (Fig. 5). In interval 1, the sedimentation rates were moderate (~1.3 cm/k.y.). Rates increased at the Chron 5/Chron 6 boundary which marks the transition from interval 1 to 2. Rates remained high (~1.8 cm/k.y.) during interval 2 until 3.4 Ma when they returned to the moderate levels (~1.3 cm/k.y.) observed during interval 3. Sedimentation rates during the interval 4 return to nearly the same level (~1.7 cm/k.y.) as in interval 2.

Exceptions to this general pattern are observed within the Olduvai (1.66 to 1.88 Ma) and Mammoth (3.08 to 3.18 Ma) Subchrons and between the subchron boundaries marking the lower Sidufjall (4.47 Ma) and the upper Thvera (4.57 Ma). Sedimentation rates during these intervals were significantly lower than during the immediately preceding or following intervals. Low sedimentation rates during the Mammoth Subchron are observed in both holes at Site 758, within Cores 121-758A-5H and 121-758B-5H. It is unlikely that missing sediment and/or a poor splice at the core break between Cores 121-758A-7H and 121-758A-8H, which separates the lower Sidufjall and the upper Thvera, can explain the low sedimentation rate of 0.76 cm/k.y. between these reversals because the same low rate (of 0.75 cm/k.y.) is observed in Core 121-758B-7H, which contains both reversals.

The dramatic drops in sedimentation rate at these reversal boundaries are curious. They most likely result from (1) a true decrease in sedimentation rate, (2) unrecognized hiatuses, (3) difficulties in reversal boundary identification, (4) unrecovered sediments, or (5) compression of the sedimentary section during the coring process. Although less likely, we cannot exclude the possibility that the age estimates for these magnetic reversal boundaries are in error. If the age estimates are erroneous, then so are the sedimentation rates. As an example, we consider different age estimates for the Olduvai Subchron and the resulting

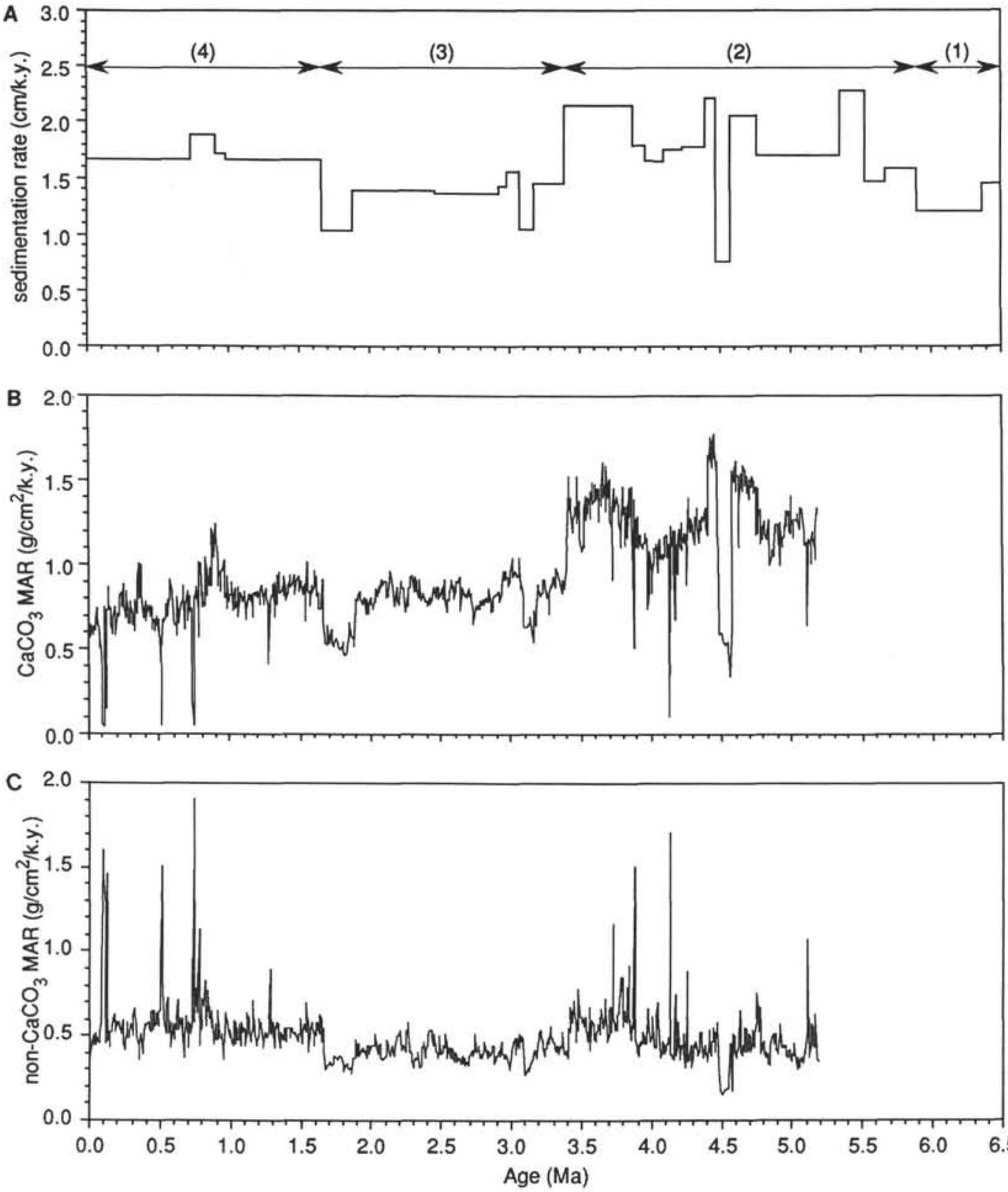

Figure 5. Comparison of Site 758 linear sedimentation rates (**A**) with mass accumulation rates of $CaCO_3$ (**B**) and non-$CaCO_3$ (**C**). Age is based on the geomagnetic reversal record (Table 2). Time intervals 1 through 4 in (A) are discussed in text. Spikes in (B) and (C) show intervals of high ash concentration.

sedimentation rates. The Berggren et al. (1985) ages for the top and bottom of the Olduvai are 1.66 and 1.88 Ma, respectively. These age estimates are slightly older than those recently proposed by Raymo et al. (1989) of 1.65 and 1.82 Ma for the top and bottom of the Olduvai. In addition, the duration of the Olduvai Subchron based on the Raymo et al. (1989) ages is shorter than the duration based on the Berggren et al. (1985) ages. The Raymo et al. (1989) ages give an Olduvai sedimentation rate of 1.33 cm/k.y., which is 22% higher than the 1.03 cm/k.y. rate based on the Berggren et al. (1985) ages. The higher sedimentation rates from the Raymo et al. (1989) ages results in a less dramatic decrease in sedimentation rates during the Olduvai compared to the time intervals preceding and following the Olduvai.

A preliminary time scale for the past 1 m.y. was constructed (Table 3; Fig. 6) by visual correlation of the Site 758 composite $\delta^{18}O$ record to the SPECMAP stack global average oxygen isotope record (Imbrie et al., 1984; Prell et al., 1986), and to the Atlantic Site 607 benthic $\delta^{18}O$ record (Ruddiman et al., 1989). The ages assigned to $\delta^{18}O$ events 1 through 20 are from Imbrie et al. (1984) and the ages for events 21 through 35 are from Ruddiman et al. (1989). Linear sedimentation rates (Table 3) are calculated between each depth interval assigned an age. Tentative identification of $\delta^{18}O$ events 23 to 105 in the Site 758 record (Fig. 7) is based on the correlation to the Site 607 record (Ruddiman et al., 1989; Raymo et al., 1989) and is supported by comparison with the planktonic and benthic $\delta^{18}O$ stratigraphies from equatorial Pacific Site 677 (Shackleton and Hall, 1989; Shackleton et al., in press). The identification of $\delta^{18}O$ events and the resulting age model for Site 758 (discussed below) is preliminary and will likely be adjusted in future work. The late Quaternary sedimenta-

Table 3. δ¹⁸O chronostratigraphy and sedimentation rates for the Site 758 composite record.

Composite depth (m)	Age (Ka)	Sedimentation rate (cm/k.y.)	$\delta^{18}O$ stages
0.00	0		(core top)
0.11	6	1.8	1.1
0.41	19	2.3	2.2
1.11	53	2.1	3.3
1.36	65	2.1	4.2
1.51	71	2.5	5.0
2.21	80	7.8	.5.1
2.41	99	1.1	5.3
2.71	122	1.3	5.5
3.01	135	2.3	6.2
3.51	171	1.6	6.5
3.71	183	1.7	6.6
3.91	194	1.8	7.1
4.01	205	0.9	7.2
4.18	216	1.5	7.3
4.41	228	1.9	7.4
4.64	238	2.3	7.5
4.96	249	2.9	8.2
5.11	257	1.9	8.3
5.32	269	1.8	8.4
5.52	287	1.1	8.5
5.67	299	1.3	8.6
6.32	331	2.0	9.3
6.62	341	3.0	10.2
7.43	405	1.3	11.3
7.63	434	0.7	12.2
8.13	478	1.1	13.0
8.23	491	0.8	13.12
8.33	513	0.5	13.2
8.43	525	0.8	13.3
8.63	538	1.5	14.2
8.73	552	0.7	14.3
9.03	563	2.7	14.4
9.38	574	3.2	15.1
9.63	585	2.3	15.2
9.83	596	1.8	15.3
9.93	607	0.9	15.4
10.03	617	1.0	15.5
10.28	631	1.8	16.23
10.98	679	1.5	17.2
11.38	700	1.9	18.23
11.58	711	1.8	18.3
11.78	721	2.0	18.4
12.03	731	2.5	19.1
12.58	750	2.9	20.23
13.18	775	2.4	21
13.73	799	2.3	22
14.03	819	1.5	23
14.28	838	1.3	24
14.58	859	1.4	25
15.18	881	2.7	26
15.53	906	1.4	27
15.73	922	1.3	28
15.93	946	0.8	29
16.33	965	2.1	30
16.83	985	2.5	31
17.92	1068	1.3	35

Note: $\delta^{18}O$ stages 1 through 20 are from Imbrie et al. (1984) and stages 21 through 35 are from Ruddiman et al. (1989).

tion rates based on $\delta^{18}O$ show much greater variations in amplitude and timing than the rates based on magnetic reversals (Fig. 6). This difference demonstrates that variations in sedimentation rate and thus ocean and climate change is inadequately captured by the geomagnetic reversal record which gives a constant sedimentation rate for the Brunhes Chron (Figs. 5 and 6). High-resolution age models are required for high-resolution paleoenvironmental analysis.

RESULTS

Isotope Stratigraphy

The $\delta^{13}C$ and $\delta^{18}O$ data are plotted vs. depth in Figure 8, plotted vs. age in Figures 9 and 10, and are listed in Appendixes D, E, and F. The d18O record can be divided into two distinct intervals at approximately 14 m ($\delta^{18}O$ stage 23; Fig. 7). The Holocene and the upper Pleistocene (0 to 14 m) contains $\delta^{18}O$ stages 1 to 22 and is characterized by high-amplitude (1‰–2‰), ~100-k.y. (100–150 cm) cycles. The most depleted (interglacial) $\delta^{18}O$ value is –2.26‰ and the most enriched (glacial) value is –0.33‰. This interval has more enriched $\delta^{18}O$ values ($\bar{x}$ = –1.21‰) and higher variability (σ = 0.43) than the interval below 14 m. The $\delta^{18}O$ record in the upper 14 m from Site 758 is quite similar to the SPECMAP-stacked $\delta^{18}O$ record (Imbrie et al., 1984; Prell et al., 1986) (Fig. 6). Compared to the SPECMAP $\delta^{18}O$ record, the record from Site 758 shows relatively enriched substages 5.5 and 18.4, and depleted substages 15.1 and 13.2.

The lower interval (14 to 39 m) lies within the upper Pliocene and lower Pleistocene, and contains $\delta^{18}O$ stages 23 to 105. Compared to the overlying interval, the $\delta^{18}O$ record in the lower interval is characterized by higher frequency (~40 k.y.) and lower amplitude (<1‰) fluctuations. The values are also more depleted ($\bar{x}$ = –1.50‰) and have a lower variability (σ = 0.24). While $\delta^{18}O$ events with depleted values reach –2.21‰, similar to those in the overlying interval, events with enriched values reach only –0.73‰ much less than in the overlying interval. In other words, the interglacial stages of the upper and lower intervals were similar while the glacial stages of the late Pleistocene were more severe, indicating some combination of greater ice volume, colder sea surface temperatures, or higher salinity during the late Pleistocene. The periodicities of ~40 k.y. in the late Pleistocene and ~100 k.y. in the late Pliocene and early Pleistocene are clearly evident, even without spectral analysis. These periodicities can be estimated by simply dividing time intervals, determined by magnetic reversal ages, by the number of $\delta^{18}O$ cycles. The $\delta^{13}C$ record also shows long- and short-term variability but the change at 14 m is not as distinct as in $\delta^{18}O$. The mean $\delta^{13}C$ value increases from 1.13‰ in the overlying interval, to 1.34‰ below, but the standard deviation is nearly the same, increasing from 0.18 to only 0.21.

Using the nomenclature of Ruddiman et al. (1989) and Raymo et al. (1989), isotope stages 23 through 105 have been identified in the Site 758 record (Fig. 7). Support for stage identification is based on the comparison to the Site 677 record (Shackleton and Hall, 1989; Shackleton et al., in press). Although we are confident in the completeness of our composite depth section and in the magnetic age control, correlation of the Site 758 record to that in Site 607 (Ruddiman et al., 1989; Raymo et al., 1989) is difficult and perhaps tenuous for several reasons. First, we are comparing significantly different $\delta^{18}O$ records. The Site 758 record is from the equatorial Indian Ocean and is based on planktonic foraminifers. The Site 607 record is from the North Atlantic and is based on benthic foraminifers. Fluctuations in global ice volume will have an identical impact on the $\delta^{18}O$ from both records. Nevertheless, water temperature and salinity also effect $\delta^{18}O$. The history of temperature and salinity fluctuations in the abyssal waters of the North Atlantic is undoubtedly different than the history in the surface waters of the equatorial Indian Ocean. Since ice volume fluctuations are the primary control of $\delta^{18}O$ in these records, the timing of the $\delta^{18}O$ fluctuations is generally similar at Sites 758 and 607. The major difference between the records is in the amplitude of the $\delta^{18}O$ variations due to differences in temperature and salinity. The second is the difference in temporal resolution of the records from Sites 758 and 607. Site 758 was

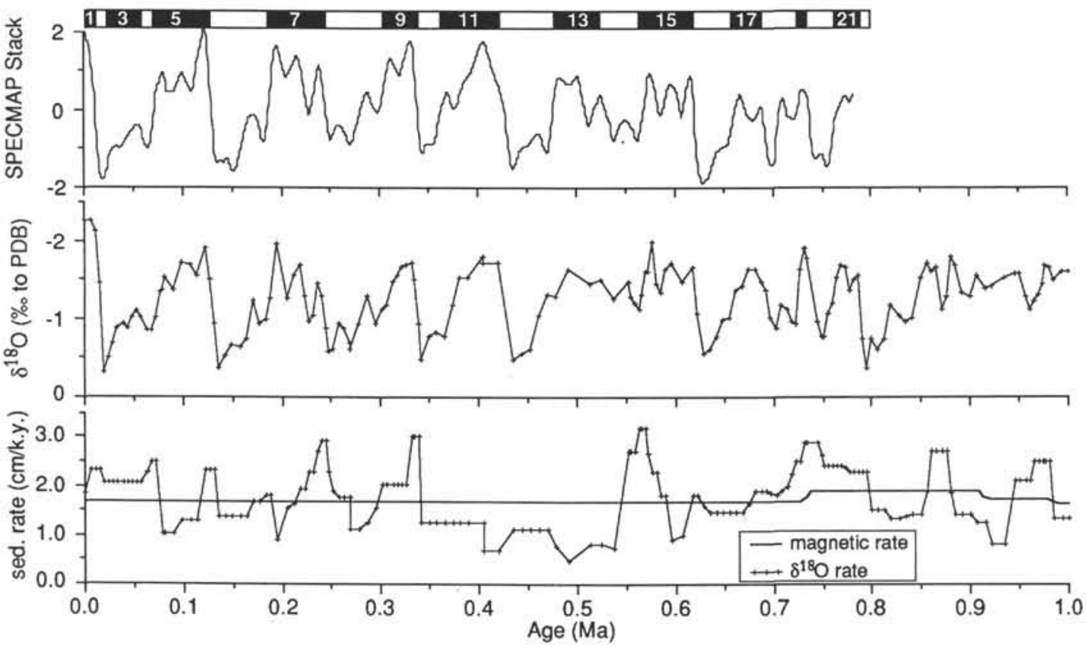

Figure 6. Oxygen isotope records from the SPECMAP stack (Imbrie et al., 1984) and from Site 758 plotted vs. age. The SPECMAP stack is plotted in standard deviation units. Odd-numbered intervals in legend refer to interglacial stages. Estimates of sedimentation rate are plotted vs. age and are based on the geomagnetic reversal record (Table 2) and on the $\delta^{18}O$ age model (Table 3).

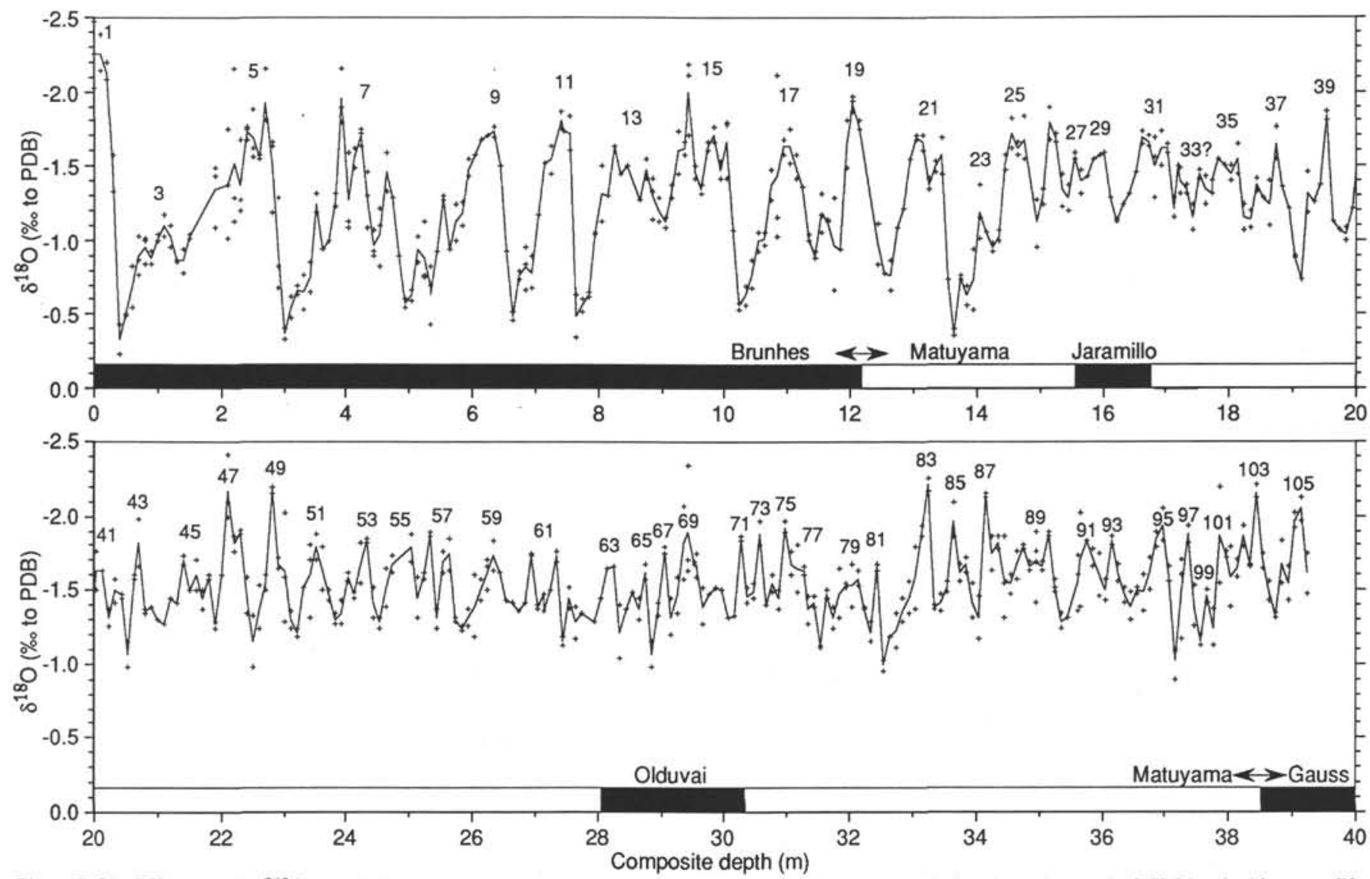

Figure 7. Site 758 composite $\delta^{18}O$ record plotted to composite depth. Solid line connects the mean of individual analyses (crosses) of *Globigerinoides sacculifera* at each depth. Odd numbers refer to interglacial stages. Stages 1 to 20 are correlated to the SPECMAP stack (Imbrie et al., 1984). Preliminary identification of stages 21 to 105 is based on correlation to the Site 607 record (Ruddiman et al., 1989; Raymo et al., 1989).

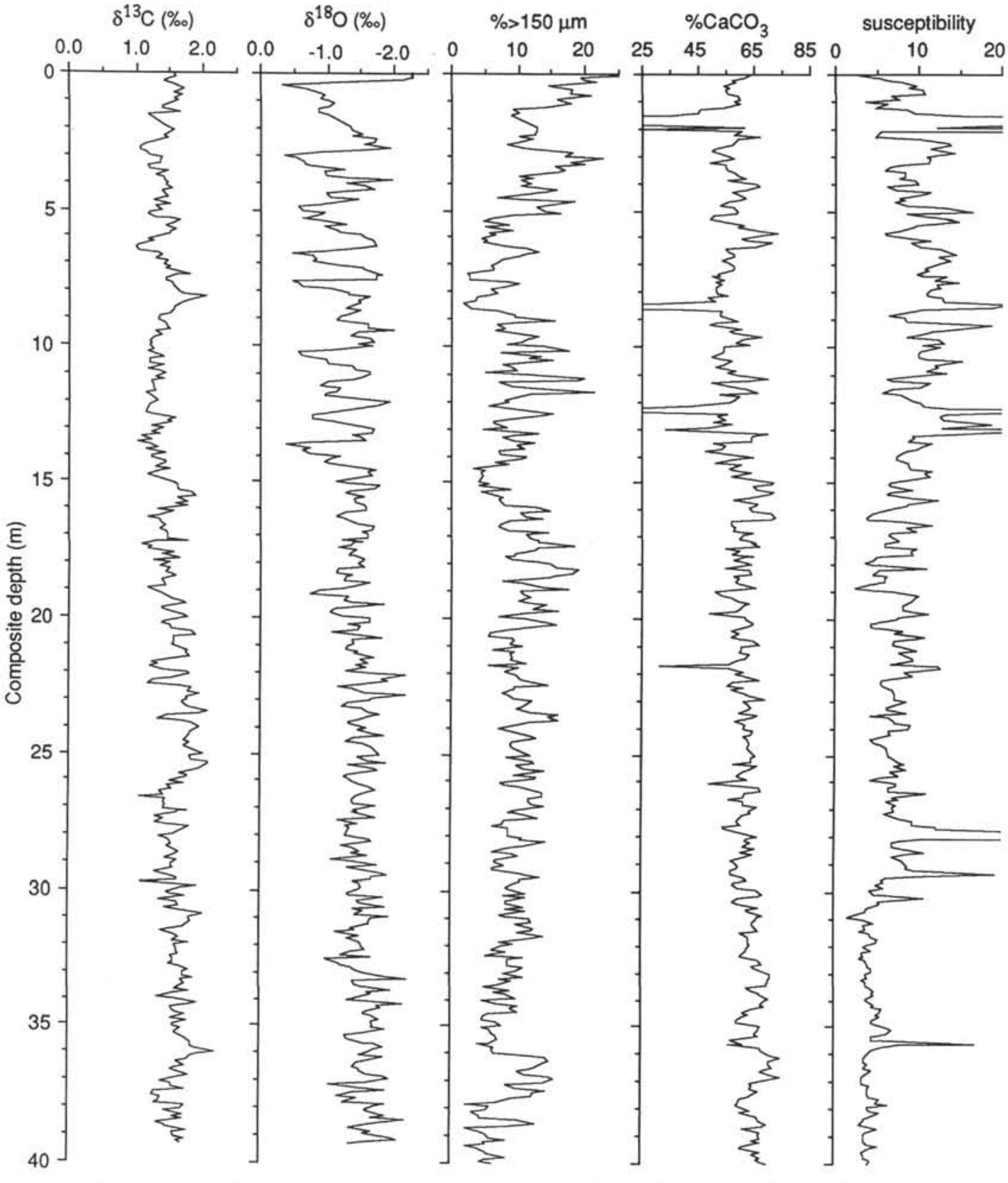

Figure 8. Site 758 composite $\delta^{13}C$ and $\delta^{18}O$ (G. sacculifera), wt% $CaCO_3$, wt% coarse fraction (>150 µm), and magnetic susceptibility (10^{-6} cgs) records vs. composite depth.

sampled at 10 cm vs. 16 cm for Site 607 (Ruddiman et al., 1989; Raymo et al, 1989). However, during the past 2.7 m.y., the average sedimentation rate at Site 607 is ~4.4 cm/k.y., which is three times greater than the average rate of 1.5 cm/k.y. at Site 758. Because the differences in sedimentation rate are much greater than the differences in sample spacing, the average sample resolution of the Site 607 record is 3.6 k.y., which is nearly twice the resolution of the 6.4-k.y. spacing in the Site 758 record. Due to the lower sedimentation rate at Site 758, the isotopic variations are more likely to be blurred compared to those in the Site 607 record. Finally, detailed biostratigraphic information that would provide additional points of correlation is not yet available.

Despite the difficulties in correlation, the general agreement between the structure and timing of the two isotope records suggests that isotope stages 21 through 105 can be correlated from Site 607 to Site 758. Particularly favorable comparisons between the two records are as follows: (1) the Brunhes/Matuyama boundary is found in stage 19; (2) the Jaramillo top occurs in stage 27 and the bottom in stage 31; (3) stages 57 and 61 are split peaks; (4) stages 78 and 82 are relatively enriched in ^{18}O compared to other glacial stages; (5) stages 96, 98, and 100 are moderately strong glacials associated with the initiation of significant Northern Hemisphere glaciation (Raymo et al., 1989); and (6) the Matuyama/Gauss boundary occurs in stage 104. Minor differences between the isotope records occur near the Olduvai Subchron. The top of the Olduvai falls within stage 63 at Site 758 but in stage 64 at Site 607. If the deepest end of the uncertainty range in Site 758 is used, the reversal occurs near the transition from stage 63 to 64. The bottom of the Olduvai falls within stage 74 at Site 758 but is found in stage 72 at Site 607. Because stage 73 is

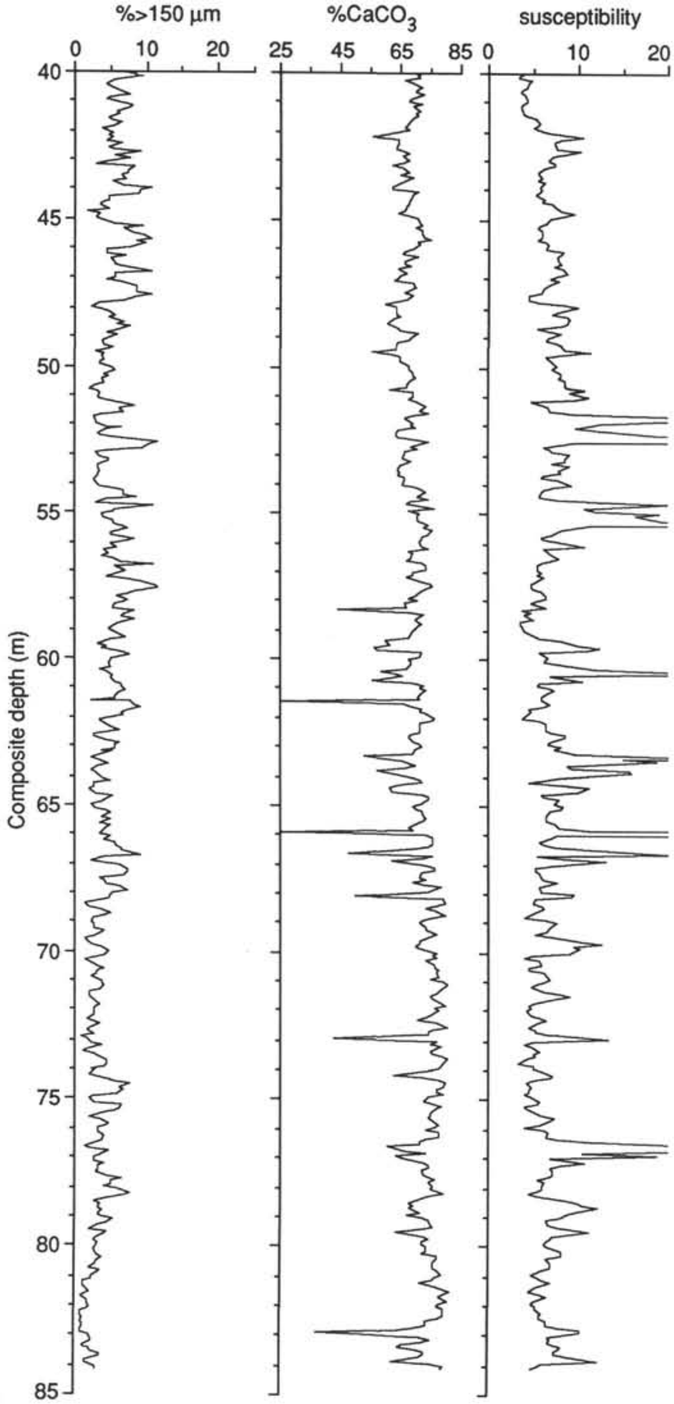

Figure 8 (continued).

poorly defined by only one point (although duplicated) in the Site 758 record, we have less confidence in our correlation to Site 607 at this interval.

Wt% $CaCO_3$ Stratigraphy

The wt% $CaCO_3$ data are plotted vs. depth in Figure 8, plotted vs. age in Figures 9, 10, and 11, and are listed in Appendixes B, C, and F. $CaCO_3$ is the dominant sedimentary component and accounts for an average of 66.3% of the bulk sediment over the past 5.2 m.y. The $CaCO_3$ content ranges from 2.7% (in volcanic ash horizons) to 81.1% and generally increases downhole (Fig. 11). This long-term downhole trend is punctuated by low wt% $CaCO_3$ intervals which mark the locations of ash layers. Excluding these layers, the mean wt% $CaCO_3$ value increases gradually from 58.3% during the interval 0–1 Ma to 73.7% during 4–5 Ma. This downhole increase is accompanied by a progressive lightening of sediment color (Shipboard Scientific Party, 1989), generally lower MS values, and lower wt% coarse fraction (Fig. 11). Higher frequency $CaCO_3$ variations, on the order of 10% to 15%, are superimposed on the long-term trend.

The late Pleistocene wt% $CaCO_3$ record is characterized by generally higher values during interglacial intervals than during glacials (Fig. 9). The $CaCO_3$ MAR, however, occasionally moves the peak $CaCO_3$ events from the middle of interglacial intervals toward the glacial to interglacial transition, a result of increased sedimentation rates at transitions between $\delta^{18}O$ stages (Fig. 6 and 9).

A shift toward higher wt% $CaCO_3$ occurs near 0.8 Ma, at about 14 m in the composite depth record (Fig. 8). Excluding obvious ash horizons, the wt% $CaCO_3$ values of the top 14 m ($\bar{x} = 57\%$) are lower than those in the next 14 m ($\bar{x} = 62\%$). The wt% $CaCO_3$ shift coincides with the $\delta^{18}O$ shift described above, a lightening of sediment color, a decrease in MS, and the distinct change in the mode of variability in the $\delta^{18}O$ record·

Coarse Fraction Stratigraphy

The wt% coarse fraction (>150 µm) data, which range from 0.79% to 28.49% and average 7.22%, are plotted vs. depth in Figure 8, plotted vs. age in Figures 9, 10, and 11, and are listed in Appendixes B, C, and F. The sediment in this fraction is almost exclusively biogenic $CaCO_3$, primarily consisting of whole and fragmented foraminifers. Volcanic ash is rarely a component. No portion of the coarse fraction is composed of nonvolcanic terrigenous sediment. The most apparent trend to the data is the long-term, downhole decrease. Superimposed on this trend are fluctuations at both high and low frequencies.

Coarse fraction percent is generally considered a reliable index of $CaCO_3$ dissolution (Berger, 1970; Berger et al., 1982). If winnowing and bottom-water turbulence are minimal, the systematic decrease in wt% coarse fraction with increasing water depth can be attributed to dissolution-induced fragmentation of foraminifer tests. Increased fragmentation of fossil assemblages and decreased wt% coarse fraction from core top and downhole samples from the Ninetyeast Ridge (near 6°S) have been directly related to dissolution (Peterson and Prell, 1985a, 1985b). The increase in dissolution with depth is attributed to a progressive increase in the corrosiveness (lower carbonate ion concentration) of the Indian Deep and Bottom Waters. Preliminary analysis of the preservation state of the foraminifer faunal assemblages at Site 758 (Chen and Farrell, this volume) shows a generally good agreement between the wt% coarse fraction and foraminifer preservation over the interval from 0 to 800 Ka. Until quantitative analysis of the assemblages is completed for the entire late Neogene interval, the wt% coarse fraction serves as the best estimate of relative dissolution at Site 758.

Magnetic Susceptibility Stratigraphy and Volcanic Ash

The MS data are plotted vs. ODP depth in Figure 3 (back pocket), plotted vs. composite depth in Figure 8, and plotted vs. age in Figures 9, 10, and 11. MS values interpolated at the depth of the samples in our wt% $CaCO_3$ and isotope database are listed in Appendix F. MS values in Site 758 sediments have increased since 7.3 Ma, but not monotonically. The low MS values in the uppermost Miocene suggest only minor input of terrigenous sediment and little to no volcanic ash; no discrete ash layers are found in the Miocene. High wt% $CaCO_3$ values in this same section support this contention. Spikes in the MS stratigraphy denote ash

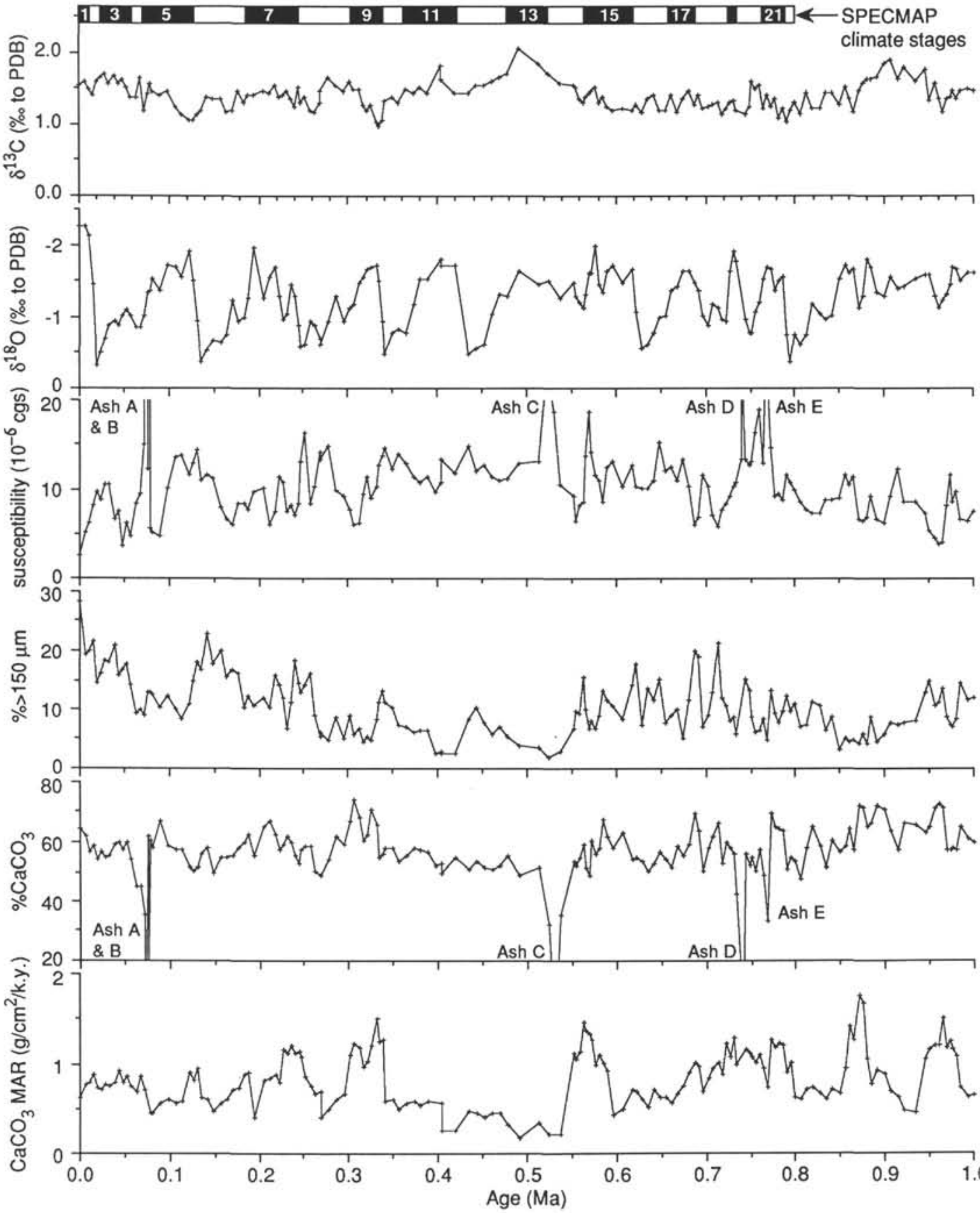

Figure 9. Site 758 composite records of $\delta^{13}C$, $\delta^{18}O$, magnetic susceptibility (10–6 cgs), wt% coarse fraction (>150 mm), wt% $CaCO_3$, and $CaCO_3$ MAR vs. age based on the $\delta^{18}O$ age model (Table 3). Depths of major ash layers are labeled. Odd-numbered intervals in the legend refer to interglacial stages.

blebs and layers which begin to appear in the early Pliocene. The increase in average MS values within the lower Pliocene (Fig. 3, back pocket) indicates the presence of disseminated ash and/or an increase in nonvolcanic terrigenous sediment (clay) input. A sharp reduction in average MS values occurs within the section between 2.7 and 1.9 Ma (Fig. 11). Since sedimentation rates are also reduced in this interval, part of the reduction in average MS values may be due to a decrease in the accumulation rate of magnetizable material. Following 1.9 Ma, the MS values increase as terrigenous sedimentation and the input of volcanic ash increased. The highest average MS values occurs within the upper Pleistocene where wt% $CaCO_3$ is lowest, the sediment color is darkest, and terrigenous sedimentation is relatively high.

Thirteen major volcanic ash layers are observed in the uppermost 116 m from Site 758. These layers appear as low wt% $CaCO_3$ spikes in Figures 5, 8, 9, 10, and 11 and as high MS spikes in Figures 3, 4, 8, 9, 10, and 11. The magnetic material in the ash is largely responsible for the high quality of the MS and magnetic declination signals. The concentration of ash in the sediments ranges from minor amounts disseminated through much of the section, to major ash layers such as the youngest Toba ash (~75 Ka), which is 34 cm thick in Hole 758A. If ages are determined for these ash layers by independent means, such as the $^{40}Ar/^{39}Ar$ method (McDougall and Harrison, 1988), these layers will become chronostratigraphic markers with the potential to test the veracity of the geomagnetic reversal and $\delta^{18}O$ chronostratigraphies.

DISCUSSION

We focus this discussion on two time scales and two time slices during which important changes are observed in one or more of the oceanic and climatic indices. We consider long-term change on the time scale from 0 to 5 Ma, and short-term change from 0 to 1 Ma. The two time slices examined are the 2.4 Ma initiation of significant Northern Hemisphere glaciation, and the mid-Pleistocene climate shift near 0.85 Ma.

Long-Term Change in the Northeastern Indian Ocean

$CaCO_3$ preservation appears to have increased since at least 5 Ma. This is based on the long-term and rather monotonic increase in wt% coarse fraction (Fig. 11). Clearly superimposed on this trend are higher frequency fluctuations at a variety of periodicities. The interpretation of enhanced preservation is based on the assumption that wt% coarse fraction measures dissolution intensity. Alternatively, the increase in wt% coarse fraction over time may reflect an increase in winnowing intensity due to faster flow of deep water. Evidence of winnowing was found at Site 707, located in intermediate-depth waters (1500 m) in the western equatorial Indian Ocean (Peterson and Backman, 1990). Beginning at 3.5 Ma, the sediments at this site show an a dramatic increase in foraminifer sand content. Most of the fine fraction, which is typical in deep-sea ooze, is not present. An abrupt increase in wt% coarse fraction did not occur at 3.5 Ma nor at any other time in the Site 758 record. Although we cannot completely discount the possibility of enhanced winnowing at Site 758, we present the following evidence to support our contention that the wt% coarse fraction record from the Ninetyeast Ridge reflects $CaCO_3$ preservation. In the late Pleistocene, $CaCO_3$ preservation is clearly correlated to wt% coarse fraction since it covaries with dissolution indices that are based on planktonic foraminifers (Chen and Farrell, this volume). Detailed analysis of the preservation state of the planktonic foraminifers in the Pliocene interval has not yet been done. However, while picking *G. sacculifera* for isotope analysis, we observed a downhole decrease in the abundance of dissolution-susceptible species and an increase in the abundance of dissolution-resistant species. Furthermore, the foraminifers in lower Pliocene and upper Miocene samples from Cores 121-758A-7H and 121-758A-8H also appear to have been greatly altered by dissolution (W. Berggren, pers. comm., 1990). In several of these samples, the abundance of *G. sacculifera*, which is moderately susceptible to dissolution, was rare to absent. One explanation of the long-term increase in wt% coarse fraction is a gradual decline in the corrosiveness of the water that bathes Site 758. Support for this contention comes from the long-term deepening of the Indian Ocean carbonate compensation depth (CCD) since ~5 Ma observed in sedimentary records from the western equatorial Indian Ocean (Peterson and Backman, 1990) and the Bengal Fan (Stow et al. (1990).

Since 5 Ma, the long-term increase in wt% coarse fraction was accompanied by a long-term decrease in wt% $CaCO_3$ (Fig. 11) and $CaCO_3$ MAR (Fig. 5). Because the increase in wt% coarse fraction apparently reflects an increase in preservation, the decline in wt% $CaCO_3$ and $CaCO_3$ MAR is considered to represent a long-term increase in dilution by non-$CaCO_3$ sediment and/or a decrease in $CaCO_3$ productivity. However, the short-term fluctuations superimposed on these long-term $CaCO_3$ trends could be controlled by dissolution. The decline in $CaCO_3$ MAR was not as monotonic as the decline in wt% $CaCO_3$. Abrupt changes in $CaCO_3$ MAR reflect fluctuations in sedimentation rate derived from the paleomagnetic reversal record. These sedimentation rate changes do not effect the wt% $CaCO_3$ record. The variations in $CaCO_3$ MAR are not affected by terrigenous dilution and are not always in phase with changes in the wt% $CaCO_3$ record. If dissolution controlled the long-term patterns observed in the $CaCO_3$ sediments, then the decrease in wt% $CaCO_3$ should be in phase with the decrease in $CaCO_3$ MAR.

The most dramatic change in the $CaCO_3$ MAR record is the 50% decrease at 3.4 Ma (Fig. 5) from a mean value of approximately 1.35 g/cm^2/k.y. to 0.7 g/cm^2/k.y. The timing and relative size (50%) of this $CaCO_3$ MAR decrease has also been observed in records from Legs 115 (Peterson and Backman, 1990) and 117 (Prell, Niitsuma, et al., 1989) suggesting that the decrease occurred over much of the Indian Ocean. This $CaCO_3$ MAR decrease in sites from Legs 115 and 117 was interpreted as a drop in productivity (Peterson and Backman, 1990; Prell, Niitsuma, et al., 1989). This interpretation is consistent with the records from Site 758. The drop in $CaCO_3$ MAR at Site 758 is interpreted as a decline in productivity because wt% coarse fraction increases across this interval, indicating enhanced preservation, and because dilution (an increase in non-$CaCO_3$ MAR) did not increase at 3.4 Ma. The widespread occurrence of this drop in $CaCO_3$ MAR near 3.4 Ma suggests a major reorganization of surface-water productivity over much of the Indian Ocean. If productivity has decreased since 5 Ma, then the long-term increase in $CaCO_3$ preservation indicated by the wt% coarse fraction record may be partly related to a decrease in the flux ratio of organic carbon (C_{org}) to $CaCO_3$ carbon (C_{CaCO_3}). If the high rates of $CaCO_3$ MAR during the latest Miocene and early Pliocene were produced by elevated productivity levels, then it is likely that the flux ratio of organic carbon to $CaCO_3$ to the seafloor was higher. Degradation of the organic carbon in the surface sediments could lead to significant dissolution and thus low wt% coarse fraction even if the hydrographic lysocline at that time was situated far below the depth of the site (Emerson and Bender, 1981; Peterson and Prell, 1985a). Secession of high productivity near 3.4 Ma may have led to a decrease in the flux ratio of C_{org}:C_{CaCO_3} and thus an increase in preservation. Elevated levels of C_{org} and $CaCO_3$ MAR during the early Pliocene at Arabian Sea Site 722 (Murray and Prell, 1991) support the link between C_{org} and $CaCO_3$ preservation.

Variations in the MS record are difficult to interpret without a greater understanding of the sedimentary components and the magnetic parameters of the record. For example, grain size as well as concentration of the magnetic minerals can determine the amplitude of the susceptibility measurements (Thompson and Oldfield, 1986). Furthermore, deconvolution of the MS record into paleoenvironmental parameters is more difficult at Site 758 than at other sites, such as those on Leg 117 (deMenocal and Bloemendal, 1991), because the signal at Site 758 contains not only silt and clay but ash as well. If we assume, however, that the average MS values at Site 758 record some measure of the long-term change in the ratio of $CaCO_3$ to clay sedimentation, then the trend of increasing MS since 7.3 Ma (Fig. 11) shows a decrease in $CaCO_3$ sedimentation and/or an increase in non-$CaCO_3$ sedimentation. This interpretation is supported by the uphole decrease in $CaCO_3$ MAR and increase in non-$CaCO_3$ MAR (Fig. 5), as well as the uphole trend of decreasing wt% $CaCO_3$ (Fig. 11).

The increase in terrigenous input from at least 7.3 to 0 Ma may be partly related to subsidence and northward movement of Site 758 closer to the source of riverine sediments. This contribution is probably minimal, however, since paleobathymetric and back-

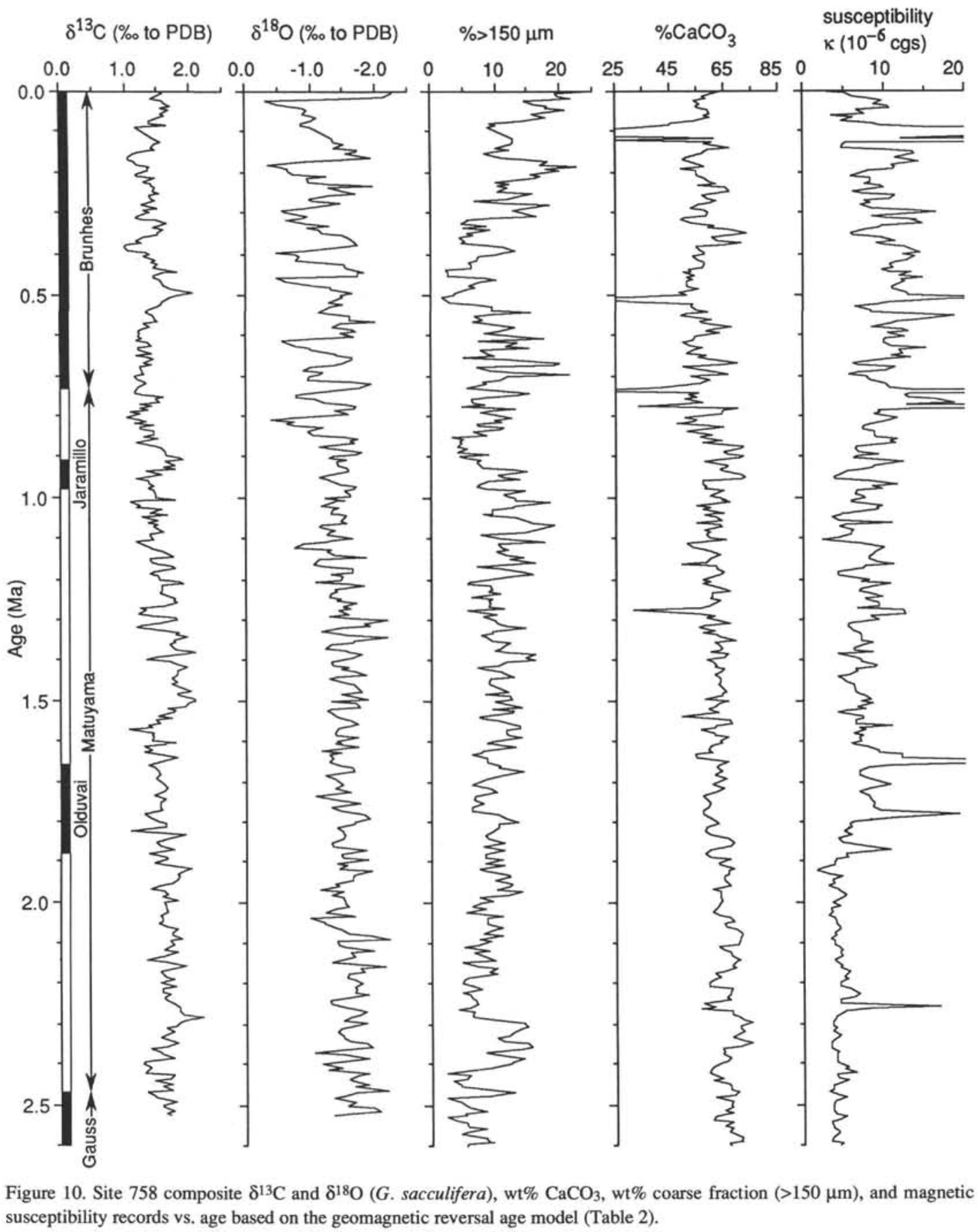

Figure 10. Site 758 composite $\delta^{13}C$ and $\delta^{18}O$ (*G. sacculifera*), wt% $CaCO_3$, wt% coarse fraction (>150 µm), and magnetic susceptibility records vs. age based on the geomagnetic reversal age model (Table 2).

track estimates suggest a deepening of no more than 200 m and northward movement of only ~2.5° since 5 Ma (Peirce, Weissel et al., 1989). Alternatively, the increase in terrigenous sedimentation could be linked to an increase in sediment discharge into the Bengal Bay. Most of the riverine sediment transported to the Ganges delta and shelf region would ultimately be deposited in the deep sea by turbidity currents. These sediments formed the Bengal Fan. Powerful turbidity currents carried sediments more than 2500 km from the Ganges delta and deposited beds up to 2.5 m thick (Stow et al., 1990). The coarser-grained sands and muds were deposited on the Bengal Fan closer to the delta. During turbidity flows, the finer sediments, predominantly silts and clays, were most likely entrained into nepheloid layers or mixed upwards into shallower waters. Some silts and clay were deposited at Site 758, atop the Ninetyeast Ridge, which lies ~1000 m above the Bengal Fan.

Greater sediment discharge by the Ganges-Brahmaputra river system over this time interval is ultimately related to increased rates of Himalayan uplift and denudation during the latest Miocene and Pliocene (Raymo et al., 1988, and references therein). Intensification of monsoonal rains resulting from an elevated Himalayan front and greater land/sea contrast due to a higher Tibetan Plateau would contribute a positive feedback by supplying greater river flow and erosional force (Raymo et al., 1988). The many causative links between uplift and terrigenous sedimentation at the Ninetyeast Ridge are complex and quite speculative

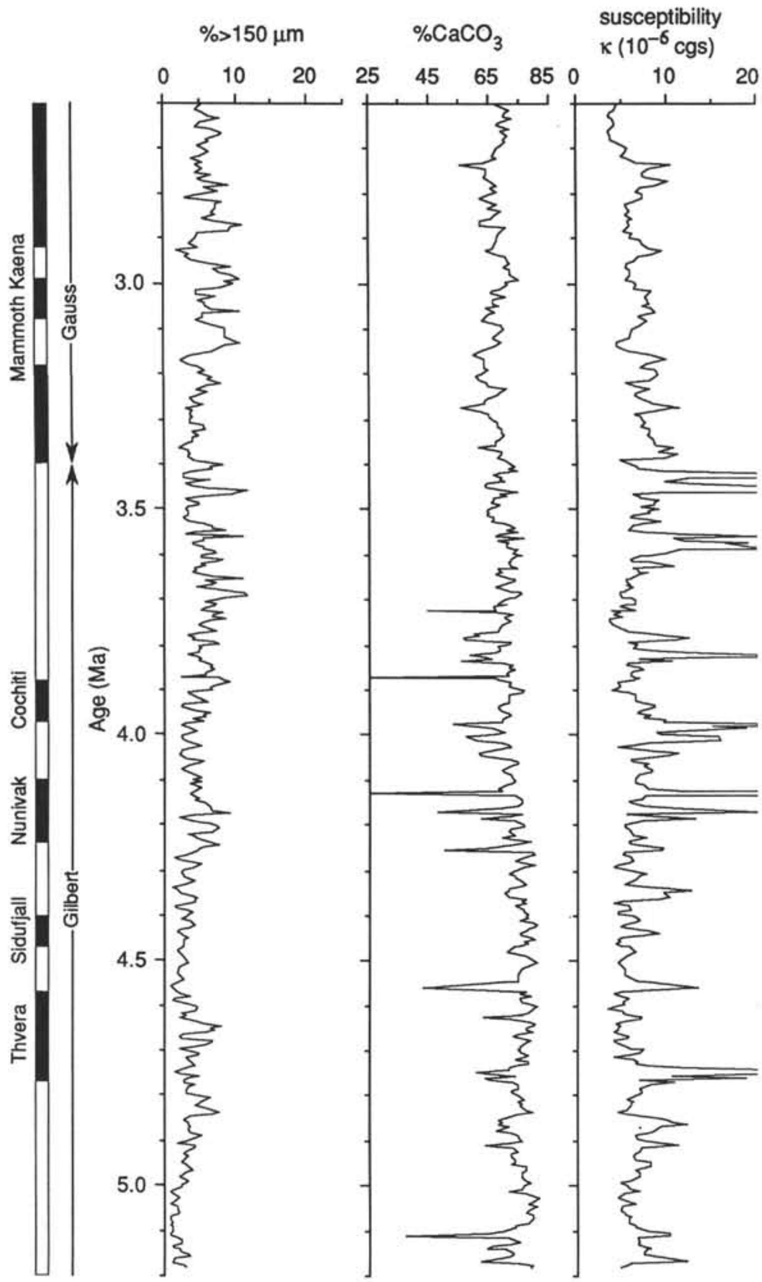

Figure 10 (continued).

at this point and will remain so until the northern Indian Ocean records and tectonic history of the Himalayas are understood in greater detail.

High-Frequency Fluctuations in the Northeastern Indian Ocean (0–1 Ma)

Over the interval from 0 to 1 Ma, the paleoenvironmental indices at Site 758 record the waxing and waning of the large Northern Hemisphere ice sheets, predominantly at a cyclicity of about 100 k.y. Glacial intervals are characterized by higher wt% coarse fraction and generally lower wt% $CaCO_3$ (Fig. 9). Interglacial intervals are characterized by lower wt% coarse fraction and generally higher wt% $CaCO_3$. High wt% coarse fraction during glacials clearly reflects enhanced $CaCO_3$ preservation. This relationship is supported by the observation that samples with high %coarse fraction also contain high percentages of foraminifer species which are moderate to highly susceptible to dissolution (Chen and Farrell, this volume). Likewise, samples with low wt% coarse fraction contain high abundances of foraminifer species, such as *Globorotalia tumida,* which are dissolution resistant. Variations in the wt% $CaCO_3$ and $CaCO_3$ MAR records are not in phase which suggests that dilution, rather than dissolution or productivity, controlled the late Pleistocene wt% $CaCO_3$ record. Higher wt% $CaCO_3$ during glacial stages is consistent with the scenario of Curray et al. (1982) which suggests that glacial low-stands of sea level allowed terrigenous sediments trapped on the continental shelf at the mouth of the Ganges-Brahmaputra river system to erode off the continental slope and into the basin, toward the northern Ninetyeast Ridge. During modern and interglacial times, when sea level was high, most of the terrigenous sediment was trapped in near-shore environments and the ocean basin was essentially starved of terrigenous sediment. This interpretation may require closer examination, however, in light of the recent study by Kuehl et al. (1989) which shows that

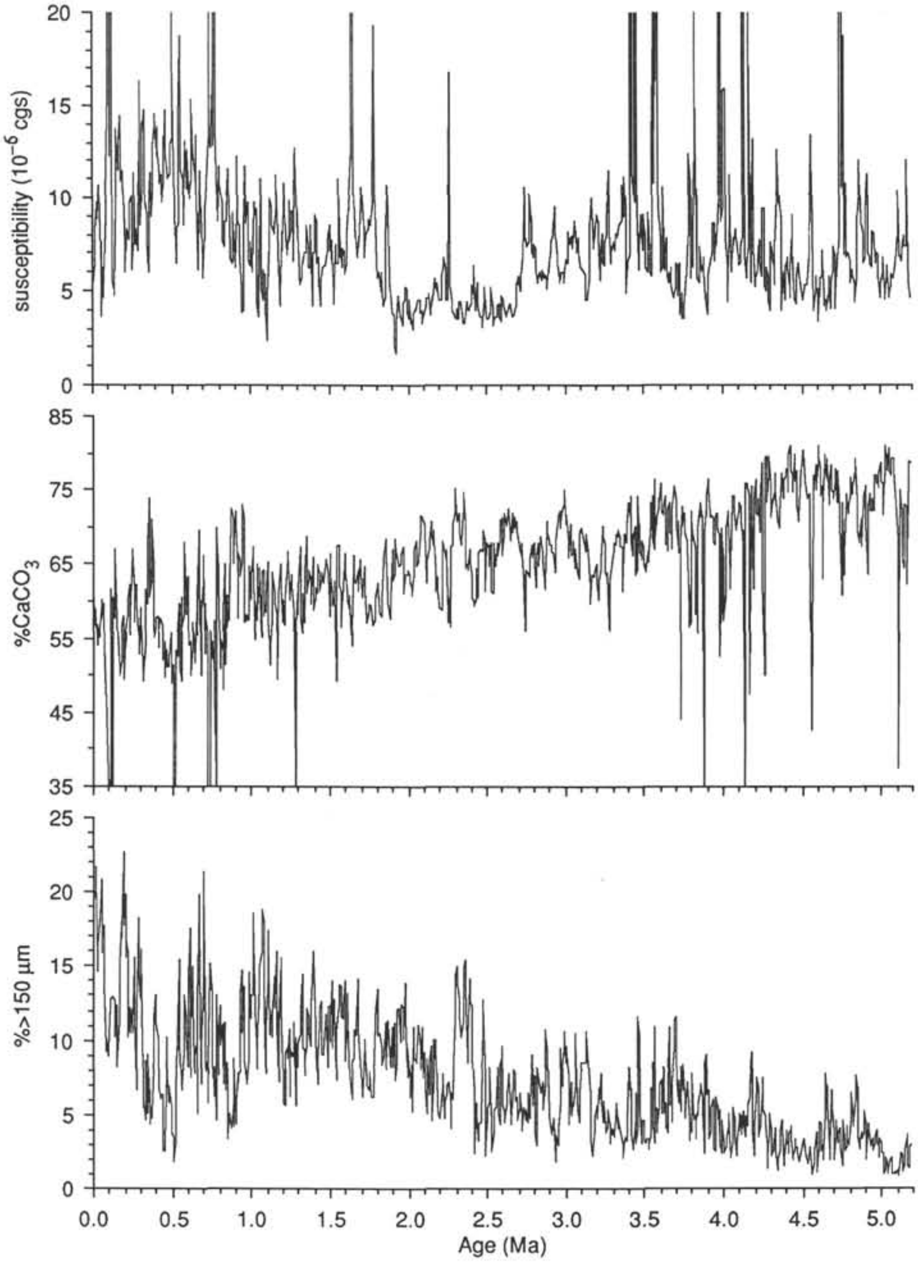

Figure 11. Site 758 composite records of magnetic susceptibility (10^{-6} cgs), wt% $CaCO_3$, and wt% coarse fraction (>150 µm) vs. age based on geomagnetic reversals.

modern terrigenous sediments are bypassing the delta and are flowing seaward onto the Bengal Fan.

The 100-k.y. cycles of the late Pleistocene are superimposed on the "Brunhes dissolution cycle" (Adelseck, 1977) which is most clearly observed in the wt% coarse fraction data. The midpoint of the cycle is between 400–525 Ka, where dissolution is greatest as indicated by the lowest wt% coarse fraction. The stronger preservation events (higher wt% coarse fraction) at ~700 Ka and at ~10 Ka mark the beginning and end of the dissolution cycle. These times are also marked by good preservation of planktonic foraminifers (Chen and Farrell, this volume). This dissolution cycle has been observed in other Indian Ocean records from shallower and deeper waters. Fluctuations in pteropod fragmentation at Site 716 record the mid-Brunhes dissolution cycle at intermediate water depths (540 m) (Droxler et al., 1990). In deeper water records, from 6°S on the Ninetyeast Ridge, Peterson and Prell (1985b) observed the Brunhes dissolution cycle as recorded by a composite dissolution index. This cycle, which has also been observed in the Pacific (Farrell and Prell, 1989) and Atlantic (Crowley, 1985), is global in extent and appears to have affected the entire water column. The cause of this cycle and its connection to the mid-Brunhes climatic event is discussed by Jansen et al. (1986).

Initiation of Significant Northern Hemisphere Glaciation Near 2.4 Ma

The onset of glaciation in the Northern Hemisphere occurred near 2.4 Ma (Backman, 1979; Shackleton et al. 1984; Raymo et al., 1989). At this time, ice-rafted debris was deposited in the

North Atlantic (Shackleton et al., 1984; Raymo et al., 1986) and $\delta^{18}O$ records from benthic (Shackleton et al., 1984; Raymo et al., 1989) and planktonic (Prell, 1985) foraminifers show ^{18}O-enriched intervals signifying strong glacials. At Site 758, the sedimentary record between 2.3–2.4 Ma is characterized by high wt% coarse fraction values, a moderate increase in wt% $CaCO_3$, and the glacial $\delta^{18}O$ stages 96, 98, and 100 (Figs. 10 and 11). The increase in wt% coarse fraction and wt% $CaCO_3$ suggests an increase in $CaCO_3$ preservation and is similar to the preservation patterns observed in the central equatorial Pacific at this time (Farrell and Prell, in press). In the $\delta^{18}O$ record from Site 758, the three glacial stages between 2.3–2.4 Ma are slightly enriched in 18O compared to the immediately preceding and following glacials. This enrichment, however, is not nearly as distinct as that observed in the benthic records (Shackleton et al., 1984; Raymo et al., 1989) and the planktonic record from DSDP 572 (Prell, 1985).

Mid-Pleistocene Shift at 850 Ka

The mid-Pleistocene shift in dominance of climate variance from a ~40-k.y. rhythm in the early Pleistocene to a ~100-k.y. rhythm in the late Pleistocene was first discussed by Pisias and Moore (1981) in Pacific records and was recently documented in Atlantic records by Ruddiman et al. (1989). In a statistical approach, Maasch (1988) examined many paleoclimatic records of the mid-Pleistocene transition and concluded that the transition was abrupt, and that it indicated an increase in global ice volume and a global SST cooling. Other studies (Ruddiman et al., 1986a, 1986b, 1989) suggest that the transition was gradual rather than abrupt. The cause of this climatic shift remains unknown.

This mid-Pleistocene shift in dominance of climatic variance has not previously been reported in records from the Indian Ocean. The shift is clearly observed in not only the $\delta^{18}O$ record from Site 758, but also in the $CaCO_3$ and MS records. The early Pleistocene record is characterized by higher wt% $CaCO_3$ (Fig. 8) and $CaCO_3$ MAR (Fig. 5), and lower MS (Fig. 8) and non-$CaCO_3$ MAR (Fig. 5), than in the late Pleistocene. The 40-k.y. rhythm, that of orbital obliquity, has been observed as the primary climatic rhythm of the early Pleistocene and the late Pliocene over much of the global ocean, and now the low-latitude Indian Ocean as well. Detailed age model construction and time-series analysis of these records will allow a more precise description of the timing, cyclicity, and phasing across this climatic shift.

CONCLUSIONS

1. Site 758 provides detailed, continuous records of planktonic foraminifer $\delta^{13}C$, $\delta^{18}O$, wt% $CaCO_3$, wt% coarse fraction, MS, and geomagnetic reversals for the Plio-Pleistocene.

2. The MS stratigraphy from Site 758 is extremely useful for correlating between holes, identifying recovery gaps, locating ash layers, and constructing a continuous composite depth section.

3. Despite core recovery in excess of 100%, about 12% of the late Neogene sedimentary sequence was not recovered in each of the two holes at Site 758. As much as 2.7 m of sediment was lost at nearly every core break. If Site 758 had not been cored twice and logged for magnetic susceptibility, the missing sediment would have been very difficult to identify. By splicing between the two holes, a continuous composite depth section was constructed for the uppermost 116 mbsf at Site 758, which spans from 0.0 to 7.3 Ma.

4. Identification of $\delta^{18}O$ stages 1 through 105 provides a high-resolution age model, permits detailed correlation to other ODP sites, and attests to the completeness of the sedimentary record at Site 758. The $\delta^{18}O$ record shows (1) the glacial stages associated with the initiation of significant Northern Hemisphere; (2) the mid-Pleistocene transition (between $\delta^{18}O$ stages 25 and 22) in variance dominance from ~40 k.y. in the late Pliocene and early Pleistocene to ~100 k.y. in the late Pleistocene; and (3) the standard sequence of 19 high-amplitude $\delta^{18}O$ stages in the Brunhes Chron. At Site 758, the relative ^{18}O enrichment of the glacial stages between 2.4 Ma and 2.3 Ma is not as great as the relative enrichment seen in benthic records from the North Atlantic (Shackleton et al., 1984; Raymo et al., 1989).

5. Preliminary interpretation of the sedimentary records suggests that (1) long-term variations in the $CaCO_3$ and MS are primarily controlled by terrigenous dilution and $CaCO_3$ productivity; (2) the long-term increase in non-$CaCO_3$ (terrigenous) accumulation is attributed to greater riverine input through complex tectonic and climatic factors such as increased rates of uplift of the Himalayas and intensification of the orogenic monsoonal rains; (3) the monotonic increase in wt% coarse fraction since 5 Ma represents a gradual increase in $CaCO_3$ preservation; (4) the mid-Pleistocene shift toward lower wt% $CaCO_3$ and higher MS coincides with the shift in $\delta^{18}O$ variability, supporting the contention that the climate and ocean systems underwent a fundamental change at that time; and (5) during the late Pleistocene, $CaCO_3$ dissolution increased during interglacials and decreased during interglacials. This ~100-k.y. pattern is superimposed on the Brunhes dissolution cycle which extends from ~700 to ~10 Ka.

6. Tephra layers occur throughout the Plio-Pleistocene and record the volcanic history of the Indonesian arc. These layers are useful lithostratigraphic and potentially chronostratigraphic markers.

ACKNOWLEDGMENTS

The authors are most grateful to Jiajie Chen, Min-Te Chen, Bob Fifer, Wei Kang, Karen Kohfeld, April Martin, Tulshi Saha, and Jack S. Vietas for their hard work and expert technical assistance, without which this study would have been impossible. We thank Jeffrey Gee, David Murray, and Maureen Raymo for useful comments and suggestions. The manuscript benefitted by thoughtful reviews from James Cullen, Larry Peterson, and Elliot Taylor. This work was supported by grants from JOI/USSAC (TAMRF-20244) and NSF/OCE 8911874 (D. W. Murray and J. W. Farrell).

REFERENCES

Adelseck, C. G., Jr., 1977. Recent and late Pleistocene sediments from the eastern equatorial Pacific Ocean: sedimentation and dissolution [Ph.D. dissert.]. Univ. of California, San Diego.

Alexandrovich, J. M., and Hays, J. D., 1989. High-resolution stratigraphic correlation of ODP Leg 111 Holes 677A and 677B and DSDP Leg 69 Hole 504. *In* Becker, K., Sakai, H., et al., *Proc. ODP, Sci. Results,* 111: College Station, TX (Ocean Drilling Program), 263–276.

Backman, J., 1979. Pliocene biostratigraphy of DSDP Sites 111 and 116 from the North Atlantic Ocean and the age of the Northern Hemisphere Glaciation. *Stockholm Contrib. Geol.*, 32:115–137.

Berger, W. H., 1970. Planktonic foraminifera: selective solution and the lysocline. *Mar. Geol.*, 8:111–138.

Berger, W. H., Bonneau, M.-C., and Parker, F. L., 1982. Foraminifera on the deep-sea floor: lysocline and dissolution rate. *Oceanol. Acta,* 5:249–258.

Berger, W. H., Killingley, J. S., and Vincent, E., 1978. Stable isotopes in deep-sea carbonates: box core ERDC-92, west equatorial Pacific. *Oceanol. Acta,* 1:203–216.

Bouquillon, A., Chamley, H., and Fröhlich, F., 1989. Sédimentation argileuse au Cénozoïque supérieur dans l'Océan Indien nord-oriental. *Oceanol. Acta,* 12:133–147.

Craig, H., 1957. Isotopic standards for carbon and oxygen correction factors for mass spectrometric analysis of CO_2. *Geochim. Cosmochim. Acta,* 12:133–149.

Crowley, T. J., 1985. Late Quaternary carbonate changes in the North Atlantic, and Atlantic-Pacific comparisons. *In* Sundquist, E. T., and Broecker, W. S. (Eds.), *The Carbon Cycle and Atmospheric CO_2:*

Natural Variations, Archaen to Present. Am. Geophys. Union Monogr., 32:271–284.

Curray, J. R., Emmel, F. J., Moore, D. G., and Raitt, R. W., 1982. Structure, tectonics and geological history of the northeastern Indian Ocean. *In* Nairn, A.E.M., and Stehli, F. G. (Eds.), *The Ocean Basins and Margins* (Vol. 6): New York (Plenum), 399–450.

Curry, W. B., and Matthews, R. K., 1981. Equilibrium ^{18}O fractionation in small size fraction planktic foraminifera: evidence from Recent Indian Ocean sediments. *Mar. Micropaleontol.*, 6:327–337.

deMenocal, P., and Bloemendal, J., in press. Episodes in the late Neogene evolution of the Asian monsoon: evidence from Leg 117 magnetic susceptibility data. *In* Prell, W. L., Niitsuma, N., et al., *Proc. ODP, Sci. Results*, 117: College Station, TX (Ocean Drilling Program).

Emerson, S., and Bender, M., 1981. Carbon fluxes at the sediment-water interface of the deep-sea: calcium carbonate preservation. *J. Mar. Res.*, 39:139–162.

Farrell, J. W., and Prell, W. L., 1989. Climatic change and $CaCO_3$ preservation: an 800,000 year bathymetric reconstruction from the central equatorial Pacific Ocean. *Paleoceanography*, 4:447–466.

_______, in press. Pacific $CaCO_3$ preservation and $\delta^{18}O$ since 4 Ma: paleoceanic and paleoclimatic implications. *Paleoceanography*.

Imbrie, J., Hays, J. D., Martinson, D. G., McIntyre, A., Mix, A. C., Morley, J. J., Pisias, N. G., Prell, W. L., and Shackleton, N. J., 1984. The orbital theory of Pleistocene climate: support from a revised chronology of the marine delta $\delta^{18}O$ record. *In* Berger, A., Imbrie, J., Hays, J., Kukla, G., and Saltzman, B. (Eds.), *Milankovitch and Climate* (Pt. 1): Dordrecht (D. Reidel), 269–305.

Jansen, J.H.F., Kuijpers, A., and Troelstra, S. R., 1986. A mid-Brunhes climatic event: long-term changes in global atmospheric and ocean circulation. *Science*, 232:619–622.

Jones, G. A., and Kaiteris, P., 1983. A vacuum-gasometric technique for rapid and precise analysis of calcium carbonate in sediments and soils. *J. Sediment. Petrol.*, 53:655–660.

Kolla, V., Moore, D. G., and Curray, J. R., 1976. Recent bottom-current activity in the deep western Bay of Bengal. *Mar. Geol.*, 21:255–270.

Kuehl, S. A., Hariu, T. M., and Moore, W. S., 1989. Shelf sedimentation off the Ganges-Brahmaputra river system: evidence for sediment bypassing to the Bengal Fan. *Geology*, 17:1132–1135.

Maasch, K. A., 1988. Statistical detection of the mid-Pleistocene transition. *Clim. Dyn.*, 2:133–143.

McDougall, I., and Harrison, T. M., 1988. *Geochronology and Thermochronology by the* $^{40}Ar/^{39}Ar$ Method. Oxford Monogr. Geol. Geophys., 9.

Milliman, J. D., and Meade, R. H., 1983. World delivery of river sediment to the oceans. *J. Geol.*, 91:1–21.

Murray, D., and Prell, W. L., in press. Pliocene to Pleistocene variations in calcium carbonate, organic carbon, and opal on the Owen Ridge, Northern Arabian Sea. *In* Prell, W. L., Niitsuma, N., et al., *Proc. ODP, Sci. Results*, 117: College Station, TX (Ocean Drilling Program).

Peirce, J., Weissel, J., et al., 1989. *Proc. ODP, Init. Repts.*, 121: College Station, TX (Ocean Drilling Program).

Peterson, L. C., and Backman, J., 1990. Late Cenozoic carbonate accumulation and the history of the carbonate compensation depth in the western equatorial Indian Ocean. *In* Duncan, R. A., Backman, J., Peterson, L. C., et al., *Proc. ODP, Sci. Results*, 115: College Station, TX (Ocean Drilling Program), 467–507.

Peterson, L. C., and Prell, W. L., 1985a. Carbonate dissolution in Recent sediments of the eastern equatorial Indian Ocean: preservation patterns and carbonate loss above the lysocline. *Mar. Geol.*, 64:259–290.

_______, 1985b. Carbonate preservation and rates of climatic change: an 800 kyr record from the Indian Ocean. *In* Sundquist, E. T., and Broecker, W. S. (Eds.), *The Carbon Cycle and Atmospheric* CO_2: Natural Variations Archean to Present: Am. Geophys. Union Monogr., 32:251–270.

Pisias, N. G., and Moore, T. C., Jr., 1981. The evolution of Pleistocene climate: a time series approach. *Earth Planet. Sci. Lett.*, 52:450–456.

Prell, W. L., 1985. Pliocene stable isotope and carbonate stratigraphy (Holes 572C and 573A): paleoceanographic data bearing on the question of Pliocene glaciation. *In* Mayer, L., and Theyer, F., Thomas, E., *Init. Repts. DSDP*, 85: Washington (U.S. Govt. Printing Office), 723–734.

Prell, W. L., Imbrie, J., Martinson, D. G., Morley, J. J., Pisias, N. G., Shackleton, N. J., and Streeter, H. F., 1986. Graphic correlation of oxygen isotope stratigraphy application to the late Quaternary. *Paleoceanography*, 1:137–162.

Prell, W. L., Niitsuma, N., et al., 1989. *Proc. ODP, Init. Repts.*, 117: College Station, TX (Ocean Drilling Program).

Prospero, J. M., 1981. Arid regions as sources of mineral aerosols in the marine atmosphere. *In* Pewe, T. L. (Ed.), *Desert Dust: Origin, Characteristics, and Effects on Man:* Spec. Pap. Geol. Soc. Am., 186:71–86.

Raymo, M. E., Ruddiman, W. F., Backman, J., Clement, B. M., and Martinson, D. G., 1989. Late Pliocene variation in Northern Hemisphere ice sheets and North Atlantic deep water circulation. *Paleoceanography*, 4:413–446.

Raymo, M. E., Ruddiman, W. F., Froelich, P. N., 1988. Influence of late Cenozoic mountain building on ocean geochemical cycles. *Geology*, 16:649–653.

Robinson, S. G., 1990. Applications for whole-core magnetic susceptibility measurements of deep-sea sediments: Leg 115 results. *In* Duncan, R. A., Backman, J., Peterson, L. C., et al., *Proc. ODP, Sci. Results*, 115: College Station, TX (Ocean Drilling Program), 737–771.

Ruddiman, W. F., Cameron, D., and Clement, B. M., 1987. Sediment disturbance and correlation of offset holes drilled with the hydraulic piston corer: Leg 94. *In* Ruddiman, W. F., Kidd, R. B., Thomas, E., et al., *Init. Repts. DSDP*, 94 (Pt. 2): Washington (U.S. Govt. Printing Office), 615–634.

Ruddiman, W. F., Raymo, M. E., Martinson, D. G., Clement, B. M., and Backman, J., 1989. Pleistocene evolution: Northern Hemisphere ice sheets and North Atlantic Ocean. *Paleoceanography*, 4:353–412.

Ruddiman, W. F., Raymo, M. E., and McIntyre, A., 1986a. Matuyama 41,000-year cycles: North Atlantic and Northern Hemisphere ice sheets. *Earth Planet. Sci. Lett.*, 80:117–129.

Ruddiman, W. F., Shackleton, N. J., and McIntyre, A., 1986b. North Atlantic sea-surface temperatures for the last 1.1 million years. *In* Summerhays, C. P., and Shackleton, N. J. (Eds.), *North Atlantic Paleoceanography*. Geol. Soc. Am. Spec. Publ., 21:155–173.

Schmitz, B., 1987. The TiO_2/Al_2O_3 ratio in the Cenozoic Bengal Abyssal Fan sediments and its use as a paleostream energy indicator. *Mar. Geol.*, 76:195–206.

Shackleton, N. J., Backman, J., Zimmerman, H., Kent, D. V., Hall, M. A., Roberts, D. G., Schnitker, D., Baldauf, J., Desprairies, A., Homrighausen, R., Huddlestun, P., Keene, J. B., Kaltenback, A. J., Krumsiek, K.A.O., Morton, A. C., Murray, J. W., and Westberg-Smith, J., 1984. Oxygen isotope calibration of the onset of ice-rafting in DSDP Site 552A: history of glaciation in the North Atlantic region. *Nature*, 307:620–623.

Shackleton, N. J., Berger, A., and Peltier, W. R., in press. An alternative astronomical calibration of the Lower Pleistocene timescale based on ODP Site 677. *Trans. R. Soc. Edinburgh*.

Shackleton, N. J., and Hall, M. A., 1989. Stable isotope history of the Pleistocene at ODP Site 677. *In* Becker, K., Sakai, H., et al., *Proc. ODP, Sci. Results*, 111: College Station, TX (Ocean Drilling Program), 295–316.

_______, 1990. Pliocene oxygen isotope stratigraphy of Hole 709C. *In* Duncan, R. A., Backman, J., Peterson, L. C., et al., *Proc. ODP, Sci. Results*, 115: College Station, TX (Ocean Drilling Program), 529–538.

Shipboard Scientific Party, 1989. Site 758. *In* Peirce, J., Weissel, J., *Proc. ODP, Init. Repts.*, 121: College Station, TX (Ocean Drilling Program), 359–453.

Stow, D.A.V., Amano, K., Balson, P. S., Brass, G. W., Corrigan, J., Raman, C. V., Tiercelin, J.-J., Townsend, M., and Wijayananda, N. P., 1990. Sediment facies and processes on the Distal Bengal Fan, Leg 116. *In* Cochran, J. R., Stow, D.A.V., et al., *Proc. ODP, Sci. Results*, 116: College Station, TX (Ocean Drilling Program), 377–396.

Thompson, R., and Oldfield, F., 1986. *Environmental Magnetism:* London (Allen and Unwin).

Date of initial receipt: 7 March 1990
Date of acceptance: 19 November 1990
Ms 121B-124

APPENDIX A
Comparison of Wt% $CaCO_3$ Data Generated at Brown University and ODP Shipboard Laboratories

Core, section, interval (cm)	ODP depth (mbsf)	1st Brown Wt% $CaCO_3$ analysis	2nd Brown Wt% $CaCO_3$ analysis	3rd Brown Wt% $CaCO_3$ analysis	Wt% $CaCO_3$ half range[a]	Mean Brown Wt% $CaCO_3$	Shipboard Wt% $CaCO_3$	Shipboard-Brown $CaCO_3$ difference
121-								
758C-1H-1, 115–117	1.15	59.6	59.7		0.0	59.6	61.5	1.9
758C-1H-2, 45–47	1.95	63.9	62.9		0.5	63.4	64.2	0.8
758C-1H-2, 115–117	2.65	59.7	58.1		0.8	58.9	59.0	0.1
758B-1H-2, 128–130	2.78	60.1	59.1		0.5	59.6	59.6	0.0
758C-1H-3, 45–47	3.45	58.6	59.1		0.2	58.9	61.2	2.3
758C-1H-3, 115–117	4.15	56.3	57.4		0.6	56.8	57.3	0.5
758C-1H-4, 45–47	4.95	62.0	61.7		0.2	61.8	63.6	1.8
758C-1H-4, 115–117	5.65	50.5	50.5		0.0	50.5	52.2	1.7
758B-1H-4, 129–131	5.79	51.5	50.4		0.6	51.0	51.1	0.1
758C-1H-5, 45–47	6.45	61.7	62.0		0.2	61.8	62.6	0.8
758C-1H-5, 115–117	7.15	59.3	58.6		0.4	58.9	59.3	0.4
758C-1H-6, 45–47	7.95	61.8	61.8		0.0	61.8	63.8	2.0
758C-1H-6, 115–117	8.65	58.3	58.3		0.0	58.3	58.7	0.4
758B-1H-6, 130–132	8.80	52.7	52.3		0.2	52.5	51.9	−0.6
758B-2H-2, 90–92	11.90	64.4	63.5		0.5	63.9	64.4	0.5
758B-2H-5, 90–92	16.40	65.1	66.2	63.4	1.4	64.9	64.8	−0.1
758B-2H-7, 38–40	18.88	56.5	56.3		0.1	56.4	57.2	0.8
758B-3H-2, 125–127	21.65	59.3	58.5		0.4	58.9	60.6	1.7
758B-3H-4, 125–127	24.65	65.9	64.3	64.9	0.8	65.0	66.1	1.1
758B-3H-6, 125–127	27.65	68.9	67.5		0.7	68.2	68.3	0.1
758A-4H-3, 25–27	28.45	64.5	65.8		0.6	65.1	65.5	0.4
758B-4H-1, 125–127	29.65	65.3	66.0		0.4	65.6	68.4	2.8
758B-4H-3, 125–127	32.65	65.4	68.1		1.4	66.8	70.0	3.3
758B-4H-5, 125–127	35.65	68.1	67.5		0.3	67.8	69.2	1.4
758B-4H-7, 34–36	37.74	70.7	69.7		0.5	70.2	71.5	1.3
758B-5H-4, 125–127	43.75	60.4	57.9		1.2	59.2	59.8	0.6
758B-5H-7, 55–57	47.55	76.8	76.6		0.1	76.7	76.9	0.2
758B-6H-2, 125–127	50.45	73.8	70.4	74.9	2.2	73.0	73.1	0.1
758B-6H-4, 125–127	53.45	75.2	73.9		0.7	74.6	75.9	1.3
758B-6H-6, 125–127	56.45	68.3	67.6		0.4	67.9	69.7	1.8
758B-7H-1, 55–57	57.85	71.2	71.4		0.1	71.3	73.4	2.1
758B-7H-3, 55–57	60.85	79.2	79.4		0.1	79.3	80.6	1.3
758B-7H-5, 55–57	63.85	81.0	80.5		0.3	80.8	82.1	1.3
758B-7H-7, 55–57	66.85	73.5	71.2		1.2	72.4	73.2	0.8
758B-8H-4, 55–57	72.05	77.5	77.3		0.1	77.4	78.0	0.6
758B-8H-6, 55–57	75.05	75.9	75.1		0.4	75.5	77.5	2.0
758A-26R-4, 95–97	243.15	88.1	88.2		0.1	88.1	88.8	0.7
758A-27R-1, 95–97	248.25	87.2	87.4	88.1	0.4	87.6	89.7	2.1

[a] Half range is one-half of the range between the two (or three) wt% $CaCO_3$ analyses.

Note: Number of comparisons of Brown vs. shipboard data = 38.0; sum of the differences = 38.5; average difference = 1.0; sum of the absolute values of the differences = 41.8; average absolute difference = 1.1; average half range of Brown results = 0.5.

APPENDIX B
Wt% $CaCO_3$, Wt% Coarse Fraction, and Dry-Bulk Density Data From Hole 758A

Core, section, interval (cm)	ODP depth (mbsf)	Composite depth (m)	Mean wt% $CaCO_3$	Number of wt% $CaCO_3$ analyses	Coarse fraction (wt% >150 μm)	Dry-bulk density (g/cm^3)	Comment
121-758A-							
1H-1, 1	0.01	0.01	64.63	2	28.490	0.527	
1H-1, 11	0.11	0.11	61.67	2	19.327	0.542	
1H-1, 21	0.21	0.21	56.96	1	20.014	0.599	
1H-1, 31	0.31	0.31	58.88	1	21.678	0.656	
1H-1, 41	0.41	0.41	54.06	2	14.596	0.656	
1H-1, 51	0.51	0.51	56.75	1	16.124	0.613	
1H-1, 61	0.61	0.61	55.03	2	18.246	0.691	
1H-1, 71	0.71	0.71	55.51	1	17.971	0.656	
1H-1, 81	0.81	0.81	59.07	1	20.852	0.648	
1H-1, 91	0.91	0.91	60.25	1	15.847	0.741	
1H-1, 101	1.01	1.01	57.70	1	16.736	0.670	
1H-1, 111	1.11	1.11	59.68	1	17.727	0.691	
1H-1, 121	1.21	1.21	54.27	1	14.036	0.656	
1H-1, 131	1.31	1.31	45.48	1	9.268	0.670	
1H-1, 141	1.41	1.41	45.20	1	10.116	0.762	
1H-2, 1	1.51	1.51	35.73	2	8.883	0.787	Contains some ash A
1H-2, 11	1.61	1.61	3.64	1		0.997	Ash A, not processed
1H-2, 21	1.71	1.71	2.70	1		0.898	Ash A, not processed
1H-2, 31	1.81	1.81	4.21	1		0.819	Ash A, not processed
1H-2, 41	1.91	1.91	61.67	2	12.791	0.727	
1H-2, 51	2.01	2.01	9.53	1		0.969	Ash B, not processed
1H-2, 61	2.11	2.11	60.48	1	12.907	0.720	
1H-2, 71	2.21	2.21	57.76	1	12.602	0.755	
1H-2, 81	2.31	2.31	67.15	2	10.231	0.777	
1H-2, 91	2.41	2.41	58.98	1	12.290	0.769	
1H-2, 101	2.51	2.51	57.66	1	9.939	0.755	
1H-2, 111	2.61	2.61	57.40	1	8.271	0.769	
1H-2, 121	2.71	2.71	51.61	1	10.927	0.755	
1H-2, 131	2.81	2.81	50.19	1	14.889	0.705	
1H-2, 141	2.91	2.91	51.83	1	18.070	0.784	
1H-3, 1	3.01	3.01	56.24	1	16.867	0.798	
1H-3, 11	3.11	3.11	57.90	1	22.754	0.755	
1H-3, 21	3.21	3.21	49.60	2	17.814	0.698	
1H-3, 31	3.31	3.31	54.77	1	19.874	0.741	
1H-3, 41	3.41	3.41	54.65	1	15.589	0.784	
1H-3, 51	3.51	3.51	55.76	1	16.851	0.755	
1H-3, 61	3.61	3.61	57.95	1	15.990	0.755	
1H-3, 71	3.71	3.71	60.11	1	10.177	0.812	
1H-3, 81	3.81	3.81	62.37	1	12.147	0.805	
1H-3, 91	3.91	3.91	55.54	2	10.532	0.812	
1H-3, 101	4.01	4.01	65.38	1	12.006	0.812	
1H-3, 111	4.11	4.11	67.08	1	10.460	0.769	
1H-3, 121	4.21	4.21	62.28	1	15.656	0.741	
1H-3, 131	4.31	4.31	57.23	1	14.323	0.727	
1H-3, 141	4.41	4.41	59.30	1	12.016	0.855	
1H-4, 1	4.51	4.51	62.19	1	6.742	0.778	
1H-4, 11	4.61	4.61	60.07	1	11.220	0.741	
1H-4, 21	4.71	4.71	55.52	2	18.392	0.698	
1H-4, 31	4.81	4.81	53.02	1	14.643	0.734	
1H-4, 41	4.91	4.91	57.60	1	12.776	0.812	
1H-4, 51	5.01	5.01	59.01	1	14.115	0.769	
1H-4, 61	5.11	5.11	58.68	1	16.238	0.727	
1H-4, 71	5.21	5.21	50.51	1	9.136	0.755	
1H-4, 81	5.31	5.31	49.31	2	5.605	0.791	Tie point
1H-4, 91	5.41	5.41	55.80	1	6.603	0.777	Not in composite
1H-4, 101	5.51	5.51	57.46	1	5.842	0.798	Not in composite
1H-4, 111	5.61	5.61	62.56	1	7.326	0.741	Not in composite
1H-4, 121	5.71	5.71	70.52	1	5.925	0.798	Not in composite
1H-CC, 1	5.76	5.76	72.81	1	6.573	0.762	Not in composite
1H-CC, 11	5.86	5.86	65.63	1	5.956	0.869	Not in composite
1H-CC, 21	5.96	5.96	60.25	1	7.640	0.762	Not in composite
2H-1, 1	6.01	7.43	49.89	1	2.681	0.742	Tie point
2H-1, 11	6.11	7.53	54.57	1	2.569	0.712	
2H-1, 21	6.21	7.63	51.28	1	8.465	0.798	
2H-1, 31	6.31	7.73	53.41	1	10.174	0.727	
2H-1, 41	6.41	7.83	51.59	1	7.881	0.712	
2H-1, 51	6.51	7.93	51.08	1	5.835	0.784	
2H-1, 61	6.61	8.03	52.04	1	6.967	0.755	
2H-1, 71	6.71	8.13	55.71	2	5.630	0.755	
2H-1, 81	6.81	8.23	48.79	1	3.887	0.748	
2H-1, 91	6.91	8.33	51.48	1	3.505	0.798	
2H-1, 101	7.01	8.43	32.42	2	1.898	0.769	Contains some ash C
2H-1, 111	7.11	8.53	3.14	1		0.933	Ash C, not processed

Appendix B (continued).

Core, section, interval (cm)	ODP depth (mbsf)	Composite depth (m)	Mean wt% $CaCO_3$	Number of wt% $CaCO_3$ analyses	Coarse fraction (wt% >150 μm)	Dry-bulk density (g/cm^3)	Comment
121-758A-(Cont.)							
2H-1, 121	7.21	8.63	35.26	1	2.953	0.812	Contains some ash C
2H-1, 131	7.31	8.73	53.42	1	6.774	0.762	
2H-1, 141	7.41	8.83	52.51	1	9.529	0.741	
2H-2, 1	7.51	8.93	54.86	1	9.410	0.758	
2H-2, 11	7.61	9.03	59.60	1	15.516	0.777	
2H-2, 21	7.71	9.13	51.44	1	9.865	0.841	
2H-2, 31	7.81	9.23	49.19	1	6.935	0.848	
2H-2, 41	7.91	9.33	60.61	1	7.991	0.784	
2H-2, 51	8.01	9.43	56.24	1	6.643	0.769	
2H-2, 61	8.11	9.53	57.91	1	8.933	0.826	
2H-2, 71	8.21	9.63	67.88	2	13.080	0.812	
2H-2, 81	8.31	9.73	61.73	1	11.700	0.826	
2H-2, 91	8.41	9.83	58.28	3	10.518	0.826	
2H-2, 101	8.51	9.93	63.34	2	8.309	0.784	
2H-2, 111	8.61	10.03	54.08	1	14.109	0.741	
2H-2, 121	8.71	10.13	54.62	1	17.629	0.712	
2H-2, 131	8.81	10.23	53.74	1	7.561	0.698	
2H-2, 141	8.91	10.33	50.07	1	13.408	0.698	
2H-3, 1	9.01	10.43	53.13	1	11.690	0.912	
2H-3, 11	9.11	10.53	57.02	1	15.111	0.748	
2H-3, 21	9.21	10.63	54.25	1	7.865	0.784	
2H-3, 31	9.31	10.73	51.69	2	8.967	0.755	
2H-3, 41	9.41	10.83	58.59	1	9.857	0.769	
2H-3, 51	9.51	10.93	55.53	1	5.077	0.826	
2H-3, 61	9.61	11.03	59.60	1	11.636	0.798	
2H-3, 71	9.71	11.13	69.72	1	19.844	0.755	
2H-3, 81	9.81	11.23	63.74	1	19.167	0.791	
2H-3, 91	9.91	11.33	50.01	2	7.056	0.741	
2H-3, 101	10.01	11.43	58.20	1	9.176	0.784	
2H-3, 111	10.11	11.53	61.90	1	12.944	0.805	
2H-3, 121	10.21	11.63	66.30	1	21.381	0.769	
2H-3, 131	10.31	11.73	52.88	2	11.882	0.755	
2H-3, 141	10.41	11.83	59.71	1	10.765	0.826	
2H-4, 1	10.51	11.93	57.90	1	8.022	0.741	
2H-4, 11	10.61	12.03	56.20	1	8.549	0.791	
2H-4, 21	10.71	12.13	42.43	1	5.756	0.812	
2H-4, 31	10.81	12.23	12.65	2		0.947	Ash D, not processed
2H-4, 41	10.91	12.33	2.69	1		1.040	Ash D, not processed
2H-4, 51	11.01	12.43	55.97	1	15.166	0.712	
2H-4, 61	11.11	12.53	52.26	1	13.376	0.812	
2H-4, 71	11.21	12.63	54.71	1	8.628	0.812	
2H-4, 81	11.31	12.73	50.57	1	6.199	0.834	
2H-4, 91	11.41	12.83	57.42	1	6.474	0.798	
2H-4, 101	11.51	12.93	48.88	1	8.298	0.812	
2H-4, 111	11.61	13.03	33.50	2	4.757	0.898	Ash E, and below
2H-4, 121	11.71	13.13	69.94	1	13.087	0.769	
2H-4, 131	11.81	13.23	65.10	1	9.458	0.798	
2H-4, 141	11.91	13.33	64.57	1	7.719	0.826	
2H-5, 1	12.01	13.43	64.08	1	9.656	0.826	
2H-5, 11	12.11	13.53	50.80	1	12.409	0.777	
2H-5, 21	12.21	13.63	54.76	1	9.686	0.812	
2H-5, 31	12.31	13.73	53.35	1	11.021	0.777	
2H-5, 41	12.41	13.83	48.03	2	7.138	0.841	
2H-5, 51	12.51	13.93	57.91	1	7.452	0.812	
2H-5, 61	12.61	14.03	65.11	1	11.285	0.855	
2H-5, 71	12.71	14.13	58.50	1	10.577	0.869	
2H-5, 81	12.81	14.23	51.56	2	6.609	0.841	
2H-5, 91	12.91	14.33	60.93	1	8.581	0.826	
2H-5, 101	13.01	14.43	56.60	1	3.371	0.826	
2H-5, 111	13.11	14.53	58.94	1	5.053	0.855	
2H-5, 121	13.21	14.63	64.39	1	4.551	0.812	
2H-5, 131	13.31	14.73	57.31	2	4.909	0.812	
2H-6, 1	13.51	14.93	72.36	1	4.145	0.895	
2H-6, 11	13.61	15.03	71.49	1	5.664	0.862	
2H-6, 21	13.71	15.13	65.04	1	4.255	0.869	
2H-6, 31	13.81	15.23	66.38	1	8.798	0.841	
2H-6, 41	13.91	15.33	72.12	1	4.448	0.912	
2H-6, 51	14.01	15.43	71.05	1	5.747	0.883	
2H-6, 61	14.11	15.53	63.91	1	7.816	0.862	
2H-6, 71	14.21	15.63	57.59	2	7.265	0.855	
2H-6, 81	14.31	15.73	66.65	1	7.730	0.855	
2H-6, 91	14.41	15.83	65.58	1	8.011	0.826	
2H-6, 101	14.51	15.93	63.49	1	12.945	0.784	
2H-6, 111	14.61	16.03	65.05	1	14.782	0.848	
2H-6, 121	14.71	16.13	71.51	1	10.494	0.798	
2H-6, 131	14.81	16.23	73.04	2	11.451	0.777	

Appendix B (continued).

Core, section, interval (cm)	ODP depth (mbsf)	Composite depth (m)	Mean wt% $CaCO_3$	Number of wt% $CaCO_3$ analyses	Coarse fraction (wt% >150 μm)	Dry-bulk density (g/cm^3)	Comment
121-758A-(Cont.)							
2H-6, 141	14.91	16.33	71.40	1	13.660	0.841	
2H-7, 1	15.01	16.43	57.22	1	8.814	0.826	
2H-7, 11	15.11	16.53	57.32	1	7.395	0.869	
2H-7, 21	15.21	16.63	58.29	1	7.102	0.798	
2H-7, 31	15.31	16.73	57.56	1	8.536	0.755	
2H-7, 41	15.41	16.83	64.97	1	14.649	0.855	
2H-7, 51	15.51	16.93	61.43	1	11.457	0.762	
2H-7, 61	15.61	17.03	60.23	1	11.954	0.819	
2H-7, 71	15.71	17.13	63.41	1	13.135	0.784	
2H-CC, 1	15.78	17.20	65.96	1	13.015	0.812	Tie point
2H-CC, 11	15.88	17.30	64.03	1	16.730	0.755	Not in composite
3H-1, 1	15.61	17.52	59.84	1	10.873	0.801	Not in composite
3H-1, 11	15.71	17.62	57.95	1	8.407	0.791	Not in composite
3H-1, 21	15.81	17.72	62.43	1	8.132	0.812	Tie point
3H-1, 31	15.91	17.82	57.61	1	9.167	0.777	
3H-1, 41	16.01	17.92	62.07	1	13.105	0.755	
3H-1, 51	16.11	18.02	64.56	1	14.854	0.812	
3H-1, 61	16.21	18.12	55.09	2	15.889	0.769	
3H-1, 71	16.31	18.22	63.84	1	18.945	0.741	
3H-1, 81	16.41	18.32	64.24	1	18.133	0.784	
3H-1, 91	16.51	18.42	58.08	1	15.853	0.841	
3H-1, 101	16.61	18.52	59.86	1	14.462	0.798	
3H-1, 111	16.71	18.62	58.53	1	7.855	0.798	
3H-1, 121	16.81	18.72	60.29	1	10.664	0.812	
3H-1, 131	16.91	18.82	65.42	1	13.728	0.777	
3H-1, 141	17.01	18.92	58.57	1	17.459	0.734	
3H-2, 1	17.11	19.02	51.56	2	10.353	0.791	
3H-2, 11	17.21	19.12	53.66	1	10.969	0.805	
3H-2, 21	17.31	19.22	56.82	1	11.968	0.869	
3H-2, 31	17.41	19.32	59.69	1	10.236	0.805	
3H-2, 41	17.51	19.42	63.90	2	11.565	0.784	
3H-2, 51	17.61	19.52	61.54	1	14.292	0.777	
3H-2, 61	17.71	19.62	60.12	1	12.156	0.826	
3H-2, 71	17.81	19.72	58.51	1	16.052	0.784	
3H-2, 81	17.91	19.82	49.49	2	11.486	0.848	
3H-2, 91	18.01	19.92	61.82	1	7.191	0.812	
3H-2, 101	18.11	20.02	61.92	1	11.004	0.812	
3H-2, 111	18.21	20.12	65.22	1	14.720	0.755	
3H-2, 121	18.31	20.22	64.48	1	15.649	0.798	
3H-2, 131	18.41	20.32	62.36	1	12.694	0.798	
3H-2, 141	18.51	20.42	57.17	1	8.042	0.855	
3H-3, 1	18.61	20.52	60.22	1	5.817	0.838	
3H-3, 11	18.71	20.62	56.85	1	5.727	0.819	
3H-3, 21	18.81	20.72	60.19	1	9.112	0.841	
3H-3, 31	18.91	20.82	64.99	1	9.542	0.819	
3H-3, 41	19.01	20.92	66.84	1	8.814	0.784	
3H-3, 51	19.11	21.02	61.05	1	10.823	0.784	
3H-3, 61	19.21	21.12	60.66	1	6.243	0.762	
3H-3, 71	19.31	21.22	60.20	1	9.642	0.798	
3H-3, 81	19.41	21.32	63.63	1	8.903	0.812	
3H-3, 91	19.51	21.42	62.33	1	9.247	0.784	
3H-3, 101	19.61	21.52	59.22	1	8.881	0.784	
3H-3, 111	19.71	21.62	56.15	2	11.166	0.748	
3H-3, 121	19.81	21.72	31.20	2	5.636	0.784	Ash F, and below
3H-3, 131	19.91	21.82	56.60	1	10.162	0.841	
3H-3, 141	20.01	21.92	61.11	1	8.168	0.784	
3H-4, 1	20.11	22.02	58.22	1	9.052	0.855	
3H-4, 11	20.21	22.12	61.41	1	9.866	0.862	
3H-4, 21	20.31	22.22	67.38	2	10.318	0.798	
3H-4, 31	20.41	22.32	58.06	1	11.628	0.805	
3H-4, 41	20.51	22.42	55.77	1	14.556	0.755	
3H-4, 51	20.61	22.52	61.14	1	9.516	0.883	
3H-4, 61	20.71	22.62	57.12	1	9.412	0.812	
3H-4, 71	20.81	22.72	62.18	1	7.607	0.912	
3H-4, 81	20.91	22.82	63.64	1	8.588	0.855	
3H-4, 91	21.01	22.92	68.93	2	9.570	0.841	
3H-4, 101	21.11	23.02	61.21	2	12.225	0.826	
3H-4, 111	21.21	23.12	62.70	1	11.613	0.812	
3H-4, 121	21.31	23.22	64.15	1	10.671	0.798	
3H-4, 131	21.41	23.32	63.22	1	9.700	0.834	
3H-4, 141	21.51	23.42	59.85	1	11.969	0.826	
3H-5, 1	21.61	23.52	66.09	1	16.097	0.849	
3H-5, 11	21.71	23.62	65.05	1	14.716	0.805	
3H-5, 21	21.81	23.72	58.88	1	16.032	0.812	
3H-5, 31	21.91	23.82	60.36	1	11.579	0.841	
3H-5, 41	22.01	23.92	61.87	1	10.369	0.869	

Appendix B (continued).

Core, section, interval (cm)	ODP depth (mbsf)	Composite depth (m)	Mean wt% $CaCO_3$	Number of wt% $CaCO_3$ analyses	Coarse fraction (wt% >150 μm)	Dry-bulk density (g/cm^3)	Comment
121-758A-(Cont.)							
3H-5, 51	22.11	24.02	61.10	1	7.100	0.855	
3H-5, 61	22.21	24.12	65.16	1	8.382	0.841	
3H-5, 71	22.31	24.22	64.04	2	10.619	0.883	
3H-5, 81	22.41	24.32	61.29	1	12.019	0.855	
3H-5, 91	22.51	24.42	62.85	1	12.710	0.855	
3H-5, 101	22.61	24.52	63.81	1	9.366	0.841	
3H-5, 111	22.71	24.62	63.85	1	9.067	0.883	
3H-5, 121	22.81	24.72	62.62	1	9.143	0.798	
3H-6, 1	23.11	25.02	65.69	1	11.851	0.831	
3H-6, 11	23.21	25.12	64.11	1	8.301	0.869	
3H-6, 21	23.31	25.22	63.98	1	12.306	0.855	
3H-6, 31	23.41	25.32	58.15	2	12.394	0.876	
3H-6, 41	23.51	25.42	66.40	1	9.939	0.826	
3H-6, 51	23.61	25.52	63.71	1	11.069	0.841	
3H-6, 61	23.71	25.62	61.54	1	14.118	0.812	
3H-6, 71	23.81	25.72	59.44	1	9.514	0.841	
3H-6, 81	23.91	25.82	60.69	1	12.723	0.855	
3H-6, 91	24.01	25.92	62.78	1	12.494	0.855	
3H-6, 101	24.11	26.02	49.17	2	7.330	0.826	
3H-6, 111	24.21	26.12	59.04	1	8.027	0.869	
3H-6, 121	24.31	26.22	67.30	1	10.501	0.912	
3H-6, 131	24.41	26.32	67.68	1	12.400	0.755	
3H-6, 141	24.51	26.42	62.31	1	13.764	0.812	
3H-7, 1	24.61	26.52	61.32	1	13.582	0.834	
3H-7, 11	24.71	26.62	56.60	2	11.633	0.812	
3H-7, 21	24.81	26.72	61.51	1	11.557	0.862	
3H-7, 31	24.91	26.82	61.69	1	12.130	0.819	
3H-7, 41	25.01	26.92	66.43	1	14.065	0.784	
3H-7, 51	25.11	27.02	63.49	1	9.605	0.826	
3H-7, 61	25.21	27.12	64.24	2	8.732	0.912	Tie point
3H-CC, 1	25.31	27.22	62.13	1	8.226	0.798	Not in composite
3H-CC, 11	25.41	27.32	61.52	1	10.370	0.855	Not in composite
4H-1, 1	25.21	29.54	62.51	1	10.353	0.771	Tie point
4H-1, 11	25.31	29.64	58.52	1	10.476	0.784	
4H-1, 21	25.41	29.74	57.88	1	9.621	0.784	
4H-1, 31	25.51	29.84	59.82	1	8.324	0.784	
4H-1, 41	25.61	29.94	66.20	1	8.905	0.869	
4H-1, 51	25.71	30.04	68.42	1	11.262	0.940	
4H-1, 61	25.81	30.14	67.20	1	8.144	0.834	
4H-1, 71	25.91	30.24	59.82	1	11.326	0.912	
4H-1, 81	26.01	30.34	57.80	1	8.364	0.855	
4H-1, 91	26.11	30.44	59.81	1	8.209	0.855	
4H-1, 101	26.21	30.54	66.98	2	10.916	0.855	
4H-1, 111	26.31	30.64	62.89	1	8.229	0.898	
4H-1, 121	26.41	30.74	63.77	1	11.289	0.912	
4H-1, 131	26.51	30.84	68.64	2	7.444	0.890	
4H-1, 141	26.61	30.94	66.08	1	8.359	0.869	
4H-2, 1	26.71	31.04	66.19	1	12.015	0.865	
4H-2, 11	26.81	31.14	64.74	1	12.170	0.869	
4H-2, 21	26.91	31.24	65.11	1	9.880	0.855	
4H-2, 31	27.01	31.34	66.19	1	12.519	0.883	
4H-2, 41	27.11	31.44	67.37	1	12.197	0.841	
4H-2, 51	27.21	31.54	61.02	2	10.085	0.834	
4H-2, 61	27.31	31.64	63.82	1	13.876	0.898	
4H-2, 71	27.41	31.74	63.68	1	12.006	0.798	
4H-2, 81	27.51	31.84	63.62	1	7.564	0.855	
4H-2, 91	27.61	31.94	64.25	1	9.453	0.912	
4H-2, 101	27.71	32.04	63.60	1	7.651	0.869	
4H-2, 111	27.81	32.14	62.81	1	6.184	0.876	
4H-2, 121	27.91	32.24	62.10	1	8.353	0.855	
4H-2, 131	28.01	32.34	60.82	2	5.309	0.955	
4H-2, 141	28.11	32.44	63.39	1	10.953	0.883	
4H-3, 1	28.21	32.54	66.84	1	8.736	0.926	
4H-3, 11	28.31	32.64	68.26	2	8.669	0.898	
4H-3, 21	28.41	32.74	64.84	1	8.522	0.912	
4H-3, 31	28.51	32.84	65.47	1	11.088	0.969	
4H-3, 41	28.61	32.94	68.96	1	9.796	0.883	
4H-3, 51	28.71	33.04	71.76	1	8.105	0.926	
4H-3, 61	28.81	33.14	71.24	1	10.873	0.890	
4H-3, 71	28.91	33.24	71.02	1	7.490	0.912	
4H-3, 81	29.01	33.34	70.38	1	9.296	0.926	
4H-3, 91	29.11	33.44	69.93	1	7.114	0.940	
4H-3, 101	29.21	33.54	62.53	2	5.117	0.926	
4H-3, 111	29.31	33.64	65.27	1	8.857	0.905	
4H-3, 121	29.41	33.74	67.12	1	6.407	0.926	
4H-3, 131	29.51	33.84	68.03	1	8.451	0.883	

Appendix B (continued).

Core, section, interval (cm)	ODP depth (mbsf)	Composite depth (m)	Mean wt% $CaCO_3$	Number of wt% $CaCO_3$ analyses	Coarse fraction (wt% > 150 μm)	Dry-bulk density (g/cm^3)	Comment
121-758A-(Cont.)							
4H-3, 141	29.61	33.94	70.92	1	9.727	0.983	
4H-4, 1	29.71	34.04	69.07	1	4.620	1.016	
4H-4, 11	29.81	34.14	67.63	1	7.040	0.933	
4H-4, 21	29.91	34.24	69.54	1	10.113	0.912	
4H-4, 31	30.01	34.34	65.05	1	8.784	0.841	
4H-4, 41	30.11	34.44	61.45	2	10.114	0.898	
4H-4, 51	30.21	34.54	63.42	1	5.589	0.983	
4H-4, 61	30.31	34.64	61.75	1	5.144	0.933	
4H-4, 71	30.41	34.74	59.18	1	4.847	0.940	
4H-4, 81	30.51	34.84	58.94	1	6.861	0.955	
4H-4, 91	30.61	34.94	68.12	1	7.750	0.955	
4H-4, 101	30.71	35.04	67.23	1	4.767	0.969	
4H-4, 111	30.81	35.14	67.03	1	5.869	0.933	
4H-4, 121	30.91	35.24	65.68	1	6.389	0.940	
4H-4, 131	31.01	35.34	67.01	1	6.911	0.905	
4H-4, 141	31.11	35.44	57.04	2	7.291	0.912	Ash H, and below
4H-5, 07	31.27	35.60	61.74	2	5.934	0.969	
4H-5, 11	31.31	35.64	56.65	2	4.087	0.962	
4H-5, 21	31.41	35.74	67.51	2	6.539	0.912	
4H-5, 31	31.51	35.84	67.66	1	6.177	0.926	
4H-5, 41	31.61	35.94	70.18	1	6.402	0.955	
4H-5, 51	31.71	36.04	72.06	1	10.875	0.926	
4H-5, 61	31.81	36.14	75.28	1	14.403	0.898	
4H-5, 71	31.91	36.24	70.74	1	15.027	0.869	
4H-5, 81	32.01	36.34	70.82	1	13.918	0.947	
4H-5, 91	32.11	36.44	71.96	1	12.894	0.912	
4H-5, 101	32.21	36.54	69.39	1	11.762	0.883	
4H-5, 111	32.31	36.64	67.54	1	10.241	0.912	
4H-5, 121	32.41	36.74	71.91	1	11.229	0.812	
4H-5, 131	32.51	36.84	74.68	1	14.764	0.890	
4H-5, 141	32.61	36.94	71.04	1	15.535	0.826	
4H-6, 1	32.71	37.04	64.54	1	13.917	0.876	
4H-6, 11	32.81	37.14	65.13	1	8.481	0.905	
4H-6, 21	32.91	37.24	64.24	1	9.937	0.940	
4H-6, 31	33.01	37.34	67.08	1	14.217	0.834	
4H-6, 41	33.11	37.44	65.60	1	12.584	0.869	
4H-6, 51	33.21	37.54	63.69	1	12.344	0.883	
4H-6, 61	33.31	37.64	60.45	1	9.122	0.905	
4H-6, 71	33.41	37.74	59.99	1	6.976	0.969	
4H-6, 81	33.51	37.84	59.48	1	2.409	0.955	
4H-6, 91	33.61	37.94	60.41	1	5.816	0.912	
4H-6, 101	33.71	38.04	64.54	2	5.239	0.883	
4H-6, 111	33.81	38.14	60.71	2	3.261	0.940	
4H-6, 121	33.91	38.24	66.59	1	4.467	0.940	
4H-6, 131	34.01	38.34	67.24	1	4.598	0.919	
4H-6, 141	34.11	38.44	66.84	1	9.985	0.869	
4H-7, 1	34.21	38.54	69.73	1	12.744	0.898	
4H-7, 11	34.31	38.64	68.39	1	9.076	0.940	
4H-7, 21	34.41	38.74	61.47	2	2.294	0.955	
4H-7, 31	34.51	38.84	68.01	1	4.518	0.912	
4H-7, 41	34.61	38.94	67.28	1	5.331	0.898	
4H-7, 51	34.71	39.04	67.72	1	5.831	0.940	
4H-7, 61	34.81	39.14	64.80	2	8.263	0.912	
4H-7, 71	34.91	39.24	68.05	1	4.964	0.997	Tie point
4H-CC, 1	34.97	39.30	66.39	1	2.195	0.969	Not in composite
4H-CC, 11	35.07	39.40	60.83	2	2.278	0.869	Not in composite
4H-CC, 20	35.16	39.49	66.10	1	4.762	0.841	Not in composite
5H-1, 1	34.81	39.96	67.90	1	5.312	0.883	Not in composite
5H-1, 11	34.91	40.06	70.57	1	6.824	0.883	Not in composite
5H-1, 21	35.01	40.16	71.26	2	9.647	0.898	Tie point
5H-1, 31	35.11	40.26	66.28	1	5.765	0.890	
5H-1, 41	35.21	40.36	68.42	1	5.202	0.912	
5H-1, 51	35.31	40.46	71.88	1	4.596	0.926	
5H-1, 61	35.41	40.56	70.53	1	5.619	0.933	
5H-1, 71	35.51	40.66	70.13	1	6.270	0.940	
5H-1, 81	35.61	40.76	72.51	1	7.880	0.940	
5H-1, 91	35.71	40.86	68.43	1	5.121	0.784	
5H-1, 101	35.81	40.96	68.20	1	4.469	0.898	
5H-1, 111	35.91	41.06	71.99	2	6.715	0.890	
5H-1, 121	36.01	41.16	69.32	1	8.116	0.883	
5H-1, 131	36.11	41.26	71.25	1	7.850	0.848	
5H-1, 141	36.21	41.36	69.99	1	5.979	0.869	
5H-2, 1	36.31	41.46	70.82	1	6.299	0.841	
5H-2, 11	36.41	41.56	69.58	1	4.738	0.912	
5H-2, 21	36.51	41.66	67.60	2	5.415	0.898	

Appendix B (continued).

Core, section, interval (cm)	ODP depth (mbsf)	Composite depth (m)	Mean wt% $CaCO_3$	Number of wt% $CaCO_3$ analyses	Coarse fraction (wt% >150 μm)	Dry-bulk density (g/cm^3)	Comment
121-758A-(Cont.)							
5H-2, 31	36.61	41.76	67.44	1	6.527	0.898	
5H-2, 41	36.71	41.86	66.33	1	5.222	0.926	
5H-2, 51	36.81	41.96	67.86	1	3.945	0.883	
5H-2, 61	36.91	42.06	63.67	1	5.505	0.855	
5H-2, 71	37.01	42.16	56.05	2	4.663	0.855	
5H-2, 81	37.11	42.26	64.13	1	5.423	0.834	
5H-2, 91	37.21	42.36	64.11	1	4.561	0.869	
5H-2, 101	37.31	42.46	63.93	1	6.571	0.855	
5H-2, 111	37.41	42.56	63.30	1	4.836	0.890	
5H-2, 121	37.51	42.66	65.71	1	5.696	0.826	
5H-2, 131	37.61	42.76	67.55	1	9.086	0.862	
5H-2, 141	37.71	42.86	65.96	1	5.669	0.855	
5H-3, 1	37.81	42.96	67.83	1	7.731	0.848	
5H-3, 11	37.91	43.06	65.51	1	4.031	0.898	
5H-3, 21	38.01	43.16	62.09	1	2.912	0.912	
5H-3, 31	38.11	43.26	66.01	1	8.278	0.898	
5H-3, 41	38.21	43.36	68.02	1	7.444	0.855	
5H-3, 51	38.31	43.46	64.79	2	7.443	0.883	
5H-3, 61	38.41	43.56	68.93	1	6.590	0.919	
5H-3, 71	38.51	43.66	66.86	1	7.276	0.869	
5H-3, 81	38.61	43.76	65.95	1	5.372	0.883	
5H-3, 91	38.71	43.86	61.91	1	6.983	0.855	
5H-3, 101	38.81	43.96	61.81	1	10.860	0.869	
5H-3, 111	38.91	44.06	70.72	1	9.336	0.848	
5H-3, 121	39.01	44.16	69.31	1	9.030	0.869	
5H-3, 131	39.11	44.26	68.33	1	4.815	0.898	
5H-3, 141	39.21	44.36	67.73	1	4.681	0.898	
5H-4, 1	39.31	44.46	67.75	1	3.893	0.912	
5H-4, 11	39.41	44.56	66.85	1	3.667	0.933	
5H-4, 21	39.51	44.66	66.59	1	4.766	0.855	
5H-4, 31	39.61	44.76	63.97	2	1.885	0.912	
5H-4, 41	39.71	44.86	68.06	1	3.710	0.883	
5H-4, 51	39.81	44.96	70.89	1	3.027	0.955	
5H-4, 61	39.91	45.06	71.42	1	3.933	0.905	
5H-4, 71	40.01	45.16	72.22	1	5.704	0.940	
5H-4, 81	40.11	45.26	69.90	1	9.530	0.926	
5H-4, 91	40.21	45.36	72.28	1	6.934	0.898	
5H-4, 101	40.31	45.46	72.16	1	8.059	0.898	
5H-4, 111	40.41	45.56	73.17	1	9.514	0.841	
5H-4, 121	40.51	45.66	74.92	1	10.683	0.841	
5H-4, 131	40.61	45.76	70.46	2	8.589	0.869	
5H-4, 141	40.71	45.86	71.56	2	9.712	0.926	
5H-5, 1	40.81	45.96	68.93	1	7.876	0.983	
5H-5, 11	40.91	46.06	66.28	1	4.453	0.902	
5H-5, 21	41.01	46.16	65.96	1	4.609	0.926	
5H-5, 31	41.11	46.26	70.61	2	7.204	0.883	
5H-5, 41	41.21	46.36	66.31	2	4.934	0.926	
5H-5, 51	41.31	46.46	66.44	1	5.766	0.898	
5H-5, 61	41.41	46.56	68.33	1	5.714	0.883	
5H-5, 71	41.51	46.66	64.60	1	6.763	0.926	
5H-5, 81	41.61	46.76	67.03	1	10.575	1.004	
5H-5, 91	41.71	46.86	64.66	1	5.631	0.855	
5H-5, 101	41.81	46.96	64.39	1	5.589	0.898	
5H-5, 111	41.91	47.06	63.21	1	4.505	0.883	
5H-5, 121	42.01	47.16	69.16	1	6.299	0.869	
5H-5, 131	42.11	47.26	69.96	1	8.550	0.862	
5H-6, 1	42.31	47.46	66.71	1	8.523	0.896	
5H-6, 11	42.41	47.56	69.16	1	10.651	0.905	
5H-6, 21	42.51	47.66	67.20	1	8.649	0.997	
5H-6, 31	42.61	47.76	62.96	1	6.699	0.933	
5H-6, 41	42.71	47.86	59.83	2	3.607	0.883	
5H-6, 51	42.81	47.96	63.57	1	2.318	1.097	
5H-6, 61	42.91	48.06	63.30	1	3.782	0.969	
5H-6, 71	43.01	48.16	63.69	2	4.773	0.883	
5H-6, 81	43.11	48.26	65.04	2	5.662	0.940	
5H-6, 91	43.21	48.36	62.77	1	4.850	0.940	
5H-6, 101	43.31	48.46	60.40	2	6.826	0.926	
5H-6, 111	43.41	48.56	62.46	1	6.085	0.912	
5H-6, 121	43.51	48.66	64.17	1	7.811	0.898	
5H-6, 131	43.61	48.76	64.98	1	6.031	0.883	
5H-6, 141	43.71	48.86	70.36	1	4.500	0.898	
5H-7, 1	43.81	48.96	68.75	1	5.970	0.919	
5H-7, 11	43.91	49.06	67.94	1	4.480	0.912	
5H-7, 21	44.01	49.16	63.94	1	3.805	0.869	
5H-7, 31	44.11	49.26	63.28	1	4.134	0.905	
5H-7, 41	44.21	49.36	63.88	1	5.431	0.869	

Appendix B (continued).

Core, section, interval (cm)	ODP depth (mbsf)	Composite depth (m)	Mean wt% $CaCO_3$	Number of wt% $CaCO_3$ analyses	Coarse fraction (wt% >150 μm)	Dry-bulk density (g/cm^3)	Comment
121-758A-(Cont.)							
5H-7, 51	44.31	49.46	56.38	2	4.467	0.862	Tie point
5H-7, 61	44.41	49.56	60.64	1	5.126	0.919	Not in composite
6H-1, 1	44.41	51.78	66.63	2	3.740	0.883	Not in composite
6H-1, 11	44.51	51.88	67.31	1	3.209	0.912	Not in composite
6H-1, 21	44.61	51.98	65.93	1	3.679	0.869	Not in composite
6H-1, 31	44.71	52.08	69.24	1	6.547	0.890	Tie point
6H-1, 41	44.81	52.18	64.19	1	4.523	0.869	
6H-1, 51	44.91	52.28	63.74	1	3.177	0.883	
6H-1, 61	45.01	52.38	64.19	2	3.998	0.919	
6H-1, 71	45.11	52.48	69.40	3	6.097	0.869	
6H-1, 81	45.21	52.58	74.29	2	11.665	0.848	
6H-1, 91	45.31	52.68	68.68	1	10.411	0.898	
6H-1, 101	45.41	52.78	70.50	1	9.563	0.855	
6H-1, 111	45.51	52.88	66.70	1	5.341	0.898	
6H-1, 121	45.61	52.98	66.23	1	3.108	1.068	
6H-1, 131	45.71	53.08	65.80	1	3.555	0.883	
6H-1, 141	45.81	53.18	68.25	1	4.735	0.940	
6H-2, 1	45.91	53.28	67.30	1	4.727	0.883	
6H-2, 11	46.01	53.38	65.22	1	3.246	0.834	
6H-2, 21	46.11	53.48	64.37	1	3.192	0.784	
6H-2, 31	46.21	53.58	65.06	1	3.452	0.784	
6H-2, 41	46.31	53.68	63.97	1	3.358	0.784	
6H-2, 51	46.41	53.78	66.74	1	3.345	0.784	
6H-2, 61	46.51	53.88	66.17	1	2.720	0.784	
6H-2, 71	46.61	53.98	65.48	1	3.020	0.841	
6H-2, 81	46.71	54.08	69.76	2	3.617	0.876	
6H-2, 91	46.81	54.18	72.10	2	5.474	0.912	
6H-2, 101	46.91	54.28	73.23	1	6.829	0.826	
6H-2, 111	47.01	54.38	70.68	1	6.745	0.834	
6H-2, 121	47.11	54.48	74.27	1	8.527	0.841	
6H-2, 131	47.21	54.58	68.85	1	4.415	0.883	
6H-2, 141	47.31	54.68	67.23	1	3.107	0.969	
6H-3, 1	47.41	54.78	76.34	2	11.005	0.834	
6H-3, 11	47.51	54.88	67.91	1	5.524	0.876	
6H-3, 21	47.61	54.98	71.13	1	5.428	0.940	
6H-3, 31	47.71	55.08	70.55	1	3.835	0.926	
6H-3, 41	47.81	55.18	70.98	1	4.178	0.912	
6H-3, 51	47.91	55.28	72.63	1	5.354	0.955	
6H-3, 61	48.01	55.38	73.93	1	5.530	0.862	
6H-3, 71	48.11	55.48	72.83	1	6.892	0.883	
6H-3, 81	48.21	55.58	75.88	1	7.318	0.905	
6H-3, 91	48.31	55.68	74.07	1	5.061	0.926	
6H-3, 101	48.41	55.78	71.96	1	5.047	0.898	
6H-3, 111	48.51	55.88	72.18	1	8.290	0.912	
6H-3, 121	48.61	55.98	71.68	1	7.264	0.940	
6H-3, 131	48.71	56.08	72.45	1	5.076	0.912	
6H-3, 141	48.81	56.18	74.14	1	5.838	0.912	
6H-4, 1	48.91	56.28	67.60	1	4.139	0.869	
6H-4, 11	49.01	56.38	69.34	1	4.705	0.933	
6H-4, 21	49.11	56.48	68.69	1	3.812	0.940	
6H-4, 31	49.21	56.58	66.87	1	5.250	0.947	
6H-4, 41	49.31	56.68	72.30	1	6.686	0.926	
6H-4, 51	49.41	56.78	73.36	1	10.886	1.012	
6H-4, 61	49.51	56.88	73.49	1	5.690	0.962	
6H-4, 71	49.61	56.98	69.43	1	7.249	0.940	
6H-4, 81	49.71	57.08	69.08	1	6.343	0.940	
6H-4, 91	49.81	57.18	67.22	1	4.578	1.026	
6H-4, 101	49.91	57.28	71.79	1	7.131	0.855	
6H-4, 111	50.01	57.38	75.31	1	9.163	0.983	
6H-4, 121	50.11	57.48	75.56	1	11.355	0.898	
6H-4, 131	50.21	57.58	73.78	1	11.620	0.883	
6H-4, 141	50.31	57.68	72.23	1	8.390	0.912	
6H-5, 1	50.41	57.78	70.10	1	7.391	1.004	
6H-5, 11	50.51	57.88	67.66	1	5.866	0.983	
6H-5, 21	50.61	57.98	70.70	1	7.322	0.841	
6H-5, 31	50.71	58.08	66.58	1	6.961	0.890	
6H-5, 41	50.81	58.18	67.10	1	5.730	0.855	
6H-5, 51	50.91	58.28	44.09	2	5.304	0.969	Ash blebs
6H-5, 61	51.01	58.38	67.55	1	8.307	0.905	
6H-5, 71	51.11	58.48	72.83	1	6.929	0.926	
6H-5, 81	51.21	58.58	70.21	1	6.639	0.919	
6H-5, 91	51.31	58.68	70.65	1	8.396	0.869	
6H-5, 101	51.41	58.78	71.80	1	6.339	0.898	
6H-5, 111	51.51	58.88	70.51	1	5.633	0.933	
6H-5, 121	51.61	58.98	69.46	1	4.857	0.940	
6H-6, 1	51.91	59.28	68.13	1	7.236	0.929	

Appendix B (continued).

Core, section, interval (cm)	ODP depth (mbsf)	Composite depth (m)	Mean wt% $CaCO_3$	Number of wt% $CaCO_3$ analyses	Coarse fraction (wt% >150 μm)	Dry-bulk density (g/cm^3)	Comment
121-758A-(Cont.)							
6H-6, 11	52.01	59.38	60.26	1	4.968	0.969	
6H-6, 21	52.11	59.48	61.28	1	3.252	0.926	
6H-6, 31	52.21	59.58	56.66	1	4.418	0.912	
6H-6, 41	52.31	59.68	57.25	1	3.851	0.926	
6H-6, 51	52.41	59.78	72.23	1	6.891	0.940	
6H-6, 61	52.51	59.88	71.35	1	7.765	0.919	
6H-6, 71	52.61	59.98	68.13	1	4.948	0.955	
6H-6, 81	52.71	60.08	68.62	1	5.100	0.883	
6H-6, 91	52.81	60.18	68.90	1	4.742	0.912	
6H-6, 101	52.91	60.28	67.26	1	5.010	0.826	
6H-6, 111	53.01	60.38	58.28	2	3.477	0.890	
6H-6, 121	53.11	60.48	63.56	1	4.600	0.997	
6H-6, 131	53.21	60.58	65.87	1	5.211	0.926	
6H-6, 141	53.31	60.68	55.85	2	4.934	0.969	
6H-7, 1	53.41	60.78	69.54	1	5.710	0.969	
6H-7, 11	53.51	60.88	72.81	1	6.613	0.826	
6H-7, 21	53.61	60.98	71.48	1	6.551	0.905	
6H-7, 31	53.71	61.08	73.40	1	7.072	0.912	
6H-7, 41	53.81	61.18	71.60	1	6.315	0.947	
6H-7, 51	53.91	61.28	70.96	1	5.706	0.926	
6H-7, 61	54.01	61.38	71.57	1	5.735	0.905	
6H-7, 71	54.11	61.48	25.13	2	2.365	0.940	Tie point
6H-CC, 1	54.13	61.50	67.37	1	5.844	0.926	Not in composite
6H-CC, 11	54.23	61.60	66.07	1	6.650	0.912	Not in composite
6H-CC, 21	54.33	61.70	69.08	1	8.585	0.940	Not in composite
7H-1, 1	54.01	63.20	69.11	1	5.378	0.829	Tie point
7H-1, 11	54.11	63.30	52.69	2	3.140	0.829	
7H-1, 21	54.21	63.40	58.65	2	2.436	0.855	
7H-1, 31	54.31	63.50	65.40	1	3.228	0.826	
7H-1, 41	54.41	63.60	69.83	1	4.670	0.940	
7H-1, 51	54.51	63.70	66.37	1	3.205	0.898	
7H-1, 61	54.61	63.80	57.42	2	2.363	0.883	
7H-1, 71	54.71	63.90	60.64	1	2.835	0.926	
7H-1, 81	54.81	64.00	69.60	1	3.222	0.876	
7H-1, 91	54.91	64.10	71.70	1	4.137	0.926	
7H-1, 101	55.01	64.20	72.09	1	5.140	0.926	
7H-1, 111	55.11	64.30	64.79	1	2.562	1.040	
7H-1, 121	55.21	64.40	61.63	1	2.573	1.111	
7H-1, 131	55.31	64.50	62.06	1	2.081	0.940	
7H-1, 141	55.41	64.60	71.98	1	2.989	0.912	
7H-2, 1	55.51	64.70	74.16	1	5.497	0.937	
7H-2, 11	55.61	64.80	74.24	1	4.878	0.883	
7H-2, 21	55.71	64.90	72.15	1	3.770	0.869	
7H-2, 31	55.81	65.00	69.64	1	2.296	0.933	
7H-2, 41	55.91	65.10	69.89	1	2.968	0.898	
7H-2, 51	56.01	65.20	72.35	1	4.521	0.883	
7H-2, 61	56.11	65.30	72.98	1	5.144	0.933	
7H-2, 71	56.21	65.40	73.27	1	4.012	0.955	
7H-2, 81	56.31	65.50	72.86	1	5.042	0.926	
7H-2, 91	56.41	65.60	71.05	1	3.650	0.912	
7H-2, 101	56.51	65.70	68.20	1	5.196	0.883	
7H-2, 111	56.61	65.80	69.60	1	4.559	0.926	
7H-2, 121	56.71	65.90	6.22	1		1.040	Ash I, not processed
7H-2, 131	56.81	66.00	73.65	1	3.507	0.862	
7H-2, 141	56.91	66.10	75.92	1	4.929	0.926	
7H-3, 1	57.01	66.20	75.79	1	4.238	0.890	
7H-3, 11	57.11	66.30	75.74	1	5.674	0.841	
7H-3, 21	57.21	66.40	74.35	1	6.073	0.926	
7H-3, 31	57.31	66.50	69.39	1	6.457	0.855	
7H-3, 41	57.41	66.60	47.57	2	6.662	0.812	
7H-3, 51	57.51	66.70	75.65	1	9.181	0.912	
7H-3, 61	57.61	66.80	72.38	1	4.137	0.926	
7H-3, 71	57.71	66.90	61.82	2	2.264	0.883	
7H-3, 81	57.81	67.00	73.25	1	4.174	0.855	
7H-3, 91	57.91	67.10	76.11	1	6.358	0.912	
7H-3, 101	58.01	67.20	76.53	1	7.307	0.883	
7H-3, 111	58.11	67.30	72.00	1	7.559	0.890	
7H-3, 121	58.21	67.40	71.76	1	6.846	0.869	
7H-3, 131	58.31	67.50	73.85	1	3.483	0.969	
7H-3, 141	58.41	67.60	69.36	1	4.288	0.962	
7H-4, 1	58.51	67.70	72.98	1	4.592	0.890	
7H-4, 11	58.61	67.80	78.75	1	6.374	0.862	
7H-4, 21	58.71	67.90	74.27	1	7.475	0.898	
7H-4, 31	58.81	68.00	64.11	1	5.427	0.962	
7H-4, 41	58.91	68.10	50.11	2	4.974	0.997	Ash
7H-4, 51	59.01	68.20	79.30	1	4.665	0.940	

Appendix B (continued).

Core, section, interval (cm)	ODP depth (mbsf)	Composite depth (m)	Mean wt% $CaCO_3$	Number of wt% $CaCO_3$ analyses	Coarse fraction (wt% >150 μm)	Dry-bulk density (g/cm^3)	Comment
121-758A-(Cont.)							
7H-4, 61	59.11	68.30	79.65	1	3.141	0.983	
7H-4, 71	59.21	68.40	77.34	1	1.399	0.926	
7H-4, 81	59.31	68.50	73.26	1	2.082	0.919	
7H-4, 91	59.41	68.60	76.42	1	3.613	0.926	
7H-4, 101	59.51	68.70	79.74	2	5.164	0.898	
7H-4, 111	59.61	68.80	76.51	1	4.051	0.912	
7H-4, 121	59.71	68.90	73.02	1	2.805	0.940	
7H-4, 131	59.81	69.00	71.29	1	2.337	0.890	
7H-4, 141	59.91	69.10	73.66	1	2.610	0.912	
7H-5, 1	60.01	69.20	73.42	1	2.688	0.983	
7H-5, 11	60.11	69.30	74.83	1	4.120	0.947	
7H-5, 21	60.21	69.40	77.45	1	3.731	0.969	
7H-5, 31	60.31	69.50	75.27	1	2.710	0.933	
7H-5, 41	60.41	69.60	71.48	1	1.346	0.898	
7H-5, 51	60.51	69.70	71.20	1	1.961	0.997	
7H-5, 61	60.61	69.80	69.91	1	2.550	0.997	
7H-5, 71	60.71	69.90	71.27	1	3.766	0.955	
7H-5, 81	60.81	70.00	76.81	1	4.667	0.898	
7H-5, 91	60.91	70.10	75.97	1	4.328	0.955	
7H-5, 101	61.01	70.20	77.33	1	4.284	0.926	
7H-5, 111	61.11	70.30	73.79	1	1.593	0.962	
7H-5, 121	61.21	70.40	76.57	1	1.970	0.983	
7H-5, 131	61.31	70.50	76.67	1	3.386	0.912	
7H-5, 141	61.41	70.60	77.77	1	4.044	0.898	
7H-6, 1	61.51	70.70	77.31	1	3.204	0.841	
7H-6, 11	61.61	70.80	78.03	1	2.957	0.955	
7H-6, 21	61.71	70.90	74.71	2	2.431	0.955	
7H-6, 31	61.81	71.00	79.61	1	3.729	0.962	
7H-6, 41	61.91	71.10	80.90	1	3.919	0.912	
7H-6, 51	62.01	71.20	80.33	1	4.234	0.983	
7H-6, 61	62.11	71.30	77.98	1	3.529	0.955	
7H-6, 71	62.21	71.40	76.94	1	2.171	0.926	
7H-6, 81	62.31	71.50	74.70	1	1.941	0.969	
7H-6, 91	62.41	71.60	75.90	1	2.315	1.026	
7H-6, 101	62.51	71.70	78.81	1	2.725	1.012	
7H-6, 111	62.61	71.80	79.75	1	3.445	0.926	
7H-6, 121	62.71	71.90	76.16	1	2.883	1.012	
7H-6, 131	62.81	72.00	77.65	1	2.804	0.983	
7H-6, 141	62.91	72.10	74.94	1	2.678	0.940	
7H-7, 1	63.01	72.20	73.28	1	2.615	0.990	
7H-7, 11	63.11	72.30	70.83	1	1.801	0.997	
7H-7, 21	63.21	72.40	77.00	1	2.601	1.012	
7H-7, 31	63.31	72.50	80.49	1	3.471	0.983	
7H-7, 41	63.41	72.60	75.99	1	2.204	0.955	
7H-7, 51	63.51	72.70	73.97	1	1.748	0.940	
7H-7, 61	63.61	72.80	74.46	1	2.784	0.969	Tie point
7H-CC, 1	63.73	72.92	61.84	2	1.909	0.926	Not in composite
7H-CC, 11	63.83	73.02	64.10	2	1.981	0.983	Not in composite
7H-CC, 21	63.93	73.12	77.17	1	2.668	0.955	Not in composite
8H-1, 1	63.71	74.02	75.51	2	3.011	0.858	Tie point
8H-1, 11	63.81	74.12	63.18	2	2.329	0.858	
8H-1, 21	63.91	74.22	71.97	1	2.039	0.912	
8H-1, 31	64.01	74.32	78.03	1	4.723	0.905	
8H-1, 41	64.11	74.42	79.85	1	5.524	0.940	
8H-1, 51	64.21	74.52	79.05	1	7.847	0.926	
8H-1, 61	64.31	74.62	76.80	1	6.373	0.940	
8H-1, 71	64.41	74.72	76.81	1	6.894	0.912	
8H-1, 81	64.51	74.82	79.36	1	5.937	0.976	
8H-1, 91	64.61	74.92	74.12	1	2.696	1.026	Ash K, and below
8H-1, 101	64.71	75.02	73.17	1	1.988	0.976	
8H-1, 111	64.81	75.12	76.04	1	2.578	0.969	
8H-1, 121	64.91	75.22	78.53	1	6.664	0.940	
8H-1, 131	65.01	75.32	77.14	1	6.331	0.905	
8H-1, 141	65.11	75.42	74.92	1	5.739	0.955	
8H-2, 1	65.21	75.52	74.67	1	4.134	0.993	
8H-2, 11	65.31	75.62	73.98	1	2.031	0.912	
8H-2, 21	65.41	75.72	75.87	1	3.431	0.969	
8H-2, 31	65.51	75.82	78.00	1	4.730	0.912	
8H-2, 41	65.61	75.92	76.77	1	4.551	0.926	
8H-2, 51	65.71	76.02	73.48	1	3.136	0.997	
8H-2, 61	65.81	76.12	77.51	1	3.302	0.955	
8H-2, 71	65.91	76.22	77.62	1	3.741	0.940	
8H-2, 81	66.01	76.32	73.45	1	4.187	0.955	
8H-2, 91	66.11	76.42	71.50	1	3.979	0.969	
8H-2, 101	66.21	76.52	71.13	1	2.988	0.997	
8H-2, 111	66.31	76.62	60.85	2	1.627	0.947	

Appendix B (continued).

Core, section, interval (cm)	ODP depth (mbsf)	Composite depth (m)	Mean wt% $CaCO_3$	Number of wt% $CaCO_3$ analyses	Coarse fraction (wt% > 150 μm)	Dry-bulk density (g/cm^3)	Comment
121-758A-(Cont.)							
8H-2, 121	66.41	76.72	66.56	1	2.432	0.969	Ash L, and below
8H-2, 131	66.51	76.82	73.28	2	4.745	0.962	
8H-2, 141	66.61	76.92	63.57	2	3.443	0.912	
8H-3, 1	66.71	77.02	65.87	1	2.613	0.955	
8H-3, 11	66.81	77.12	72.74	1	2.812	0.912	
8H-3, 21	66.91	77.22	74.10	1	4.312	0.898	
8H-3, 31	67.01	77.32	74.48	1	3.300	0.976	
8H-3, 41	67.11	77.42	72.02	1	3.195	0.940	
8H-3, 51	67.21	77.52	72.53	1	2.932	0.997	
8H-3, 61	67.31	77.62	74.25	1	4.522	0.940	
8H-3, 71	67.41	77.72	76.66	1	6.549	0.969	
8H-3, 81	67.51	77.82	74.54	1	5.056	0.940	
8H-3, 91	67.61	77.92	75.45	1	4.973	0.898	
8H-3, 101	67.71	78.02	75.27	1	4.293	0.940	
8H-3, 111	67.81	78.12	77.21	1	5.917	0.883	
8H-3, 121	67.91	78.22	79.40	1	7.664	0.940	
8H-3, 131	68.01	78.32	74.59	1	6.842	0.905	
8H-3, 141	68.11	78.42	69.72	1	3.727	0.841	
8H-4, 1	68.21	78.52	68.17	1	2.638	0.905	
8H-4, 11	68.31	78.62	69.03	1	3.478	0.926	
8H-4, 21	68.41	78.72	67.83	1	3.214	0.940	
8H-4, 31	68.51	78.82	71.19	1	3.814	0.933	
8H-4, 41	68.61	78.92	67.41	1	3.355	0.926	
8H-4, 51	68.71	79.02	72.49	1	3.737	0.997	
8H-4, 61	68.81	79.12	73.99	1	5.243	0.955	
8H-4, 71	68.91	79.22	75.15	1	4.460	0.969	
8H-4, 81	69.01	79.32	75.51	1	3.183	0.962	
8H-4, 91	69.11	79.42	71.07	1	1.958	1.012	
8H-4, 101	69.21	79.52	63.77	2	4.395	0.926	
8H-4, 111	69.31	79.62	72.55	1	4.194	0.912	
8H-4, 121	69.41	79.72	74.53	1	3.002	0.983	
8H-4, 131	69.51	79.82	72.34	1	2.795	0.905	
8H-4, 141	69.61	79.92	72.14	1	3.348	0.940	
8H-5, 1	69.71	80.02	73.30	1	2.964	0.940	
8H-5, 11	69.81	80.12	73.87	2	2.538	0.983	
8H-5, 21	69.91	80.22	72.12	1	3.021	0.955	
8H-5, 31	70.01	80.32	76.98	1	3.374	1.004	
8H-5, 41	70.11	80.42	77.08	1	4.008	0.940	
8H-5, 51	70.21	80.52	75.89	1	3.104	0.997	
8H-5, 61	70.31	80.62	75.89	1	2.834	1.026	
8H-5, 71	70.41	80.72	75.40	1	2.110	0.940	
8H-5, 81	70.51	80.82	77.10	1	3.478	0.905	
8H-5, 91	70.61	80.92	78.84	1	3.130	1.054	
8H-5, 101	70.71	81.02	76.22	1	2.458	0.983	
8H-5, 111	70.81	81.12	76.01	1	2.451	0.955	
8H-5, 121	70.91	81.22	71.69	2	1.056	0.955	
8H-5, 131	71.01	81.32	77.14	1	1.260	0.969	
8H-6, 1	71.21	81.52	81.12	1	2.128	0.919	
8H-6, 11	71.31	81.62	79.23	1	1.583	0.933	
8H-6, 21	71.41	81.72	77.67	1	0.968	0.983	
8H-6, 31	71.51	81.82	80.77	1	1.824	0.933	
8H-6, 41	71.61	81.92	77.64	1	1.836	0.926	
8H-6, 51	71.71	82.02	77.15	1	2.082	0.969	
8H-6, 61	71.81	82.12	79.25	1	1.705	0.997	
8H-6, 71	71.91	82.22	79.24	1	1.026	0.983	
8H-6, 81	72.01	82.32	79.19	1	0.995	0.990	
8H-6, 91	72.11	82.42	77.79	1	1.093	0.912	
8H-6, 101	72.21	82.52	73.92	1	0.933	0.955	
8H-6, 111	72.31	82.62	73.58	1	1.108	0.898	
8H-6, 121	72.41	82.72	69.21	1	1.209	0.969	
8H-6, 131	72.51	82.82	64.42	1	1.019	0.976	
8H-6, 141	72.61	82.92	37.42	3	0.794	1.012	Ash
8H-7, 1	72.71	83.02	71.23	1	1.977	0.933	
8H-7, 11	72.81	83.12	75.18	1	2.361	0.898	
8H-7, 21	72.91	83.22	72.41	1	2.311	0.919	
8H-7, 31	73.01	83.32	65.99	1	1.157	0.983	
8H-7, 41	73.11	83.42	64.57	1	1.629	0.919	Tie point
8H-7, 51	73.21	83.52	72.22	1	1.919	0.983	Not in composite
8H-7, 61	73.31	83.62	71.78	1	2.153	0.955	Not in composite
8H-8, 1	73.35	83.66	71.51	2	3.589	0.898	Not in composite
8H-8, 11	73.45	83.76	72.51	1	1.420	0.983	Not in composite
8H-8, 21	73.55	83.86	65.74	2	2.797	0.940	Not in composite

APPENDIX C
Wt% $CaCO_3$, Wt% Coarse Fraction, and Dry-Bulk Density Data From Hole 758B

Core, section, interval (cm)	ODP depth (mbsf)	Composite depth (m)	Mean wt% $CaCO_3$	Number of wt% $CaCO_3$ analyses	Coarse fraction (wt% >150 μm)	Dry-bulk density (g/cm^3)	Comment
121-758B-							
1H-3, 61	3.61	5.12	59.98	2	14.18	0.705	Not in composite
1H-3, 71	3.71	5.22	51.70	1	9.19	0.727	Not in composite
1H-3, 81	3.81	5.32	49.10	2	6.09	0.741	Tie point
1H-3, 91	3.91	5.42	53.90	2	4.70	0.841	
1H-3, 101	4.01	5.52	61.74	2	8.73	0.769	
1H-3, 111	4.11	5.62	59.60	2	5.07	0.712	
1H-3, 121	4.21	5.72	66.99	1	9.09	0.812	
1H-3, 131	4.31	5.82	73.88	2	5.76	0.819	
1H-3, 141	4.41	5.92	68.69	1	6.66	0.855	
1H-4, 1	4.51	6.02	60.63	2	4.41	0.791	
1H-4, 11	4.61	6.12	62.54	1	5.48	0.812	
1H-4, 21	4.71	6.22	71.18	2	4.90	0.841	
1H-4, 31	4.81	6.32	65.70	1	8.33	0.762	
1H-4, 41	4.91	6.42	55.04	1	11.35	0.755	
1H-4, 51	5.01	6.52	56.28	1	13.08	0.755	
1H-4, 61	5.11	6.62	57.75	1	11.24	0.798	
1H-4, 71	5.21	6.72	57.88	1	10.22	0.812	
1H-4, 81	5.31	6.82	53.87	2	7.49	0.741	
1H-4, 91	5.41	6.92	55.63	1	7.00	0.784	
1H-4, 101	5.51	7.02	57.83	1	6.09	0.784	
1H-4, 111	5.61	7.12	57.61	1	6.36	0.748	
1H-4, 121	5.71	7.22	56.79	1	6.35	0.798	
1H-4, 131	5.81	7.32	52.04	1	2.49	0.805	
1H-4, 141	5.91	7.42	53.18	1	2.82	0.841	Tie point
1H-5, 1	6.01	7.52	55.82	1	10.87	0.758	Not in composite
1H-5, 11	6.11	7.62	50.21	2	7.41	0.698	Not in composite
1H-5, 21	6.21	7.72	51.78	1	8.47	0.769	Not in composite
1H-5, 31	6.31	7.82	54.67	1	9.65	0.784	Not in composite
1H-5, 41	6.41	7.92	53.42	1	7.65	0.784	Not in composite
1H-5, 51	6.51	8.02	56.09	1	8.03	0.769	Not in composite
1H-5, 61	6.61	8.12	54.46	1	5.87	0.784	Not in composite
2H-5, 1	15.51	17.01	53.00	2	10.20	0.762	Not in composite
2H-5, 11	15.61	17.11	61.11	2	14.08	0.819	Not in composite
2H-5, 21	15.71	17.21	63.96	1	13.63	0.784	Tie point
2H-5, 31	15.81	17.31	67.40	1	18.57	0.805	
2H-5, 41	15.91	17.41	54.76	1	13.03	0.798	
2H-5, 51	16.01	17.51	59.97	2	12.42	0.784	
2H-5, 61	16.11	17.61	57.46	1	9.49	0.841	
2H-5, 71	16.21	17.71	65.09	1	9.45	0.798	Tie point
2H-5, 81	16.31	17.81	61.51	2	12.01	0.769	Not in composite
3H-3, 111	23.01	26.83	63.39	1	12.13	0.855	Not in composite
3H-3, 121	23.11	26.93	63.78	1	13.68	0.826	Not in composite
3H-3, 131	23.21	27.03	65.99	1	14.15	0.812	Not in composite
3H-3, 141	23.31	27.13	64.63	1	9.11	0.841	Tie point
3H-4, 1	23.41	27.23	61.54	1	10.60	0.912	
3H-4, 11	23.51	27.33	60.24	1	13.16	0.819	
3H-4, 21	23.61	27.43	59.22	1	8.06	0.855	
3H-4, 31	23.71	27.53	60.81	1	7.84	0.784	
3H-4, 41	23.81	27.63	53.93	1	6.12	0.826	
3H-4, 51	23.91	27.73	55.08	1	8.49	0.812	Ash G, and below
3H-4, 73	24.13	27.95	66.21	1	8.75	0.841	
3H-4, 81	24.21	28.03	62.79	1	10.73	0.883	
3H-4, 91	24.31	28.13	62.44	1	10.44	0.912	
3H-4, 101	24.41	28.23	64.18	1	14.27	0.812	
3H-4, 111	24.51	28.33	61.37	1	10.88	0.841	
3H-4, 121	24.61	28.43	65.67	1	8.76	0.955	
3H-4, 131	24.71	28.53	60.71	1	6.21	0.869	
3H-4, 141	24.81	28.63	64.96	1	9.25	0.926	
3H-5, 1	24.91	28.73	61.92	1	10.04	0.872	
3H-5, 11	25.01	28.83	57.02	1	6.95	0.883	
3H-5, 21	25.11	28.93	58.70	1	6.62	0.898	
3H-5, 31	25.21	29.03	59.82	1	7.99	0.905	
3H-5, 41	25.31	29.13	59.51	1	6.21	0.869	
3H-5, 51	25.41	29.23	56.86	1	6.29	0.869	
3H-5, 61	25.51	29.33	57.48	1	10.50	0.841	
3H-5, 71	25.61	29.43	60.25	1	11.55	0.841	
3H-5, 81	25.71	29.53	62.31	1	13.46	0.855	Tie point
3H-5, 91	25.81	29.63	60.62	1	11.99	0.883	Not in composite
3H-5, 101	25.91	29.73	62.47	1	12.42	0.883	Not in composite
3H-5, 111	26.01	29.83	66.04	1	12.06	0.912	Not in composite
4H-5, 71	35.11	38.95	66.59	1	5.32	0.883	Not in composite
4H-5, 81	35.21	39.05	69.99	2	6.58	0.940	Not in composite
4H-5, 91	35.31	39.15	64.76	1	5.48	0.912	Not in composite
4H-5, 101	35.41	39.25	64.06	2	5.30	0.940	Tie point
4H-5, 111	35.51	39.35	61.53	1	2.52	0.969	

Appendix C (continued).

Core, section, interval (cm)	ODP depth (mbsf)	Composite depth (m)	Mean wt% $CaCO_3$	Number of wt% $CaCO_3$ analyses	Coarse fraction (wt% >150 μm)	Dry-bulk density (g/cm^3)	Comment
121-758B-(Cont.)							
4H-5, 121	35.61	39.45	61.04	1	3.73	0.869	
4H-5, 131	35.71	39.55	67.95	1	5.40	0.869	
4H-5, 141	35.81	39.65	64.71	1	5.56	0.898	
4H-6, 1	35.91	39.75	68.03	1	8.28	0.876	
4H-6, 11	36.01	39.85	66.15	1	5.31	0.926	
4H-6, 21	36.11	39.95	67.84	1	4.34	0.969	
4H-6, 31	36.21	40.05	71.13	1	8.40	0.947	
4H-6, 41	36.31	40.15	70.62	1	8.83	0.883	Tie point
5H-4, 111	43.61	49.27	63.35	2	4.273	0.905	Not in composite
5H-4, 121	43.71	49.37	62.33	1	3.603	0.869	Not in composite
5H-4, 131	43.81	49.47	55.90	1	3.072	0.862	Tie point
5H-4, 141	43.91	49.57	62.48	1	4.078	0.919	
5H-5, 1	44.01	49.67	64.95	1	3.723	0.940	
5H-5, 11	44.11	49.77	64.87	1	4.110	0.919	
5H-5, 21	44.21	49.87	66.68	1	3.634	0.955	
5H-5, 31	44.31	49.97	67.88	1	3.542	0.926	
5H-5, 41	44.41	50.07	67.80	1	5.370	0.883	
5H-5, 51	44.51	50.17	69.19	1	5.759	0.983	
5H-5, 61	44.61	50.27	68.94	1	4.084	0.940	
5H-5, 71	44.71	50.37	69.79	1	4.784	0.912	
5H-5, 81	44.81	50.47	68.70	2	3.954	0.940	
5H-5, 91	44.91	50.57	67.36	1	4.044	0.926	
5H-5, 101	45.01	50.67	67.43	1	3.109	0.912	
5H-5, 111	45.11	50.77	61.32	2	2.092	0.933	
5H-5, 121	45.21	50.87	69.18	1	3.392	0.912	
5H-5, 131	45.31	50.97	69.05	1	3.605	0.883	
5H-5, 141	45.41	51.07	67.93	1	3.301	0.865	
5H-6, 1	45.51	51.17	69.99	1	4.160	0.955	
5H-6, 21	45.71	51.37	73.35	1	8.298	0.855	
5H-6, 30	45.80	51.46	71.68	1	6.304	0.912	
5H-6, 41	45.91	51.57	74.09	1	6.753	0.955	
5H-6, 51	46.01	51.67	68.75	1	3.913	0.898	
5H-6, 61	46.11	51.77	66.34	1	2.753	0.940	
5H-6, 71	46.21	51.87	69.05	1	2.887	0.926	
5H-6, 81	46.31	51.97	68.31	1	2.855	0.955	
5H-6, 91	46.41	52.07	70.24	2	4.492	0.926	Tie point
6H-4, 1	52.21	60.89	72.28	1	6.052	0.826	Not in composite
6H-4, 11	52.31	60.99	71.87	1	6.294	0.905	Not in composite
6H-4, 21	52.41	61.09	71.32	2	5.848	0.912	Not in composite
6H-4, 31	52.51	61.19	75.37	2	7.103	0.947	Not in composite
6H-4, 41	52.61	61.29	73.03	1	6.676	0.926	Not in composite
6H-4, 51	52.71	61.39	73.65	1	6.916	0.905	Not in composite
6H-4, 61	52.81	61.49	66.31	1	7.721	0.940	Tie point
6H-4, 71	52.91	61.59	68.83	1	8.289	0.940	
6H-4, 81	53.01	61.69	72.27	1	9.101	0.926	
6H-4, 91	53.11	61.79	71.66	1	7.097	0.869	
6H-4, 101	53.21	61.89	73.83	1	6.416	0.898	
6H-4, 111	53.31	61.99	76.58	1	6.708	0.926	
6H-4, 121	53.41	62.09	75.71	1	3.474	0.955	
6H-4, 131	53.51	62.19	71.46	1	3.800	0.898	
6H-4, 141	53.61	62.29	71.40	1	4.833	0.862	
6H-5, 1	53.71	62.39	71.52	1	5.399	0.922	
6H-5, 11	53.81	62.49	71.29	1	6.164	0.898	
6H-5, 21	53.91	62.59	68.38	1	2.765	0.898	
6H-5, 31	54.01	62.69	67.59	1	2.567	0.919	
6H-5, 41	54.11	62.79	69.46	1	4.378	0.898	
6H-5, 51	54.21	62.89	71.26	1	6.255	0.898	
6H-5, 61	54.31	62.99	72.05	1	5.522	0.926	
6H-5, 71	54.41	63.09	69.91	1	5.690	0.912	
6H-5, 81	54.51	63.19	69.13	1	3.834	0.940	Tie point
6H-5, 91	54.61	63.29	65.24	1	3.516	0.926	Not in composite
6H-5, 101	54.71	63.39	58.17	2	3.166	0.855	Not in composite
6H-5, 111	54.81	63.49	62.26	1	3.081	0.862	Not in composite
7H-4, 91	62.71	72.51	79.37	1	2.761	0.955	Not in composite
7H-4, 101	62.81	72.61	76.97	1	2.346	1.012	Not in composite
7H-4, 111	62.91	72.71	70.85	1	2.100	0.955	Not in composite
7H-4, 121	63.01	72.81	71.91	1	2.796	0.969	Tie point
7H-4, 131	63.11	72.91	42.71	2	0.924	1.047	Ash J, and below
7H-4, 141	63.21	73.01	77.08	1	1.696	0.926	
7H-5, 1	63.31	73.11	75.12	1	2.374	1.012	
7H-5, 11	63.41	73.21	78.35	1	3.790	0.962	
7H-5, 21	63.51	73.31	75.11	1	1.667	0.969	
7H-5, 31	63.61	73.41	75.37	1	1.184	0.962	
7H-5, 41	63.71	73.51	78.58	1	2.543	0.955	
7H-5, 51	63.81	73.61	80.91	1	3.784	0.969	

Appendix C (continued).

Core, section, interval (cm)	ODP depth (mbsf)	Composite depth (m)	Mean wt% $CaCO_3$	Number of wt% $CaCO_3$ analyses	Coarse fraction (wt% >150 μm)	Dry-bulk density (g/cm^3)	Comment
121-758B-(Cont.)							
7H-5, 61	63.91	73.71	79.64	1	4.541	0.969	
7H-5, 71	64.01	73.81	78.25	1	4.424	0.898	
7H-5, 81	64.11	73.91	77.91	2	4.170	0.955	
7H-5, 91	64.21	74.01	74.12	1	2.495	0.997	Tie point
7H-5, 101	64.31	74.11	73.11	1	0.854	0.912	Not in composite
7H-5, 111	64.41	74.21	77.10	1	2.023	0.890	Not in composite
7H-5, 121	64.51	74.31	81.42	1	4.345	0.969	Not in composite
8H-4, 141	72.91	83.23	73.94	1	2.798	0.883	Not in composite
8H-5, 1	73.01	83.33	69.06	1	1.329	0.855	Not in composite
8H-5, 11	73.11	83.43	70.06	1	2.177	0.947	Tie point
8H-5, 21	73.21	83.53	72.97	1	2.494	0.969	
8H-5, 31	73.31	83.63	72.85	1	3.468	0.947	
8H-5, 41	73.41	83.73	71.61	1	3.656	0.898	
8H-5, 51	73.51	83.83	62.22	2	1.623	0.983	
8H-5, 61	73.61	83.93	74.82	1	1.351	0.940	
8H-5, 71	73.71	84.03	79.03	1	2.842	0.997	
8H-5, 81	73.81	84.13	78.64	2	3.020	0.969	Tie point
8H-5, 91	73.91	84.23	79.43	1	3.345	0.955	Not in composite
8H-5, 99	73.99	84.31	78.69	1	2.920	0.947	Not in composite
8H-5, 111	74.11	84.43	73.95	1	0.758	0.947	Not in composite

APPENDIX D
$\delta^{13}C$ and $\delta^{18}O$ Data, G. *sacculifera* (300-355 μm), Hole 758A

Core, section, interval (cm)	ODP depth (mbsf)	Composite depth (m)	Number of foraminifers analyzed	Number of foraminifers with sacs	Transducer pressure (mbar)	$\delta^{13}C$ ‰ to (PDB)	$\delta^{18}O$ ‰ to (PDB)
121-758A-							
1H-1, 1	0.01	0.01	11	0	4.8	1.46	−2.26
1H-1, 1	0.01	0.01	11	0	4.8	1.72	−2.02
1H-1, 1	0.01	0.01	11	0	3.7	1.51	−2.47
1H-1, 11	0.11	0.11	13	0	6.7	1.40	−2.14
1H-1, 11	0.11	0.11	12	0	4.8	1.79	−2.38
1H-1, 21	0.21	0.21	13	0	6.3	1.34	−2.19
1H-1, 21	0.21	0.21	12	0	5.9	1.64	−2.08
1H-1, 31	0.31	0.31	11	0	6.7	1.49	−1.58
1H-1, 31	0.31	0.31	11	0	5.2	1.34	−1.33
1H-1, 41	0.41	0.41	13	0	7.0	1.42	−0.44
1H-1, 41	0.41	0.41	12	0	6.3	1.78	−0.23
1H-1, 51	0.51	0.51	11	0	4.8	1.49	−0.49
1H-1, 51	0.51	0.51	11	0	4.8	1.83	−0.51
1H-1, 61	0.61	0.61	12	0	5.6	1.75	−0.55
1H-1, 61	0.61	0.61	10	0	4.1	1.68	−0.83
1H-1, 71	0.71	0.71	10	0	4.1	1.45	−0.87
1H-1, 71	0.71	0.71	9	0	3.3	1.76	−1.03
1H-1, 71	0.71	0.71	9	0	3.0	1.52	−0.76
1H-1, 81	0.81	0.81	10	0	3.0	1.80	−0.84
1H-1, 81	0.81	0.81	10	0	4.8	1.43	−1.01
1H-1, 81	0.81	0.81	10	0	3.7	1.81	−1.00
1H-1, 91	0.91	0.91	13	0	5.2	1.56	−0.84
1H-1, 91	0.91	0.91	12	0	4.4	1.59	−0.93
1H-1, 101	1.01	1.01	13	0	5.2	1.65	−0.99
1H-1, 101	1.01	1.01	14	0	5.9	1.63	−1.04
1H-1, 111	1.11	1.11	12	0	5.2	1.54	−1.02
1H-1, 111	1.11	1.11	12	0	5.9	1.53	−1.17
1H-1, 121	1.21	1.21	13	0	5.6	1.43	−1.10
1H-1, 121	1.21	1.21	12	0	5.2	1.37	−0.95
1H-1, 131	1.31	1.31	15	0	6.7	1.37	−0.87
1H-1, 131	1.31	1.31	12	0	5.2	1.40	−0.85
1H-1, 141	1.41	1.41	13	0	7.8	1.68	−0.78
1H-1, 141	1.41	1.41	12	0	7.4	1.67	−0.94
1H-2, 1	1.51	1.51	13	0	3.3	1.12	−1.01
1H-2, 1	1.51	1.51	12	0	5.9	1.26	−1.04
1H-2, 41	1.91	1.91	11	0	7.8	1.33	−1.09
1H-2, 41	1.91	1.91	11	0	4.4	1.45	−1.43
1H-2, 41	1.91	1.91	11	0	4.1	1.57	−1.49
1H-2, 61	2.11	2.11	12	0	4.1	1.34	−1.01
1H-2, 61	2.11	2.11	12	0	4.8	1.63	−1.38
1H-2, 61	2.11	2.11	12	0	4.1	1.75	−1.75
1H-2, 71	2.21	2.21	13	0	5.6	1.24	−2.16
1H-2, 71	2.21	2.21	12	0	4.4	1.68	−1.28
1H-2, 71	2.21	2.21	14	0	5.2	1.53	−1.13
1H-2, 81	2.31	2.31	13	0	4.4	1.30	−1.67
1H-2, 81	2.31	2.31	12	0	4.8	1.48	−1.20
1H-2, 81	2.31	2.31	15	0	6.3	1.44	−1.27
1H-2, 91	2.41	2.41	15	0	5.9	1.29	−1.76
1H-2, 91	2.41	2.41	12	0	4.4	1.62	−1.67
1H-2, 91	2.41	2.41	10	0	2.6	1.53	−1.75
1H-2, 101	2.51	2.51	13	0	4.8	1.24	−1.88
1H-2, 101	2.51	2.51	12	0	4.4	1.03	−1.56
1H-2, 101	2.51	2.51	13	0	4.8	1.51	−1.62
1H-2, 111	2.61	2.61	11	0	4.4	1.23	−1.55
1H-2, 111	2.61	2.61	10	0	3.0	1.10	−1.58
1H-2, 121	2.71	2.71	14	0	4.1	0.97	−1.80
1H-2, 121	2.71	2.71	13	0	3.0	1.10	−2.16
1H-2, 121	2.71	2.71	10	0	3.3	1.13	−1.80
1H-2, 131	2.81	2.81	12	0	5.9	1.07	−1.19
1H-2, 131	2.81	2.81	11	0	3.7	0.87	−1.64
1H-2, 131	2.81	2.81	11	0	4.8	1.24	−1.66
1H-2, 141	2.91	2.91	15	0	8.9	1.04	−1.28
1H-2, 141	2.91	2.91	15	0	7.8	1.30	−0.68
1H-2, 141	2.91	2.91	12	0	6.3	1.09	−0.82
1H-3, 1	3.01	3.01	15	0	8.1	1.23	−0.33
1H-3, 1	3.01	3.01	12	0	5.2	1.17	−0.41
1H-3, 11	3.11	3.11	15	0	7.8	1.36	−0.47
1H-3, 11	3.11	3.11	12	0	5.6	1.41	−0.62
1H-3, 21	3.21	3.21	14	0	7.0	1.42	−0.64
1H-3, 21	3.21	3.21	12	0	5.6	1.32	−0.69
1H-3, 31	3.31	3.31	15	0	8.5	1.52	−0.53
1H-3, 31	3.31	3.31	12	0	5.6	1.17	−0.77
1H-3, 41	3.41	3.41	13	0	6.7	1.15	−0.65
1H-3, 41	3.41	3.41	12	0	5.6	1.20	−0.85
1H-3, 51	3.51	3.51	13	0	6.3	1.21	−1.19

Appendix D (continued).

Core, section, interval (cm)	ODP depth (mbsf)	Composite depth (m)	Number of foraminifers analyzed	Number of foraminifers with sacs	Transducer pressure (mbar)	$\delta^{13}C$ ‰ to (PDB)	$\delta^{18}O$ ‰ to (PDB)
121-758A-(Cont.)							
1H-3, 51	3.51	3.51	12	0	4.4	1.22	−1.32
1H-3, 61	3.61	3.61	15	0	8.9	1.47	−0.94
1H-3, 71	3.71	3.71	14	0	8.1	1.31	−0.99
1H-3, 81	3.81	3.81	10	0	4.4	1.33	−1.31
1H-3, 81	3.81	3.81	10	0	4.8	1.49	−1.23
1H-3, 91	3.91	3.91	12	0	4.4	1.65	−1.79
1H-3, 91	3.91	3.91	12	0	4.4	1.03	−2.15
1H-3, 91	3.91	3.91	12	0	4.4	1.55	−1.90
1H-3, 101	4.01	4.01	9	0	3.0	1.52	−1.13
1H-3, 101	4.01	4.01	8	0	2.6	1.52	−1.59
1H-3, 101	4.01	4.01	8	0	2.2	1.40	−1.08
1H-3, 111	4.11	4.11	15	0	6.3	1.42	−1.49
1H-3, 111	4.11	4.11	12	0	6.3	1.49	−1.62
1H-3, 121	4.21	4.21	15	0	7.4	1.57	−1.75
1H-3, 121	4.21	4.21	12	0	5.9	1.59	−1.72
1H-3, 121	4.21	4.21	12	0	5.6	1.50	−1.63
1H-3, 131	4.31	4.31	14	0	7.0	1.49	−1.08
1H-3, 131	4.31	4.31	12	0	5.6	1.36	−1.46
1H-3, 131	4.31	4.31	12	0	5.6	1.36	−1.30
1H-3, 141	4.41	4.41	15	0	8.1	1.40	−1.07
1H-3, 141	4.41	4.41	12	0	6.3	1.42	−0.90
1H-3, 141	4.41	4.41	12	0	5.6	1.44	−0.93
1H-4, 1	4.51	4.51	12	0	5.6	1.28	−1.10
1H-4, 1	4.51	4.51	12	0	7.0	1.54	−0.82
1H-4, 1	4.51	4.51	12	0	4.4	1.60	−1.21
1H-4, 11	4.61	4.61	15	0	7.0	1.32	−1.59
1H-4, 11	4.61	4.61	12	0	4.8	1.38	−1.33
1H-4, 21	4.71	4.71	15	0	7.4	1.26	−1.29
1H-4, 31	4.81	4.81	15	0	8.5	1.52	−0.90
1H-4, 41	4.91	4.91	15	0	8.5	1.45	−0.55
1H-4, 41	4.91	4.91	12	0	6.3	1.14	−0.61
1H-4, 51	5.01	5.01	15	0	8.1	1.38	−0.59
1H-4, 51	5.01	5.01	12	0	5.6	1.40	−0.66
1H-4, 61	5.11	5.11	15	0	7.4	1.28	−0.85
1H-4, 61	5.11	5.11	12	0	6.3	1.15	−1.02
1H-4, 71	5.21	5.21	15	0	7.8	1.18	−0.75
1H-4, 71	5.21	5.21	12	0	7.0	0.99	−1.12
1H-4, 71	5.21	5.21	12	0	6.3	1.34	−0.77
1H-4, 81	5.31	5.31	15	0	9.6	1.22	−0.70
1H-4, 81	5.31	5.31	12	0	6.7	1.40	−0.69
1H-4, 91	5.41	5.41	15	0	8.9	1.45	−0.99
1H-4, 101	5.51	5.51	11	0	4.1	1.31	−1.29
1H-4, 111	5.61	5.61	15	0	8.9	1.79	−1.07
1H-4, 121	5.71	5.71	15	0	8.1	1.54	−0.95
1H-CC, 1	5.76	5.76	15	0	7.4	1.47	−1.05
1H-CC, 11	5.86	5.86	12	0	6.3	1.42	−1.40
1H-CC, 21	5.96	5.96	10	0	4.1	1.32	−1.74
2H-1, 1	6.01	7.43	13	0	5.2	1.62	−1.73
2H-1, 11	6.11	7.53	9	0	3.0	1.45	−1.60
2H-1, 11	6.11	7.53	8	4	2.2	1.44	−1.84
2H-1, 21	6.21	7.63	15	0	7.8	1.28	−0.63
2H-1, 21	6.21	7.63	12	0	5.9	1.61	−0.34
2H-1, 31	6.31	7.73	15	0	8.1	1.62	−0.52
2H-1, 31	6.31	7.73	12	0	6.3	1.45	−0.61
2H-1, 41	6.41	7.83	15	0	8.1	1.63	−0.62
2H-1, 41	6.41	7.83	12	0	6.3	1.49	−0.65
2H-1, 51	6.51	7.93	15	0	10.0	1.49	−1.04
2H-1, 51	6.51	7.93	12	0	7.4	1.73	−1.06
2H-1, 61	6.61	8.03	15	0	6.7	1.64	−1.12
2H-1, 61	6.61	8.03	12	0	4.4	1.68	−1.51
2H-1, 71	6.71	8.13	15	0	8.5	1.87	−1.30
2H-1, 71	6.71	8.13	12	0	4.1	1.58	−1.30
2H-1, 81	6.81	8.23	13	0	6.3	2.06	−1.64
2H-1, 91	6.91	8.33	9	0	2.6	1.84	−1.45
2H-1, 101	7.01	8.43	8	0	4.1	1.71	−1.50
2H-1, 121	7.21	8.63	8	0	1.9	1.57	−1.27
2H-1, 131	7.31	8.73	9	0	3.0	1.71	−1.42
2H-1, 131	7.31	8.73	13	0	6.3	1.41	−1.55
2H-1, 141	7.41	8.83	15	0	6.7	1.48	−1.42
2H-1, 141	7.41	8.83	12	0	5.9	1.63	−1.33
2H-1, 141	7.41	8.83	12	0	5.9	1.45	−1.14
2H-2, 1	7.51	8.93	15	0	7.4	1.28	−1.12
2H-2, 1	7.51	8.93	12	0	5.6	1.43	−1.29
2H-2, 11	7.61	9.03	15	0	9.3	1.28	−1.16
2H-2, 11	6.61	9.03	12	0	7.4	1.36	−1.09
2H-2, 21	7.71	9.13	15	0	10.0	1.24	−1.28

Appendix D (continued).

Core, section, interval (cm)	ODP depth (mbsf)	Composite depth (m)	Number of foraminifers analyzed	Number of foraminifers with sacs	Transducer pressure (mbar)	$\delta^{13}C$ ‰ to (PDB)	$\delta^{18}O$ ‰ to (PDB)
121-758A-(Cont.)							
2H-2, 21	7.71	9.13	12	0	6.3	1.56	−1.38
2H-2, 31	7.81	9.23	11	0	4.1	1.35	−1.45
2H-2, 31	7.81	9.23	11	0	3.7	1.54	−1.74
2H-2, 41	7.91	9.33	12	0	4.8	1.50	−1.57
2H-2, 41	7.91	9.33	12	0	5.6	1.46	−1.66
2H-2, 51	8.01	9.43	10	0	3.3	1.45	−2.18
2H-2, 51	8.01	9.43	10	0	4.1	1.62	−2.11
2H-2, 51	8.01	9.43	8	0	2.6	1.48	−1.70
2H-2, 61	8.11	9.53	15	0	6.3	1.30	−1.42
2H-2, 61	8.11	9.53	12	0	5.2	1.32	−1.50
2H-2, 71	8.21	9.63	15	0	7.8	1.45	−1.31
2H-2, 71	8.21	9.63	12	0	5.9	1.53	−1.32
2H-2, 71	8.21	9.63	12	0	5.6	1.23	−1.38
2H-2, 81	8.31	9.73	15	0	8.5	1.26	−1.60
2H-2, 81	8.31	9.73	12	0	4.8	1.25	−1.66
2H-2, 91	8.41	9.83	12	0	4.8	1.28	−1.66
2H-2, 91	8.41	9.83	12	0	4.1	1.15	−1.76
2H-2, 101	8.51	9.93	10	0	3.0	1.21	−1.53
2H-2, 101	8.51	9.93	10	0	3.7	1.25	−1.41
2H-2, 111	8.61	10.03	10	0	4.8	1.10	−1.79
2H-2, 111	8.61	10.03	10	0	4.8	1.36	−1.41
2H-2, 111	8.61	10.03	13	10	4.4	1.16	−1.78
2H-2, 121	8.71	10.13	11	0	6.3	1.28	−1.07
2H-2, 131	8.81	10.23	10	0	4.8	1.15	−0.58
2H-2, 131	8.81	10.23	11	0	6.3	1.22	−0.54
2H-2, 141	8.91	10.33	12	0	5.9	1.29	−0.57
2H-2, 141	8.91	10.33	12	0	7.8	1.44	−0.70
2H-3, 1	9.01	10.43	11	0	6.3	1.41	−0.68
2H-3, 1	9.01	10.43	11	0	7.0	1.41	−0.87
2H-3, 11	9.11	10.53	11	0	5.6	1.36	−1.05
2H-3, 11	9.11	10.53	12	0	6.3	1.04	−0.93
2H-3, 21	9.21	10.63	11	0	6.7	1.21	−0.97
2H-3, 21	9.21	10.63	12	0	6.3	1.21	−1.06
2H-3, 31	9.31	10.73	11	0	6.7	1.36	−1.27
2H-3, 31	9.31	10.73	12	0	8.5	1.47	−1.47
2H-3, 41	9.41	10.83	12	0	5.2	1.29	−1.03
2H-3, 41	9.41	10.83	12	0	4.8	0.96	−2.11
2H-3, 41	9.41	10.83	12	6	5.6	1.27	−1.15
2H-3, 51	9.51	10.93	12	0	7.0	1.43	−1.57
2H-3, 51	9.51	10.93	11	0	5.6	1.31	−1.68
2H-3, 61	9.61	11.03	12	0	5.2	1.34	−1.75
2H-3, 61	9.61	11.03	12	0	5.6	1.59	−1.52
2H-3, 71	9.71	11.13	12	0	5.9	1.28	−1.58
2H-3, 71	9.71	11.13	12	0	6.3	1.31	−1.41
2H-3, 81	9.81	11.23	12	0	7.0	1.42	−1.36
2H-3, 91	9.91	11.33	12	0	5.2	1.22	−0.99
2H-3, 91	9.91	11.33	12	0	6.3	1.24	−1.04
2H-3, 101	10.01	11.43	12	0	5.2	1.26	−0.88
2H-3, 101	10.01	11.43	12	0	5.2	1.26	−0.93
2H-3, 111	10.11	11.53	12	0	6.7	1.44	−1.17
2H-3, 111	10.11	11.53	12	0	6.7	1.04	−1.31
2H-3, 111	10.11	11.53	12	12	6.7	1.35	−1.05
2H-3, 121	10.21	11.63	13	0	6.7	1.34	−1.14
2H-3, 121	10.21	11.63	12	0	7.4	1.29	−1.13
2H-3, 131	10.31	11.73	10	0	5.9	1.23	−0.67
2H-3, 131	10.31	11.73	12	0	9.3	1.05	−1.28
2H-3, 141	10.41	11.83	9	0	3.7	1.22	−0.94
2H-4, 1	10.51	11.93	10	0	3.7	1.18	−1.49
2H-4, 1	10.51	11.93	12	0	4.8	1.43	−1.81
2H-4, 11	10.61	12.03	11	0	4.8	1.17	−1.86
2H-4, 11	10.61	12.03	11	0	4.4	1.30	−1.93
2H-4, 11	10.61	12.03	10	0	3.0	1.54	−1.96
2H-4, 21	10.71	12.13	13	0	3.7	1.09	−1.75
2H-4, 21	10.71	12.13	12	0	4.8	1.34	−1.80
2H-4, 51	11.01	12.43	13	0	6.7	1.03	−1.11
2H-4, 51	11.01	12.43	12	0	6.3	1.30	−0.84
2H-4, 61	11.11	12.53	13	0	7.4	1.26	−0.78
2H-4, 71	11.21	12.63	13	0	8.1	1.67	−0.67
2H-4, 71	11.21	12.63	12	0	8.5	1.52	−0.87
2H-4, 81	11.31	12.73	11	0	4.8	1.49	−1.08
2H-4, 91	11.41	12.83	13	0	6.7	1.54	−1.21
2H-4, 101	11.51	12.93	10	0	4.4	1.24	−1.54
2H-4, 111	11.61	13.03	13	0	8.5	1.55	−1.71
2H-4, 111	11.61	13.03	13	0	7.0	1.30	−1.67
2H-4, 121	11.71	13.13	13	0	7.0	1.17	−1.61
2H-4, 121	11.71	13.13	12	0	6.7	1.33	−1.71

Appendix D (continued).

Core, section, interval (cm)	ODP depth (mbsf)	Composite depth (m)	Number of foraminifers analyzed	Number of foraminifers with sacs	Transducer pressure (mbar)	$\delta^{13}C$ ‰ to (PDB)	$\delta^{18}O$ ‰ to (PDB)
121-758A-(Cont.)							
2H-4, 131	11.81	13.23	13	0	6.3	1.32	−1.42
2H-4, 131	11.81	13.23	12	0	6.3	1.39	−1.34
2H-4, 141	11.91	13.33	12	0	5.9	1.10	−1.53
2H-4, 141	11.91	13.33	12	0	5.2	1.10	−1.46
2H-5, 1	12.01	13.43	15	0	7.8	1.19	−1.69
2H-5, 1	12.01	13.43	12	0	7.4	1.28	−1.45
2H-5, 11	12.11	13.53	15	0	9.3	1.03	−0.74
2H-5, 21	12.21	13.63	15	0	9.6	1.22	−0.40
2H-5, 21	12.21	13.63	13	6	9.3	1.21	−0.36
2H-5, 31	12.31	13.73	15	0	10.4	1.32	−0.73
2H-5, 31	12.31	13.73	12	0	8.5	1.32	−0.77
2H-5, 41	12.41	13.83	13	0	8.1	1.20	−0.57
2H-5, 41	12.41	13.83	12	0	7.0	1.12	−0.69
2H-5, 51	12.51	13.93	15	0	10.0	1.35	−0.94
2H-5, 51	12.51	13.93	11	0	7.4	1.54	−0.54
2H-5, 61	12.61	14.03	13	0	7.8	1.16	−1.38
2H-5, 61	12.61	14.03	7	0	4.1	1.33	−1.15
2H-5, 61	12.61	14.03	12	7	7.8	1.22	−1.01
2H-5, 71	12.71	14.13	12	8	6.7	1.23	−1.06
2H-5, 81	12.81	14.23	15	0	11.5	1.53	−0.93
2H-5, 81	12.81	14.23	12	0	8.5	1.37	−0.98
2H-5, 91	12.91	14.33	15	0	10.7	1.42	−1.07
2H-5, 91	12.91	14.33	12	0	8.9	1.49	−1.00
2H-5, 101	13.01	14.43	10	0	5.2	1.18	−1.58
2H-5, 101	13.01	14.43	12	0	9.6	1.40	−1.47
2H-5, 111	13.11	14.53	10	0	5.2	1.41	−1.82
2H-5, 111	13.11	14.53	12	5	5.9	1.64	−1.62
2H-5, 121	13.21	14.63	8	0	2.6	1.16	−1.66
2H-5, 121	13.21	14.63	8	0	4.8	1.57	−1.57
2H-5, 131	13.31	14.73	12	0	4.8	1.13	−1.83
2H-5, 131	13.31	14.73	12	0	6.3	1.22	−1.54
2H-6, 1	13.51	14.93	12	0	6.7	1.54	−1.27
2H-6, 1	13.51	14.93	12	0	6.7	1.41	−0.96
2H-6, 11	13.61	15.03	15	0	9.6	1.57	−1.35
2H-6, 11	13.61	15.03	12	0	6.7	1.60	−1.24
2H-6, 21	13.71	15.13	13	0	9.3	1.64	−1.90
2H-6, 21	13.71	15.13	12	0	7.0	1.65	−1.68
2H-6, 31	13.81	15.23	12	0	7.0	1.68	−1.72
2H-6, 31	13.81	15.23	12	0	5.9	1.57	−1.66
2H-6, 41	13.91	15.33	12	0	7.0	1.74	−1.44
2H-6, 41	13.91	15.33	12	0	5.6	1.61	−1.23
2H-6, 51	14.01	15.43	10	0	4.4	1.85	−1.37
2H-6, 51	14.01	15.43	12	0	7.4	1.83	−1.20
2H-6, 61	14.11	15.53	11	0	7.0	1.92	−1.54
2H-6, 61	14.11	15.53	12	0	7.4	1.87	−1.59
2H-6, 71	14.21	15.63	15	0	7.8	1.61	−1.32
2H-6, 71	14.21	15.63	12	0	6.3	1.63	−1.48
2H-6, 81	14.31	15.73	15	0	8.1	1.79	−1.43
2H-6, 91	14.41	15.83	12	0	5.6	1.60	−1.54
2H-6, 101	14.51	15.93	15	0	8.1	1.77	−1.58
2H-6, 111	14.61	16.03	13	0	7.4	1.33	−1.59
2H-6, 121	14.71	16.13	13	0	8.9	1.58	−1.29
2H-6, 131	14.81	16.23	12	0	7.8	1.33	−1.14
2H-6, 131	14.81	16.23	12	0	8.9	1.37	−1.12
2H-6, 141	14.91	16.33	15	0	10.0	1.18	−1.25
2H-7, 1	15.01	16.43	15	0	8.1	1.37	−1.31
2H-7, 11	15.11	16.53	14	0	9.6	1.40	−1.46
2H-7, 21	15.21	16.63	14	0	8.5	1.48	−1.65
2H-7, 21	15.21	16.63	12	0	7.4	1.44	−1.73
2H-7, 31	15.31	16.73	15	0	6.7	1.25	−1.63
2H-7, 31	15.31	16.73	12	0	5.2	1.48	−1.70
2H-7, 41	15.41	16.83	15	0	8.5	1.24	−1.29
2H-7, 41	15.41	16.83	12	0	7.0	1.37	−1.56
2H-7, 41	15.41	16.83	12	0	7.4	1.77	−1.69
2H-7, 51	15.51	16.93	12	0	7.8	1.47	−1.73
2H-7, 51	15.51	16.93	12	0	8.1	1.51	−1.50
2H-7, 61	15.61	17.03	12	0	7.4	1.37	−1.65
2H-7, 61	15.61	17.03	9	0	4.1	1.58	−1.59
2H-7, 71	15.71	17.13	12	0	6.3	1.28	−1.28
2H-7, 71	15.71	17.13	12	0	7.8	1.68	−1.16
2H-c, 01	15.78	17.20	12	0	8.1	1.77	−1.51
2H-c, 11	15.88	17.30	12	0	6.3	1.30	−1.61
2H-c, 11	15.88	17.30	12	0	6.3	1.42	−1.50
3H-1, 1	15.61	17.52	12	0	5.6	1.44	−1.37
3H-1, 11	15.71	17.62	15	0	9.3	1.31	−1.28
3H-1, 11	15.71	17.62	12	0	7.0	1.35	−1.43

Appendix D (continued).

Core, section, interval (cm)	ODP depth (mbsf)	Composite depth (m)	Number of foraminifers analyzed	Number of foraminifers with sacs	Transducer pressure (mbar)	$\delta^{13}C$ ‰ to (PDB)	$\delta^{18}O$ ‰ to (PDB)
121-758A-(Cont.)							
3H-1, 11	15.71	17.62	12	0	9.6	1.50	−1.44
3H-1, 21	15.81	17.72	12	0	5.2	1.41	−1.40
3H-1, 31	15.91	17.82	12	0	6.7	1.66	−1.55
3H-1, 41	16.01	17.92	10	0	4.4	1.26	−1.51
3H-1, 51	16.11	18.02	12	0	7.4	1.40	−1.40
3H-1, 51	16.11	18.02	12	0	7.8	1.61	−1.50
3H-1, 61	16.21	18.12	12	0	6.3	1.34	−1.65
3H-1, 61	16.21	18.12	12	0	7.0	1.40	−1.44
3H-1, 71	16.31	18.22	12	0	7.8	1.51	−1.07
3H-1, 71	16.31	18.22	12	0	8.5	1.50	−1.24
3H-1, 81	16.41	18.32	12	0	8.9	1.36	−1.08
3H-1, 81	16.41	18.32	12	0	9.3	1.52	−1.20
3H-1, 91	16.51	18.42	12	0	8.5	1.44	−1.33
3H-1, 91	16.51	18.42	12	0	9.3	1.65	−1.41
3H-1, 101	16.61	18.52	12	0	7.8	1.61	−1.29
3H-1, 111	16.71	18.62	12	0	6.3	1.21	−1.40
3H-1, 111	16.71	18.62	12	5	6.7	1.56	−1.10
3H-1, 121	16.81	18.72	12	0	5.6	1.28	−1.77
3H-1, 121	16.81	18.72	12	0	6.7	1.55	−1.54
3H-1, 131	16.91	18.82	12	0	6.7	1.46	−1.36
3H-1, 141	17.01	18.92	12	0	7.0	1.18	−1.21
3H-2, 1	17.11	19.02	12	0	7.8	1.30	−0.88
3H-2, 1	17.11	19.02	12	0	6.7	1.16	−0.89
3H-2, 11	17.21	19.12	12	0	8.9	1.51	−0.73
3H-2, 11	17.21	19.12	12	0	8.1	1.28	−0.73
3H-2, 21	17.31	19.22	12	0	6.7	1.35	−1.18
3H-2, 21	17.31	19.22	12	0	7.8	1.58	−1.46
3H-2, 31	17.41	19.32	12	0	5.9	1.57	−1.26
3H-2, 41	17.51	19.42	12	0	6.3	1.68	−1.37
3H-2, 51	17.61	19.52	12	0	8.1	1.78	−1.80
3H-2, 51	17.61	19.52	12	0	6.3	1.73	−1.87
3H-2, 61	17.71	19.62	12	0	7.0	1.39	−1.12
3H-2, 71	17.81	19.72	12	0	7.8	1.43	−1.07
3H-2, 81	17.91	19.82	12	0	8.1	1.56	−0.99
3H-2, 81	17.91	19.82	12	0	8.1	1.46	−1.09
3H-2, 91	18.01	19.92	12	0	6.7	1.72	−1.21
3H-2, 101	18.11	20.02	12	0	6.7	1.72	−1.51
3H-2, 101	18.11	20.02	12	0	7.0	1.86	−1.77
3H-2, 111	18.21	20.12	12	0	7.4	1.44	−1.64
3H-2, 121	18.31	20.22	12	0	8.5	1.45	−1.37
3H-2, 121	18.31	20.22	12	0	8.5	1.34	−1.26
3H-2, 131	18.41	20.32	12	0	6.7	1.51	−1.58
3H-2, 131	18.41	20.32	12	0	7.8	1.48	−1.42
3H-2, 141	18.51	20.42	12	0	6.7	1.51	−1.48
3H-2, 141	18.51	20.42	12	0	4.4	1.57	−1.45
3H-3, 1	18.61	20.52	12	0	6.3	1.76	−1.15
3H-3, 1	18.61	20.52	13	0	7.0	1.89	−0.98
3H-3, 11	18.71	20.62	12	0	7.4	1.91	−1.60
3H-3, 11	18.71	20.62	12	0	7.8	1.90	−1.57
3H-3, 21	18.81	20.72	12	0	6.3	1.47	−1.66
3H-3, 21	18.81	20.72	12	0	5.9	1.64	−1.98
3H-3, 31	18.91	20.82	12	0	7.4	1.60	−1.37
3H-3, 31	18.91	20.82	12	0	7.0	1.53	−1.34
3H-3, 41	19.01	20.92	12	0	7.0	1.57	−1.39
3H-3, 51	19.11	21.02	12	0	8.1	1.54	−1.30
3H-3, 61	19.21	21.12	12	0	6.7	1.68	−1.27
3H-3, 71	19.31	21.22	12	0	7.0	1.79	−1.45
3H-3, 81	19.41	21.32	12	0	6.3	1.75	−1.41
3H-3, 91	19.51	21.42	12	0	7.0	1.83	−1.73
3H-3, 91	19.51	21.42	12	0	6.7	1.79	−1.68
3H-3, 101	19.61	21.52	12	0	6.3	1.57	−1.50
3H-3, 101	19.61	21.52	12	0	6.7	1.65	−1.51
3H-3, 111	19.71	21.62	12	0	6.3	1.39	−1.51
3H-3, 111	19.71	21.62	12	0	7.0	1.10	−1.71
3H-3, 121	19.81	21.72	12	0	6.7	1.39	−1.51
3H-3, 121	19.81	21.72	12	0	4.4	1.27	−1.37
3H-3, 131	19.91	21.82	12	0	7.4	1.14	−1.60
3H-3, 131	19.91	21.82	12	0	7.8	1.26	−1.58
3H-3, 141	20.01	21.92	12	0	5.2	1.30	−1.29
3H-3, 141	20.01	21.92	12	0	6.3	1.52	−1.25
3H-4, 1	20.11	22.02	12	0	7.0	1.78	−1.60
3H-4, 11	20.21	22.12	12	0	6.7	1.78	−1.99
3H-4, 11	20.21	22.12	12	0	7.8	1.86	−2.41
3H-4, 11	20.21	22.12	12	0	6.7	1.78	−2.10
3H-4, 21	20.31	22.22	12	0	7.4	1.58	−1.87

Appendix D (continued).

Core, section, interval (cm)	ODP depth (mbsf)	Composite depth (m)	Number of foraminifers analyzed	Number of foraminifers with sacs	Transducer pressure (mbar)	$\delta^{13}C$ ‰ to (PDB)	$\delta^{18}O$ ‰ to (PDB)
121-758A-(Cont.)							
3H-4, 21	20.31	22.22	12	0	5.9	1.53	−1.77
3H-4, 31	20.41	22.32	12	0	5.9	1.30	−1.88
3H-4, 31	20.41	22.32	12	0	6.3	1.23	−1.91
3H-4, 41	20.51	22.42	12	0	7.8	1.20	−1.34
3H-4, 41	20.51	22.42	12	0	6.7	1.18	−1.59
3H-4, 51	20.61	22.52	12	0	7.4	1.71	−0.98
3H-4, 51	20.61	22.52	12	0	6.7	1.55	−1.33
3H-4, 61	20.71	22.62	12	0	8.1	1.83	−1.53
3H-4, 61	20.71	22.62	12	0	7.4	1.83	−1.24
3H-4, 71	20.81	22.72	12	0	7.4	1.96	−1.60
3H-4, 71	20.81	22.72	12	0	4.8	1.61	−1.50
3H-4, 81	20.91	22.82	12	0	7.0	2.14	−2.20
3H-4, 81	20.91	22.82	12	0	5.6	1.80	−2.15
3H-4, 91	21.01	22.92	12	0	5.9	1.81	−1.72
3H-4, 91	21.01	22.92	12	0	4.8	1.68	−1.65
3H-4, 101	21.11	23.02	12	0	5.9	1.81	−2.02
3H-4, 101	21.11	23.02	12	0	5.9	1.68	−1.59
3H-4, 101	21.11	23.02	12	0	5.2	1.86	−1.29
3H-4, 111	21.21	23.12	12	0	5.9	1.79	−1.24
3H-4, 111	21.21	23.12	12	0	6.3	1.57	−1.36
3H-4, 121	21.31	23.22	12	0	6.7	1.81	−1.24
3H-4, 121	21.31	23.22	12	0	5.9	1.71	−1.19
3H-4, 131	21.41	23.32	12	0	6.3	1.80	−1.52
3H-4, 141	21.51	23.42	12	0	6.7	2.08	−1.70
3H-4, 141	21.51	23.42	12	0	1.5	1.93	−1.32
3H-4, 141	21.51	23.42	13	0	8.9	2.25	−1.80
3H-5, 1	21.61	23.52	12	0	7.0	2.05	−1.70
3H-5, 1	21.61	23.52	12	0	6.7	1.88	−1.88
3H-5, 11	21.71	23.62	12	0	5.9	1.53	−1.50
3H-5, 11	21.71	23.62	12	0	7.0	1.42	−1.79
3H-5, 21	21.81	23.72	12	0	6.3	1.57	−1.51
3H-5, 21	21.81	23.72	12	0	7.0	1.08	−1.43
3H-5, 31	21.91	23.82	12	0	7.8	1.81	−1.27
3H-5, 31	21.91	23.82	12	0	7.4	1.55	−1.34
3H-5, 41	22.01	23.92	12	0	7.4	1.88	−1.27
3H-5, 41	22.01	23.92	12	0	7.8	1.80	−1.43
3H-5, 51	22.11	24.02	12	0	6.7	1.97	−1.56
3H-5, 51	22.11	24.02	12	0	7.0	1.93	−1.62
3H-5, 61	22.21	24.12	12	0	7.0	1.80	−1.44
3H-5, 61	22.21	24.12	12	0	7.4	2.01	−1.49
3H-5, 71	22.31	24.22	12	0	5.9	1.71	−1.82
3H-5, 71	22.31	24.22	12	0	7.0	1.92	−1.55
3H-5, 81	22.41	24.32	12	0	7.4	1.94	−1.85
3H-5, 81	22.41	24.32	12	0	5.6	1.70	−1.82
3H-5, 91	22.51	24.42	12	0	7.0	1.61	−1.31
3H-5, 91	22.51	24.42	12	0	8.5	1.93	−1.52
3H-5, 101	22.61	24.52	12	0	8.9	1.75	−1.32
3H-5, 101	22.61	24.52	12	0	8.1	1.70	−1.25
3H-5, 111	22.71	24.62	12	0	8.5	1.90	−1.39
3H-5, 111	22.71	24.62	12	0	8.5	1.70	−1.65
3H-5, 121	22.81	24.72	12	0	5.9	1.73	−1.62
3H-5, 121	22.81	24.72	12	0	6.7	1.70	−1.73
3H-6, 1	23.11	25.02	12	0	7.4	1.97	−1.69
3H-6, 1	23.11	25.02	12	0	7.4	2.05	−1.88
3H-6, 11	23.21	25.12	12	0	7.0	1.83	−1.31
3H-6, 11	23.21	25.12	12	0	7.4	1.79	−1.59
3H-6, 21	23.31	25.22	12	0	7.8	1.69	−1.58
3H-6, 21	23.31	25.22	12	0	8.9	2.01	−1.62
3H-6, 31	23.41	25.32	12	0	6.7	1.91	−1.86
3H-6, 31	23.41	25.32	12	0	8.9	2.24	−1.89
3H-6, 41	23.51	25.42	12	0	6.7	1.95	−1.24
3H-6, 41	23.51	25.42	12	0	8.9	2.21	−1.38
3H-6, 51	23.61	25.52	12	0	6.7	1.88	−1.77
3H-6, 51	23.61	25.52	12	0	6.3	2.08	−1.62
3H-6, 61	23.71	25.62	12	0	5.9	1.75	−1.85
3H-6, 61	23.71	25.62	12	0	7.4	2.14	−1.64
3H-6, 71	23.81	25.72	12	0	7.0	1.52	−1.29
3H-6, 71	23.81	25.72	12	0	5.6	1.78	−1.32
3H-6, 81	23.91	25.82	12	0	7.4	1.64	−1.23
3H-6, 81	23.91	25.82	12	0	9.3	1.94	−1.26
3H-6, 91	24.01	25.92	12	0	8.1	1.62	−1.37
3H-6, 91	24.01	25.92	12	0	8.9	1.86	−1.26
3H-6, 101	24.11	26.02	12	0	8.5	1.38	−1.61
3H-6, 101	24.11	26.02	12	0	5.6	1.61	−1.18
3H-6, 111	24.21	26.12	12	0	7.8	1.62	−1.43
3H-6, 111	24.21	26.12	12	0	8.5	1.82	−1.58

Appendix D (continued).

Core, section, interval (cm)	ODP depth (mbsf)	Composite depth (m)	Number of foraminifers analyzed	Number of foraminifers with sacs	Transducer pressure (mbar)	$\delta^{13}C$ ‰ to (PDB)	$\delta^{18}O$ ‰ to (PDB)
121-758A-(Cont.)							
3H-6, 121	24.31	26.22	12	0	7.8	1.59	−1.70
3H-6, 121	24.31	26.22	12	0	8.5	1.41	−1.51
3H-6, 121	24.31	26.22	12	0	9.3	1.48	−1.66
3H-6, 131	24.41	26.32	12	0	5.9	1.36	−1.64
3H-6, 131	24.41	26.32	12	0	7.4	1.72	−1.83
3H-6, 141	24.51	26.42	12	0	7.4	1.35	−1.62
3H-7, 1	24.61	26.52	12	0	7.8	1.42	−1.43
3H-7, 11	24.71	26.62	12	0	7.0	1.06	−1.41
3H-7, 21	24.81	26.72	12	0	7.8	1.45	−1.36
3H-7, 31	24.91	26.82	12	0	7.4	1.41	−1.41
3H-7, 41	25.01	26.92	12	0	6.7	1.30	−1.75
3H-7, 41	25.01	26.92	12	0	8.5	1.61	−1.73
3H-7, 51	25.11	27.02	12	0	7.4	1.48	−1.40
3H-7, 51	25.11	27.02	12	0	6.3	1.36	−1.38
3H-7, 61	25.21	27.12	12	0	11.1	1.77	−1.47
3H-c, 01	25.31	27.22	12	0	11.5	1.86	−1.60
3H-c, 11	25.41	27.32	12	0	7.8	1.57	−1.72
4H-1, 1	25.21	29.54	12	0	7.0	1.77	−1.59
4H-1, 1	25.21	29.54	15	0	7.0	1.51	−1.75
4H-1, 11	25.31	29.64	12	0	6.7	1.57	−1.27
4H-1, 11	25.31	29.64	13	0	7.8	1.66	−1.52
4H-1, 21	25.41	29.74	12	0	7.8	1.10	−1.48
4H-1, 31	25.51	29.84	12	0	10.4	1.93	−1.52
4H-1, 41	25.61	29.94	12	0	8.1	1.70	−1.50
4H-1, 51	25.71	30.04	12	0	5.6	1.47	−1.32
4H-1, 61	25.81	30.14	12	0	6.3	1.54	−1.33
4H-1, 71	25.91	30.24	12	0	7.8	1.82	−1.83
4H-1, 71	25.91	30.24	13	0	7.8	1.71	−1.87
4H-1, 81	26.01	30.34	12	0	6.7	1.23	−1.52
4H-1, 81	26.01	30.34	12	0	5.9	1.51	−1.41
4H-1, 91	26.11	30.44	12	0	7.8	1.71	−1.54
4H-1, 91	26.11	30.44	12	0	7.4	1.54	−1.44
4H-1, 101	26.21	30.54	12	0	5.2	1.82	−1.80
4H-1, 101	26.21	30.54	12	0	6.3	1.49	−1.96
4H-1, 111	26.31	30.64	12	0	6.3	1.46	−1.40
4H-1, 121	26.41	30.74	12	0	5.9	1.46	−1.61
4H-1, 121	26.41	30.74	12	0	6.3	1.73	−1.49
4H-1, 131	26.51	30.84	12	0	6.3	1.82	−1.50
4H-1, 131	26.51	30.84	13	0	8.5	2.20	−1.38
4H-1, 141	26.61	30.94	12	0	6.7	1.87	−1.96
4H-1, 141	26.61	30.94	13	0	7.8	1.97	−1.89
4H-2, 1	26.71	31.04	12	0	8.1	1.87	−1.76
4H-2, 1	26.71	31.04	12	0	6.3	1.74	−1.60
4H-2, 11	26.81	31.14	12	0	9.6	1.90	−1.81
4H-2, 11	26.81	31.14	12	0	8.5	1.79	−1.49
4H-2, 21	26.91	31.24	12	0	6.7	1.81	−1.61
4H-2, 21	26.91	31.24	12	0	7.4	1.80	−1.66
4H-2, 31	27.01	31.34	12	0	6.3	1.57	−1.27
4H-2, 31	27.01	31.34	12	0	8.5	1.87	−1.46
4H-2, 41	27.11	31.44	12	0	7.4	1.65	−1.46
4H-2, 41	27.11	31.44	12	0	6.7	1.45	−1.39
4H-2, 51	27.21	31.54	12	0	5.2	1.23	−1.11
4H-2, 51	27.21	31.54	12	0	6.7	1.57	−1.12
4H-2, 61	27.31	31.64	12	0	7.8	1.54	−1.51
4H-2, 61	27.31	31.64	12	0	8.5	1.65	−1.44
4H-2, 71	27.41	31.74	12	0	7.0	1.68	−1.24
4H-2, 71	27.41	31.74	12	0	7.0	1.63	−1.39
4H-2, 81	27.51	31.84	12	0	7.8	1.70	−1.65
4H-2, 81	27.51	31.84	14	0	7.0	1.45	−1.32
4H-2, 91	27.61	31.94	12	0	7.4	1.72	−1.52
4H-2, 91	27.61	31.94	12	0	7.4	1.89	−1.54
4H-2, 101	27.71	32.04	12	0	6.3	1.67	−1.67
4H-2, 101	27.71	32.04	12	0	6.7	1.53	−1.39
4H-2, 111	27.81	32.14	10	0	5.2	1.62	−1.63
4H-2, 111	27.81	32.14	10	10	5.2	1.67	−1.53
4H-2, 121	27.91	32.24	12	0	6.7	1.67	−1.38
4H-2, 121	27.91	32.24	12	0	5.9	1.61	−1.39
4H-2, 131	28.01	32.34	12	0	6.3	1.65	−1.29
4H-2, 131	28.01	32.34	12	0	8.5	1.66	−1.16
4H-2, 141	28.11	32.44	12	0	7.0	1.47	−1.64
4H-2, 141	28.11	32.44	12	0	7.8	1.59	−1.68
4H-3, 1	28.21	32.54	12	0	8.1	1.46	−0.96
4H-3, 1	28.21	32.54	12	0	8.5	1.65	−1.02
4H-3, 11	28.31	32.64	12	0	7.4	1.57	−1.19
4H-3, 21	28.41	32.74	12	0	8.1	1.71	−1.11
4H-3, 21	28.41	32.74	12	0	6.3	1.28	−1.35

Appendix D (continued).

Core, section, interval (cm)	ODP depth (mbsf)	Composite depth (m)	Number of foraminifers analyzed	Number of foraminifers with sacs	Transducer pressure (mbar)	$\delta^{13}C$ ‰ to (PDB)	$\delta^{18}O$ ‰ to (PDB)
121-758A-(Cont.)							
4H-3, 31	28.51	32.84	12	0	0.4	1.46	−1.44
4H-3, 31	28.51	32.84	14	0	6.7	1.86	−1.28
4H-3, 41	28.61	32.94	12	0	7.8	1.86	−1.35
4H-3, 41	28.61	32.94	13	0	7.8	1.74	−1.56
4H-3, 51	28.71	33.04	12	0	6.7	1.71	−1.79
4H-3, 51	28.71	33.04	12	0	6.7	1.74	−1.38
4H-3, 61	28.81	33.14	12	0	7.4	1.67	−1.93
4H-3, 61	28.81	33.14	12	0	6.3	1.80	−1.87
4H-3, 71	28.91	33.24	12	0	9.3	1.91	−2.17
4H-3, 71	28.91	33.24	12	0	8.1	1.83	−2.25
4H-3, 81	29.01	33.34	12	0	6.7	1.62	−1.40
4H-3, 81	29.01	33.34	12	0	8.5	1.76	−1.38
4H-3, 91	29.11	33.44	12	0	7.8	1.74	−1.48
4H-3, 91	29.11	33.44	12	0	8.5	1.79	−1.36
4H-3, 101	29.21	33.54	12	0	7.8	1.66	−1.56
4H-3, 101	29.21	33.54	12	0	6.3	1.71	−1.49
4H-3, 111	29.31	33.64	12	0	7.4	1.66	−1.86
4H-3, 111	29.31	33.64	15	0	11.1	1.55	−2.09
4H-3, 121	29.41	33.74	12	0	8.1	1.84	−1.68
4H-3, 121	29.41	33.74	12	0	8.5	1.79	−1.56
4H-3, 131	29.51	33.84	12	0	7.4	1.52	−1.62
4H-3, 131	29.51	33.84	12	0	7.4	1.66	−1.72
4H-3, 141	29.61	33.94	12	0	7.8	1.69	−1.54
4H-3, 141	29.61	33.94	12	0	7.4	0.95	−1.31
4H-4, 1	29.71	34.04	12	0	5.6	1.62	−1.17
4H-4, 1	29.71	34.04	13	0	9.6	1.58	−1.46
4H-4, 11	29.81	34.14	12	0	7.0	1.83	−2.16
4H-4, 11	29.81	34.14	14	3	8.5	2.06	−2.13
4H-4, 21	29.91	34.24	12	0	7.8	1.76	−1.63
4H-4, 21	29.91	34.24	13	0	7.8	1.86	−1.86
4H-4, 31	30.01	34.34	12	0	6.3	1.46	−1.78
4H-4, 31	30.01	34.34	13	0	8.1	1.63	−1.86
4H-4, 41	30.11	34.44	12	0	8.1	1.60	−1.31
4H-4, 41	30.11	34.44	15	0	11.1	1.54	−1.87
4H-4, 41	30.11	34.44	11	0	9.3	1.61	−1.54
4H-4, 51	30.21	34.54	12	0	7.0	1.78	−1.47
4H-4, 51	30.21	34.54	15	0	7.8	1.50	−1.61
4H-4, 61	30.31	34.64	12	0	8.1	1.87	−1.57
4H-4, 61	30.31	34.64	13	0	8.1	1.64	−1.77
4H-4, 71	30.41	34.74	12	0	7.4	1.51	−1.81
4H-4, 71	30.41	34.74	12	0	7.8	1.57	−1.78
4H-4, 81	30.51	34.84	12	0	10.0	1.82	−1.69
4H-4, 81	30.51	34.84	13	0	4.1	1.75	−1.63
4H-4, 91	30.61	34.94	12	0	8.5	1.55	−1.77
4H-4, 91	30.61	34.94	12	0	8.5	1.52	−1.41
4H-4, 91	30.61	34.94	13	0	9.3	1.60	−1.89
4H-4, 91	30.61	34.94	7	7	11.1	1.61	−1.69
4H-4, 101	30.71	35.04	12	0	8.1	1.51	−1.63
4H-4, 101	30.71	35.04	15	0	10.0	1.65	−1.69
4H-4, 111	30.81	35.14	15	0	9.3	1.75	−1.90
4H-4, 111	30.81	35.14	12	0	6.3	1.64	−1.86
4H-4, 121	30.91	35.24	12	0	6.3	1.41	−1.52
4H-4, 121	30.91	35.24	13	0	8.1	1.81	−1.49
4H-4, 121	30.91	35.24	12	0	7.0	1.59	−1.58
4H-4, 131	31.01	35.34	12	0	9.6	1.69	−1.25
4H-4, 131	31.01	35.34	12	0	15.6	1.56	−1.25
4H-4, 131	31.01	35.34	15	0	8.9	1.65	−1.35
4H-4, 141	31.11	35.44	12	0	5.9	1.76	−1.31
4H-5, 7	31.27	35.60	12	0	8.5	1.91	−1.36
4H-5, 7	31.27	35.60	13	0	10.0	1.76	−1.73
4H-5, 7	31.27	35.60	12	0	7.0	1.87	−1.60
4H-5, 11	31.31	35.64	15	0	9.3	1.80	−2.03
4H-5, 11	31.31	35.64	11	0	5.9	1.89	−1.39
4H-5, 21	31.41	35.74	14	0	8.1	1.62	−1.84
4H-5, 21	31.41	35.74	12	0	5.9	2.03	−1.84
4H-5, 31	31.51	35.84	15	0	11.5	2.13	−1.66
4H-5, 31	31.51	35.84	12	0	7.0	1.70	−1.78
4H-5, 41	31.61	35.94	12	0	8.1	2.21	−1.46
4H-5, 41	31.61	35.94	15	0	10.0	2.15	−1.75
4H-5, 51	31.71	36.04	12	0	8.1	1.94	−1.43
4H-5, 51	31.71	36.04	13	0	8.5	1.94	−1.57
4H-5, 61	31.81	36.14	15	0	12.2	1.70	−1.80
4H-5, 61	31.81	36.14	13	0	8.9	1.97	−1.87
4H-5, 71	31.91	36.24	12	0	10.4	1.78	−1.56
4H-5, 71	31.91	36.24	12	0	7.8	1.80	−1.67
4H-5, 81	32.01	36.34	12	0	8.1	1.66	−1.42

Appendix D (continued).

Core, section, interval (cm)	ODP depth (mbsf)	Composite depth (m)	Number of foraminifers analyzed	Number of foraminifers with sacs	Transducer pressure (mbar)	$\delta^{13}C$ ‰ to (PDB)	$\delta^{18}O$ ‰ to (PDB)
121-758A-(Cont.)							
4H-5, 81	32.01	36.34	15	0	8.9	1.60	−1.52
4H-5, 91	32.11	36.44	12	0	6.3	1.81	−1.30
4H-5, 91	32.11	36.44	15	0	12.6	1.69	−1.49
4H-5, 101	32.21	36.54	12	0	7.4	1.69	−1.47
4H-5, 101	32.21	36.54	14	0	9.6	1.53	−1.52
4H-5, 111	32.31	36.64	12	0	6.3	1.55	−1.36
4H-5, 111	32.31	36.64	15	0	7.0	1.53	−1.61
4H-5, 121	32.41	36.74	12	0	7.0	1.67	−1.51
4H-5, 121	32.41	36.74	12	0	7.4	1.77	−1.72
4H-5, 131	32.51	36.84	12	0	8.5	1.75	−1.79
4H-5, 131	32.51	36.84	12	0	8.1	1.89	−1.90
4H-5, 141	32.61	36.94	12	0	7.4	1.70	−1.83
4H-5, 141	32.61	36.94	12	0	9.3	1.55	−2.05
4H-6, 1	32.71	37.04	12	0	9.6	1.47	−1.56
4H-6, 1	32.71	37.04	12	0	7.4	1.33	−1.66
4H-6, 11	32.81	37.14	12	0	8.9	1.57	−1.09
4H-6, 11	32.81	37.14	12	0	8.5	1.45	−0.90
4H-6, 11	32.81	37.14	12	0	7.4	1.62	−1.10
4H-6, 21	32.91	37.24	12	0	6.7	1.52	−1.17
4H-6, 21	32.91	37.24	12	0	10.0	1.81	−1.70
4H-6, 21	32.91	37.24	15	0	9.3	1.42	−1.60
4H-6, 31	33.01	37.34	12	0	7.4	1.51	−1.82
4H-6, 31	33.01	37.34	12	0	5.6	1.96	−1.93
4H-6, 41	33.11	37.44	12	0	7.8	1.28	−1.26
4H-6, 41	33.11	37.44	12	0	8.1	1.33	−1.53
4H-6, 51	33.21	37.54	12	0	7.8	1.24	−1.13
4H-6, 51	33.21	37.54	12	0	8.5	1.29	−1.20
4H-6, 61	33.31	37.64	12	0	9.6	1.32	−1.51
4H-6, 61	33.31	37.64	12	0	9.3	1.45	−1.41
4H-6, 71	33.41	37.74	12	0	6.7	1.27	−1.13
4H-6, 71	33.41	37.74	12	0	9.3	1.42	−1.38
4H-6, 81	33.51	37.84	12	0	7.8	1.25	−2.19
4H-6, 81	33.51	37.84	15	0	9.3	1.35	−1.54
4H-6, 91	33.61	37.94	12	0	6.3	1.73	−1.76
4H-6, 91	33.61	37.94	12	0	0.4	1.77	−1.72
4H-6, 101	33.71	38.04	12	0	7.0	1.75	−1.39
4H-6, 101	33.71	38.04	13	2	7.4	1.63	−1.79
4H-6, 111	33.81	38.14	12	0	6.3	1.50	−1.59
4H-6, 111	33.81	38.14	12	0	5.9	1.40	−1.71
4H-6, 121	33.91	38.24	12	0	7.4	1.84	−1.79
4H-6, 121	33.91	38.24	12	0	7.4	1.63	−1.94
4H-6, 131	34.01	38.34	12	0	6.7	1.67	−1.68
4H-6, 131	34.01	38.34	12	0	6.3	1.49	−1.66
4H-6, 141	34.11	38.44	12	0	8.5	1.71	−2.21
4H-6, 141	34.11	38.44	12	0	6.7	1.75	−2.12
4H-7, 1	34.21	38.54	12	0	7.8	1.30	−1.75
4H-7, 1	34.21	38.54	12	0	7.4	1.36	−1.65
4H-7, 11	34.31	38.64	12	0	7.8	1.49	−1.43
4H-7, 11	34.31	38.64	12	0	7.4	1.42	−1.56
4H-7, 21	34.41	38.74	12	0	8.1	1.55	−1.35
4H-7, 21	34.41	38.74	12	0	8.1	1.42	−1.31
4H-7, 31	34.51	38.84	12	0	6.3	1.76	−1.83
4H-7, 31	34.51	38.84	12	0	7.0	1.81	−1.54
4H-7, 41	34.61	38.94	12	0	6.7	1.75	−1.66
4H-7, 41	34.61	38.94	12	0	5.9	1.39	−1.43
4H-7, 51	34.71	39.04	12	0	4.8	1.52	−2.03
4H-7, 51	34.71	39.04	12	0	6.7	1.67	−1.92

APPENDIX E
$\delta^{13}C$ and $\delta^{18}O$ Data, G. *sacculifera* (300-355 μm), Hole 758B

Core, section, interval (cm)	ODP depth (mbsf)	Composite depth (m)	Number of foraminifers analyzed	Number of foraminifers with sacs	Transducer pressure (mbar)	$\delta^{13}C$ ‰ to (PDB)	$\delta^{18}O$ ‰ to (PDB)
121-758B-							
1H-3, 61	3.61	5.12	15	0	8.5	1.39	−1.10
1H-3, 61	3.61	5.12	13	0	7.0	1.20	−0.80
1H-3, 71	3.71	5.22	15	0	9.3	1.26	−0.74
1H-3, 81	3.81	5.32	15	0	8.5	1.56	−0.44
1H-3, 81	3.81	5.32	15	0	7.8	1.41	−0.83
1H-3, 91	3.91	5.42	9	0	4.4	1.65	−0.93
1H-3, 101	4.01	5.52	15	0	7.8	1.57	−1.27
1H-3, 101	4.01	5.52	13	0	5.9	1.53	−1.30
1H-3, 111	4.11	5.62	15	0	5.9	1.46	−0.94
1H-3, 121	4.21	5.72	15	0	7.4	1.61	−0.99
1H-3, 121	4.21	5.72	15	0	8.1	1.60	−1.24
1H-3, 131	4.31	5.82	15	0	9.3	1.66	−1.10
1H-3, 131	4.31	5.82	12	0	6.7	1.36	−1.26
1H-3, 141	4.41	5.92	13	0	7.8	1.49	−1.54
1H-3, 141	4.41	5.92	13	0	5.6	1.50	−1.43
1H-4, 1	4.51	6.02	9	0	3.0	1.29	−1.57
1H-4, 11	4.61	6.12	10	0	2.6	1.19	−1.68
1H-4, 21	4.71	6.22	11	0	3.3	1.28	−1.70
1H-4, 31	4.81	6.32	12	0	4.8	1.12	−1.69
1H-4, 31	4.81	6.32	12	0	5.6	0.97	−1.76
1H-4, 41	4.91	6.42	15	0	7.4	0.99	−1.50
1H-4, 51	5.01	6.52	13	0	7.4	1.06	−0.93
1H-4, 61	5.11	6.62	10	0	6.3	1.41	−0.46
1H-4, 61	5.11	6.62	9	0	5.9	1.26	−0.52
1H-4, 71	5.21	6.72	13	0	7.4	1.32	−0.80
1H-4, 71	5.21	6.72	12	0	5.9	1.49	−0.74
1H-4, 81	5.31	6.82	15	0	7.4	1.47	−0.67
1H-4, 81	5.31	6.82	12	0	6.3	1.44	−0.95
1H-4, 81	5.31	6.82	12	0	5.6	1.00	−0.84
1H-4, 91	5.41	6.92	15	0	5.9	1.50	−0.68
1H-4, 91	5.41	6.92	12	0	6.3	1.47	−0.89
1H-4, 101	5.51	7.02	12	0	5.2	1.43	−1.17
1H-4, 111	5.61	7.12	15	0	7.8	1.52	−1.52
1H-4, 121	5.71	7.22	13	0	5.9	1.49	−1.64
1H-4, 121	5.71	7.22	12	0	6.3	1.41	−1.44
1H-4, 141	5.91	7.42	6	0	2.6	1.85	−1.87
1H-4, 141	5.91	7.42	9	4	6.7	1.78	−1.75
1H-5, 1	6.01	7.52	15	0	6.3	1.27	−1.15
1H-5, 1	6.01	7.52	12	0	4.8	1.27	−1.10
1H-5, 11	6.11	7.62	15	0	9.3	1.40	−0.64
1H-5, 21	6.21	7.72	15	0	8.9	1.55	−0.34
1H-5, 31	6.31	7.82	13	0	5.9	1.51	−0.64
1H-5, 41	6.41	7.92	13	0	8.1	1.77	−0.97
1H-5, 51	6.51	8.02	13	0	8.1	1.65	−0.98
1H-5, 61	6.61	8.12	13	0	7.0	1.80	−0.84
1H-5, 61	6.61	8.12	12	0	6.7	1.51	−0.88
2H-5, 1	15.51	17.01	12	0	5.6	1.43	−1.52
2H-5, 11	15.61	17.11	12	0	5.9	1.49	−1.30
2H-5, 11	15.61	17.11	12	0	5.9	1.59	−1.22
2H-5, 21	15.71	17.21	12	0	5.6	1.21	−1.32
2H-5, 21	15.71	17.21	12	0	4.8	1.47	−1.49
2H-5, 31	15.81	17.31	12	0	6.7	1.12	−1.38
2H-5, 31	15.81	17.31	12	0	6.7	1.06	−1.31
2H-5, 41	15.91	17.41	12	0	5.6	1.21	−1.24
2H-5, 41	15.91	17.41	12	0	6.3	1.29	−1.07
2H-5, 51	16.01	17.51	12	0	5.6	1.22	−1.41
2H-5, 51	16.01	17.51	12	0	6.3	1.17	−1.47
2H-5, 61	16.11	17.61	12	0	5.2	1.63	−1.43
2H-5, 61	16.11	17.61	12	0	6.7	1.52	−1.25
2H-5, 71	16.21	17.71	12	0	4.1	1.31	−1.32
2H-5, 71	16.21	17.71	12	0	4.4	1.47	−1.32
2H-5, 81	16.31	17.81	12	0	5.6	1.36	−1.59
2H-5, 81	16.31	17.81	12	0	5.6	1.35	−1.40

Appendix E (continued).

Core, section, interval (cm)	ODP depth (mbsf)	Composite depth (m)	Number of foraminifers analyzed	Number of foraminifers with sacs	Transducer pressure (mbar)	$\delta^{13}C$ ‰ to (PDB)	$\delta^{18}O$ ‰ to (PDB)
121-758B- (Cont).							
3H-3, 111	23.01	26.83	12	0	5.9	1.19	−1.16
3H-3, 111	23.01	26.83	13	0	6.7	1.31	−1.37
3H-3, 121	23.11	26.93	12	0	7.0	1.33	−1.64
3H-3, 121	23.11	26.93	12	0	7.0	1.35	−1.54
3H-3, 131	23.21	27.03	12	0	7.8	1.31	−1.43
3H-3, 141	23.31	27.13	12	0	8.1	1.62	−1.36
3H-4, 1	23.41	27.23	12	0	8.1	1.62	−1.50
3H-4, 11	23.51	27.33	12	0	6.7	1.22	−1.76
3H-4, 11	23.51	27.33	12	0	8.5	1.39	−1.69
3H-4, 21	23.61	27.43	12	0	7.4	1.42	−1.12
3H-4, 21	23.61	27.43	12	0	7.0	1.41	−1.18
3H-4, 31	23.71	27.53	12	0	7.4	1.34	−1.38
3H-4, 31	23.71	27.53	16	0	10.0	1.25	−1.52
3H-4, 41	23.81	27.63	12	0	7.0	1.52	−1.17
3H-4, 41	23.81	27.63	12	0	8.1	1.42	−1.39
3H-4, 51	23.91	27.73	12	0	6.7	1.80	−1.34
3H-4, 73	24.13	27.95	12	0	6.3	1.57	−1.29
3H-4, 81	24.21	28.03	12	0	6.3	1.37	−1.45
3H-4, 91	24.31	28.13	12	0	7.8	1.44	−1.65
3H-4, 101	24.41	28.23	12	0	8.1	1.51	−1.66
3H-4, 111	24.51	28.33	12	0	7.4	1.59	−1.04
3H-4, 111	24.51	28.33	12	0	9.3	1.49	−1.40
3H-4, 121	24.61	28.43	12	0	7.4	1.49	−1.38
3H-4, 131	24.71	28.53	12	0	5.6	1.61	−1.49
3H-4, 141	24.81	28.63	12	0	7.0	1.67	−1.30
3H-4, 141	24.81	28.63	12	0	7.4	1.64	−1.45
3H-5, 1	24.91	28.73	12	0	5.9	1.51	−1.57
3H-5, 1	24.91	28.73	12	5	5.9	1.66	−1.67
3H-5, 11	25.01	28.83	12	0	1.9	1.55	−0.98
3H-5, 11	25.01	28.83	12	2	5.2	1.36	−1.16
3H-5, 21	25.11	28.93	12	0	6.7	1.63	−1.33
3H-5, 21	25.11	28.93	12	0	5.9	1.60	−1.42
3H-5, 31	25.21	29.03	12	0	5.9	1.61	−1.75
3H-5, 31	25.21	29.03	12	0	6.3	1.48	−1.79
3H-5, 41	25.31	29.13	12	0	4.8	1.62	−1.20
3H-5, 41	25.31	29.13	12	0	7.4	1.48	−1.44
3H-5, 51	25.41	29.23	12	0	2.6	1.44	−1.35
3H-5, 51	25.41	29.23	12	0	7.4	1.72	−1.59
3H-5, 61	25.51	29.33	12	0	5.6	1.35	−1.57
3H-5, 61	25.51	29.33	12	0	5.9	1.28	−2.07
3H-5, 71	25.61	29.43	12	0	4.4	1.07	−2.34
3H-5, 71	25.61	29.43	12	0	5.2	1.60	−1.63
3H-5, 71	25.61	29.43	12	0	5.9	1.52	−1.70
3H-5, 81	25.71	29.53	12	0	5.6	1.49	−1.67
3H-5, 81	25.71	29.53	12	0	5.9	1.54	−1.69
3H-5, 91	25.81	29.63	12	0	6.7	1.54	−1.38
3H-5, 101	25.91	29.73	12	0	7.4	1.60	−1.10
3H-5, 111	26.01	29.83	12	0	7.8	1.53	−1.21
4H-5, 71	35.11	38.95	12	0	5.2	1.41	−1.35
4H-5, 81	35.21	39.05	12	0	5.6	1.26	−1.53
4H-5, 91	35.31	39.15	12	0	7.0	1.45	−1.80
4H-5, 101	35.41	39.25	12	0	6.7	1.44	−1.35
4H-5, 111	35.51	39.35	12	0	7.4	1.28	−1.23
4H-5, 121	35.61	39.45	12	0	5.6	1.04	−1.53
4H-5, 131	35.71	39.55	12	0	5.9	1.49	−1.46
4H-5, 141	35.81	39.65	12	0	5.9	1.35	−1.53
4H-6, 1	35.91	39.75	12	0	6.3	1.33	−1.64
4H-6, 11	36.01	39.85	12	0	6.7	1.38	−0.95
4H-6, 21	36.11	39.95	12	0	7.4	1.25	−1.30
4H-6, 31	36.21	40.05	12	0	6.7	1.28	−1.50
4H-6, 41	36.31	40.15	12	0	6.3	1.38	−1.67

APPENDIX F
Site 758 Composite Records of Mean $\delta^{13}C$, $\delta^{18}O$, $CaCO_3$, Density, Coarse Fraction, and Interpolated Magnetic Susceptibility Data

Core, section, interval (cm)	ODP depth (mbsf)	Composite depth (m)	Magnetic age (m.y.)	Magnetic sedimentation rate (m/m.y.)	$\delta^{18}O$ age (m.y.)	$\delta^{18}O$ sedimentation rate (m/m.y.)	Mean (wt% $CaCO_3$)	Magnetic $CaCO_3$ MAR (g/cm²/k.y.)	$\delta^{13}C$ ‰ to (PDB)	$\delta^{18}O$ ‰ to (PDB)	Dry-bulk density (g/cm³)	Coarse fraction (wt% >150 μm)	Interpolated MS K (10-6) (cgs)	Comment
121-758A-														
1H-1, 1	0.01	0.01	0.00060	16.7	0.00055	23.08	64.63	0.56	1.56	−2.25	0.527	28.49	2.50	
1H-1, 11	0.11	0.11	0.00660	16.7	0.00600	23.08	61.67	0.56	1.60	−2.26	0.542	19.33	5.23	
1H-1, 21	0.21	0.21	0.01260	16.7	0.01033	23.08	56.96	0.57	1.49	−2.13	0.599	20.01	6.20	
1H-1, 31	0.31	0.31	0.01859	16.7	0.01467	23.08	58.88	0.64	1.41	−1.45	0.656	21.68	8.07	
1H-1, 41	0.41	0.41	0.02459	16.7	0.01900	20.59	54.06	0.59	1.60	−0.33	0.656	14.60	9.77	
1H-1, 51	0.51	0.51	0.03059	16.7	0.02386	20.59	56.75	0.58	1.66	−0.50	0.613	16.12	8.90	
1H-1, 61	0.61	0.61	0.03659	16.7	0.02871	20.59	55.03	0.63	1.71	−0.69	0.691	18.25	10.53	
1H-1, 71	0.71	0.71	0.04259	16.7	0.03357	20.59	55.51	0.61	1.58	−0.89	0.656	17.97	10.63	
1H-1, 81	0.81	0.81	0.04859	16.7	0.03843	20.59	59.07	0.64	1.68	−0.95	0.648	20.85	6.70	
1H-1, 91	0.91	0.91	0.05459	16.7	0.04329	20.59	60.25	0.74	1.57	−0.88	0.741	15.85	7.57	
1H-1, 101	1.01	1.01	0.06058	16.7	0.04814	20.59	57.70	0.64	1.64	−1.01	0.670	16.74	3.63	
1H-1, 111	1.11	1.11	0.06658	16.7	0.05300	20.83	59.68	0.69	1.53	−1.10	0.691	17.73	6.20	
1H-1, 121	1.21	1.21	0.07258	16.7	0.05780	20.83	54.27	0.59	1.40	−1.02	0.656	14.04	4.67	
1H-1, 131	1.31	1.31	0.07858	16.7	0.06260	22.73	45.48	0.51	1.39	−0.86	0.670	9.27	8.47	
1H-1, 141	1.41	1.41	0.08458	16.7	0.06700	25.00	45.20	0.57	1.67	−0.86	0.762	10.12	9.50	
1H-2, 1	1.51	1.51	0.09058	16.7	0.07100	25.00	35.73	0.47	1.19	−1.02	0.787	8.88	15.03	Contains some ash A
1H-2, 11	1.61	1.61	0.09657	16.7			3.64	0.06			0.997		50.90	Ash A, not processed
1H-2, 21	1.71	1.71	0.10257	16.7			2.70	0.04			0.898		35.90	Ash A, not processed
1H-2, 31	1.81	1.81	0.10857	16.7			4.21	0.06			0.819		31.27	Ash A, not processed
1H-2, 41	1.91	1.91	0.11457	16.7	0.07614		61.67	0.75	1.45	−1.34	0.727	12.79	12.23	
1H-2, 51	2.01	2.01	0.12057	16.7			9.53	0.15			0.969		113.50	Ash B, not processed
1H-2, 61	2.11	2.11	0.12657	16.7	0.07871	10.53	60.48	0.73	1.57	−1.38	0.720	12.91	5.57	
1H-2, 71	2.21	2.21	0.13256	16.7	0.08000	10.53	57.76	0.73	1.48	−1.52	0.755	12.60	5.07	
1H-2, 81	2.31	2.31	0.13856	16.7	0.08950	10.53	67.15	0.87	1.41	−1.38	0.777	10.23	4.80	
1H-2, 91	2.41	2.41	0.14456	16.7	0.09900	13.04	58.98	0.76	1.48	−1.73	0.769	12.29	10.17	
1H-2, 101	2.51	2.51	0.15056	16.7	0.10667	13.04	57.66	0.73	1.26	−1.69	0.755	9.94	13.63	
1H-2, 111	2.61	2.61	0.15656	16.7	0.11433	13.04	57.40	0.74	1.16	−1.56	0.769	8.27	13.80	
1H-2, 121	2.71	2.71	0.16256	16.7	0.12200	23.08	51.61	0.65	1.07	−1.92	0.755	10.93	11.53	
1H-2, 131	2.81	2.81	0.16855	16.7	0.12633	23.07	50.19	0.59	1.06	−1.50	0.705	14.89	12.83	
1H-2, 141	2.91	2.91	0.17455	16.7	0.13067	23.08	51.83	0.68	1.14	−0.93	0.784	18.07	14.40	
1H-3, 1	3.01	3.01	0.18055	16.7	0.13500	13.89	56.24	0.75	1.20	−0.37	0.798	16.87	10.90	
1H-3, 11	3.11	3.11	0.18655	16.7	0.14220	13.89	57.90	0.73	1.39	−0.55	0.755	22.75	11.53	
1H-3, 21	3.21	3.21	0.19255	16.7	0.14940	13.89	49.60	0.58	1.37	−0.66	0.698	17.81	11.20	
1H-3, 31	3.31	3.31	0.19855	16.7	0.15660	13.89	54.77	0.68	1.35	−0.65	0.741	19.87	8.00	
1H-3, 41	3.41	3.41	0.20454	16.7	0.16380	13.89	54.65	0.71	1.17	−0.75	0.784	15.59	6.73	
1H-3, 51	3.51	3.51	0.21054	16.7	0.17100	16.67	55.76	0.70	1.21	−1.25	0.755	16.85	6.00	
1H-3, 61	3.61	3.61	0.21654	16.7	0.17700	16.67	57.95	0.73	1.47	−0.94	0.755	15.99	8.30	
1H-3, 71	3.71	3.71	0.22254	16.7	0.18300	18.18	60.11	0.81	1.31	−0.99	0.812	10.18	8.30	
1H-3, 81	3.81	3.81	0.22854	16.7	0.18850	18.18	62.37	0.84	1.41	−1.27	0.805	12.15	7.70	
1H-3, 91	3.91	3.91	0.23454	16.7	0.19400	9.09	55.54	0.75	1.41	−1.95	0.812	10.53	9.63	
1H-3, 101	4.01	4.01	0.24053	16.7	0.20500	15.45	65.38	0.89	1.48	−1.27	0.812	12.01	10.10	
1H-3, 111	4.11	4.11	0.24653	16.7	0.21147	16.41	67.08	0.86	1.45	−1.56	0.769	10.46	6.10	
1H-3, 121	4.21	4.21	0.25253	16.7	0.21757	19.16	62.28	0.77	1.55	−1.70	0.741	15.66	7.50	
1H-3, 131	4.31	4.31	0.25853	16.7	0.22278	19.17	57.23	0.69	1.40	−1.28	0.727	14.32	11.37	
1H-3, 141	4.41	4.41	0.26453	16.7	0.22800	23.00	59.30	0.85	1.42	−0.97	0.855	12.02	10.70	
1H-4, 1	4.51	4.51	0.27053	16.7	0.23235	23.00	62.19	0.81	1.47	−1.04	0.778	6.74	7.54	
1H-4, 11	4.61	4.61	0.27652	16.7	0.23670	26.95	60.07	0.74	1.35	−1.46	0.741	11.22	8.27	
1H-4, 21	4.71	4.71	0.28252	16.7	0.24041	29.09	55.52	0.65	1.26	−1.29	0.698	18.39	7.20	
1H-4, 31	4.81	4.81	0.28852	16.7	0.24384	29.10	53.02	0.65	1.52	−0.90	0.734	14.64	8.47	
1H-4, 41	4.91	4.91	0.29452	16.7	0.24728	22.80	57.60	0.78	1.30	−0.58	0.812	12.78	13.10	
1H-4, 51	5.01	5.01	0.30052	16.7	0.25167	18.75	59.01	0.76	1.39	−0.63	0.769	14.12	16.40	
1H-4, 61	5.11	5.11	0.30652	16.7	0.25700	17.50	58.68	0.71	1.21	−0.94	0.727	16.24	8.47	
1H-4, 71	5.21	5.21	0.31251	16.7	0.26271	17.50	50.51	0.64	1.17	−0.88	0.755	9.14	10.27	
1H-4, 81	5.31	5.31	0.31851	16.7	0.26843	17.51	49.31	0.65	1.31	−0.69	0.791	5.61	14.10	

121-758B-														
1H-3, 81	3.81	5.32	0.31911	16.7	0.26900	11.11	49.10	0.61	1.48	−0.63	0.741	6.09	13.30	
1H-3, 91	3.91	5.42	0.32511	16.7	0.27800	11.11	53.90	0.76	1.65	−0.93	0.841	4.70	14.80	
1H-3, 101	4.01	5.52	0.33111	16.7	0.28700	12.50	61.74	0.79	1.55	−1.28	0.769	8.73	9.87	
1H-3, 111	4.11	5.62	0.33711	16.7	0.29500	15.48	59.60	0.71	1.46	−0.94	0.712	5.07	9.20	
1H-3, 121	4.21	5.72	0.34311	16.7	0.30146	20.31	66.99	0.91	1.61	−1.12	0.812	9.09	7.70	
1H-3, 131	4.31	5.82	0.34910	16.7	0.30639	20.31	73.88	1.01	1.51	−1.18	0.819	5.76	6.00	
1H-3, 141	4.41	5.92	0.35510	16.7	0.31131	20.31	68.69	0.98	1.50	−1.48	0.855	6.66	6.20	
1H-4, 1	4.51	6.02	0.36110	16.7	0.31623	20.31	60.63	0.80	1.29	−1.57	0.791	4.41	9.43	
1H-4, 11	4.61	6.12	0.36710	16.7	0.32115	20.31	62.54	0.85	1.19	−1.68	0.812	5.48	11.40	
1H-4, 21	4.71	6.22	0.37310	16.7	0.32608	20.31	71.18	1.00	1.28	−1.70	0.841	4.90	9.00	
1H-4, 31	4.81	6.32	0.37910	16.7	0.33100	30.00	65.70	0.84	1.04	−1.73	0.762	8.33	10.23	
1H-4, 41	4.91	6.42	0.38510	16.7	0.33433	29.99	55.04	0.69	0.99	−1.50	0.755	11.35	12.70	
1H-4, 51	5.01	6.52	0.39109	16.7	0.33767	30.00	56.28	0.71	1.06	−0.93	0.755	13.08	13.80	
1H-4, 61	5.11	6.62	0.39709	16.7	0.34100	12.66	57.75	0.77	1.34	−0.49	0.798	11.24	14.57	
1H-4, 71	5.21	6.72	0.40309	16.7	0.34890	12.66	57.88	0.78	1.40	−0.77	0.812	10.22	12.30	
1H-4, 81	5.31	6.82	0.40909	16.7	0.35680	12.66	53.87	0.67	1.30	−0.82	0.741	7.49	13.90	
1H-4, 91	5.41	6.92	0.41509	16.7	0.36470	12.66	55.63	0.73	1.49	−0.78	0.784	7.00	12.87	
1H-4, 101	5.51	7.02	0.42109	16.7	0.37261	12.66	57.83	0.76	1.43	−1.17	0.784	6.09	11.47	
1H-4, 111	5.61	7.12	0.42708	16.7	0.38051	12.66	57.61	0.72	1.52	−1.52	0.748	6.36	10.80	
1H-4, 121	5.71	7.22	0.43308	16.7	0.38841	12.66	56.79	0.76	1.45	−1.54	0.798	6.35	11.30	
1H-4, 131	5.81	7.32	0.43908	16.7			52.04	0.70			0.805	2.49	9.73	Insufficient foraminifers
1H-4, 141	5.91	7.42	0.44508	16.7	0.40421	12.66	53.18	0.75	1.81	−1.81	0.841	2.82	10.70	
121-758A-														
2H-1, 1	6.01	7.43	0.44568	16.7	0.40500	6.90	49.89	0.62	1.62	−1.73	0.742	2.68	13.30	
2H-1, 11	6.11	7.53	0.45168	16.7	0.41950	6.90	54.57	0.65	1.44	−1.72	0.712	2.57	11.90	
2H-1, 21	6.21	7.63	0.45768	16.7	0.43400	11.36	51.28	0.68	1.44	−0.49	0.798	8.46	14.80	
2H-1, 31	6.31	7.73	0.46367	16.7	0.44280	11.36	53.41	0.65	1.54	−0.56	0.727	10.17	12.10	
2H-1, 41	6.41	7.83	0.46967	16.7	0.45160	11.36	51.59	0.61	1.56	−0.63	0.712	7.88	12.63	
2H-1, 51	6.51	7.93	0.47567	16.7	0.46040	11.36	51.08	0.67	1.61	−1.05	0.784	5.83	11.40	
2H-1, 61	6.61	8.03	0.48167	16.7	0.46920	11.36	52.04	0.66	1.66	−1.32	0.755	6.97	11.07	
2H-1, 71	6.71	8.13	0.48767	16.7	0.47800	7.69	55.71	0.70	1.72	−1.30	0.755	5.63	11.20	
2H-1, 81	6.81	8.23	0.49367	16.7	0.49100	4.55	48.79	0.61	2.06	−1.64	0.748	3.89	12.80	
2H-1, 91	6.91	8.33	0.49966	16.7	0.51300	8.33	51.48	0.68	1.84	−1.45	0.798	3.51	13.13	
2H-1, 101	7.01	8.43	0.50566	16.7	0.52500	8.33	32.42	0.42	1.71	−1.50	0.769	1.90	23.13	Contains some ash C
2H-1, 111	7.11	8.53	0.51166	16.7			3.14	0.05			0.933		18.80	Ash C, not processed
2H-1, 121	7.21	8.63	0.51766	16.7	0.53800	7.14	35.26	0.48	1.57	−1.27	0.812	2.95	10.57	Contains some ash C
2H-1, 131	7.31	8.73	0.52366	16.7	0.55200	27.27	53.42	0.68	1.56	−1.48	0.762	6.77	9.27	
2H-1, 141	7.41	8.83	0.52966	16.7	0.55567	27.28	52.51	0.65	1.52	−1.30	0.741	9.53	6.50	
2H-2, 1	7.51	8.93	0.53565	16.7	0.55933	27.27	54.86	0.69	1.36	−1.20	0.758	9.41	8.24	
2H-2, 11	7.61	9.03	0.54165	16.7	0.56300	31.82	59.60	0.77	1.32	−1.13	0.777	15.52	8.60	
2H-2, 21	7.71	9.13	0.54765	16.7	0.56614	31.82	51.44	0.72	1.40	−1.33	0.841	9.86	13.80	
2H-2, 31	7.81	9.23	0.55365	16.7	0.56929	31.82	49.19	0.70	1.44	−1.60	0.848	6.94	18.77	
2H-2, 41	7.91	9.33	0.55965	16.7	0.57243	26.52	60.61	0.79	1.48	−1.62	0.784	7.99	14.27	
2H-2, 51	8.01	9.43	0.56565	16.7	0.57620	22.73	56.24	0.72	1.52	−2.00	0.769	6.64	11.60	
2H-2, 61	8.11	9.53	0.57164	16.7	0.58060	22.73	57.91	0.80	1.31	−1.46	0.826	8.93	11.03	
2H-2, 71	8.21	9.63	0.57764	16.7	0.58500	18.18	67.88	0.92	1.40	−1.34	0.812	13.08	8.57	
2H-2, 81	8.31	9.73	0.58364	16.7	0.59050	18.18	61.73	0.85	1.26	−1.63	0.826	11.70	12.50	
2H-2, 91	8.41	9.83	0.58964	16.7	0.59600	9.09	58.28	0.80	1.21	−1.71	0.826	10.52	13.07	
2H-2, 101	8.51	9.93	0.59564	16.7	0.60700	10.00	63.34	0.83	1.23	−1.47	0.784	8.31	10.43	
2H-2, 111	8.61	10.03	0.60164	16.7	0.61700	17.86	54.08	0.67	1.21	−1.66	0.741	14.11	12.60	
2H-2, 121	8.71	10.13	0.60763	16.7	0.62260	17.86	54.62	0.65	1.28	−1.07	0.712	17.63	10.27	
2H-2, 131	8.81	10.23	0.61363	16.7	0.62820	16.05	53.74	0.63	1.18	−0.56	0.698	7.56	10.03	
2H-2, 141	8.91	10.33	0.61963	16.7	0.63443	14.58	50.07	0.58	1.37	−0.63	0.698	13.41	10.10	
2H-3, 1	9.01	10.43	0.62563	16.7	0.64129	14.58	53.13	0.81	1.41	−0.77	0.912	11.69	10.93	
2H-3, 11	9.11	10.53	0.63163	16.7	0.64814	14.58	57.02	0.71	1.20	−0.99	0.748	15.11	15.30	
2H-3, 21	9.21	10.63	0.63763	16.7	0.65500	14.58	54.25	0.71	1.21	−1.01	0.784	7.87	12.00	
2H-3, 31	9.31	10.73	0.64362	16.7	0.66186	14.58	51.69	0.65	1.41	−1.37	0.755	8.97	12.43	
2H-3, 41	9.41	10.83	0.64962	16.7	0.66871	14.58	58.59	0.75	1.17	−1.43	0.769	9.86	10.90	
2H-3, 51	9.51	10.93	0.65562	16.7	0.67557	16.52	55.53	0.76	1.37	−1.63	0.826	5.08	13.40	
2H-3, 61	9.61	11.03	0.66162	16.7	0.68163	19.05	59.60	0.79	1.46	−1.63	0.798	11.64	10.23	

Appendix F (continued).

Core, section, interval (cm)	ODP depth (mbsf)	Composite depth (m)	Magnetic age (m.y.)	Magnetic sedimentation rate (m/m.y.)	$\delta^{18}O$ age (m.y.)	$\delta^{18}O$ sedimentation rate (m/m.y.)	Mean (wt% $CaCO_3$)	Magnetic $CaCO_3$ MAR ($g/cm^2/k.y.$)	$\delta^{13}C$ ‰ to (PDB)	$\delta^{18}O$ ‰ to (PDB)	Dry-bulk density (g/cm^3)	Coarse fraction (wt% >150 μm)	Interpolated MS K (10-6) (cgs)	Comment
121-758A-(Cont.)														
2H-3, 71	9.71	11.13	0.66762	16.7	0.68688	19.05	69.72	0.88	1.29	−1.49	0.755	19.84	6.10	
2H-3, 81	9.81	11.23	0.67362	16.7	0.69213	19.05	63.74	0.84	1.42	−1.36	0.791	19.17	6.90	
2H-3, 91	9.91	11.33	0.67961	16.7	0.69738	18.60	50.01	0.62	1.23	−1.01	0.741	7.06	11.53	
2H-3, 101	10.01	11.43	0.68561	16.7	0.70275	18.18	58.20	0.76	1.26	−0.90	0.784	9.18	10.23	
2H-3, 111	10.11	11.53	0.69161	16.7	0.70825	19.05	61.90	0.83	1.28	−1.18	0.805	12.94	7.00	
2H-3, 121	10.21	11.63	0.69761	16.7	0.71350	20.00	66.30	0.85	1.31	−1.13	0.769	21.38	5.70	
2H-3, 131	10.31	11.73	0.70361	16.7	0.71850	22.22	52.88	0.67	1.14	−0.97	0.755	11.88	7.77	
2H-3, 141	10.41	11.83	0.70961	16.7	0.72300	25.00	59.71	0.82	1.22	−0.94	0.826	10.77	8.40	
2H-4, 1	10.51	11.93	0.71560	16.7	0.72700	25.00	57.90	0.72	1.30	−1.65	0.741	8.02	9.30	
2H-4, 11	10.61	12.03	0.72160	16.7	0.73100	28.94	56.20	0.74	1.34	−1.92	0.791	8.55	10.30	
2H-4, 21	10.71	12.13	0.72760	16.7	0.73446	28.94	42.43	0.57	1.21	−1.77	0.812	5.76	10.70	
2H-4, 31	10.81	12.23	0.73318	17.9			12.65	0.21			0.947		13.23	Ash D, not processed
2H-4, 41	10.91	12.33	0.73847	18.9			2.69	0.05			1.040		34.80	Ash D, not processed
2H-4, 51	11.01	12.43	0.74377	18.9	0.74482	28.94	55.97	0.75	1.16	−0.98	0.712	15.17	13.40	
2H-4, 61	11.11	12.53	0.74906	18.9	0.74827	26.25	52.26	0.80	1.26	−0.78	0.812	13.38	12.70	
2H-4, 71	11.21	12.63	0.75435	18.9	0.75208	24.00	54.71	0.84	1.60	−0.77	0.812	8.63	13.07	
2H-4, 81	11.31	12.73	0.75965	18.9	0.75625	24.00	50.57	0.80	1.49	−1.08	0.834	6.20	16.40	
2H-4, 91	11.41	12.83	0.76494	18.9	0.76042	24.00	57.42	0.87	1.54	−1.21	0.798	6.47	18.83	Ash D
2H-4, 101	11.51	12.93	0.77024	18.9	0.76458	24.00	48.88	0.75	1.24	−1.54	0.812	8.30	12.87	
2H-4, 111	11.61	13.03	0.77553	18.9	0.76875	24.00	33.50	0.57	1.42	−1.69	0.898	4.76	33.70	Ash E, and below
2H-4, 121	11.71	13.13	0.78082	18.9	0.77292	23.45	69.94	1.02	1.25	−1.66	0.769	13.09	14.57	
2H-4, 131	11.81	13.23	0.78612	18.9	0.77718	22.92	65.10	0.98	1.36	−1.38	0.798	9.46	9.30	
2H-4, 141	11.91	13.33	0.79141	18.9	0.78155	22.91	64.57	1.01	1.10	−1.50	0.826	7.72	9.50	
2H-5, 1	12.01	13.43	0.79671	18.9	0.78591	22.91	64.08	1.00	1.24	−1.57	0.826	9.66	8.73	
2H-5, 11	12.11	13.53	0.80200	18.9	0.79027	22.92	50.80	0.75	1.03	−0.74	0.777	12.41	11.70	
2H-5, 21	12.21	13.63	0.80729	18.9	0.79464	22.91	54.76	0.84	1.21	−0.38	0.812	9.69	10.80	
2H-5, 31	12.31	13.73	0.81259	18.9	0.79900	15.00	53.35	0.78	1.32	−0.75	0.777	11.02	9.80	
2H-5, 41	12.41	13.83	0.81788	18.9	0.80567	15.00	48.03	0.76	1.16	−0.63	0.841	7.14	8.60	
2H-5, 51	12.51	13.93	0.82318	18.9	0.81233	15.00	57.91	0.89	1.44	−0.74	0.812	7.45	7.70	
2H-5, 61	12.61	14.03	0.82847	18.9	0.81900	13.16	65.11	1.05	1.24	−1.18	0.855	11.29	7.40	
2H-5, 71	12.71	14.13	0.83377	18.9	0.82660	13.16	58.50	0.96	1.23	−1.06	0.869	10.58	7.37	
2H-5, 81	12.81	14.23	0.83906	18.9	0.83420	13.70	51.56	0.82	1.45	−0.96	0.841	6.61	8.80	
2H-5, 91	12.91	14.33	0.84435	18.9	0.84150	14.29	60.93	0.95	1.45	−1.03	0.826	8.58	8.73	
2H-5, 101	13.01	14.43	0.84965	18.9	0.84850	14.29	56.60	0.88	1.29	−1.52	0.826	3.37	9.10	
2H-5, 111	13.11	14.53	0.85494	18.9	0.85550	18.75	58.94	0.95	1.52	−1.72	0.855	5.05	11.60	
2H-5, 121	13.21	14.63	0.86024	18.9	0.86083	27.27	64.39	0.99	1.37	−1.62	0.812	4.55	10.63	
2H-5, 131	13.31	14.73	0.86553	18.9	0.86450	27.27	57.31	0.88	1.17	−1.68	0.812	4.91	11.40	
2H-6, 1	13.51	14.93	0.87612	18.9	0.87183	27.27	72.36	1.22	1.47	−1.12	0.895	4.14	6.66	
2H-6, 11	13.61	15.03	0.88141	18.9	0.87550	27.27	71.49	1.16	1.58	−1.30	0.862	5.66	6.47	
2H-6, 21	13.71	15.13	0.88671	18.9	0.87917	18.50	65.04	1.07	1.64	−1.79	0.869	4.25	6.90	
2H-6, 31	13.81	15.23	0.89200	18.9	0.88457	14.00	66.38	1.05	1.63	−1.69	0.841	8.80	9.17	
2H-6, 41	13.91	15.33	0.89729	18.9	0.89171	14.00	72.12	1.24	1.67	−1.34	0.912	4.45	6.60	
2H-6, 51	14.01	15.43	0.90259	18.9	0.89886	14.00	71.05	1.19	1.84	−1.29	0.883	5.75	6.20	
2H-6, 61	14.11	15.53	0.90788	18.9	0.90600	12.50	63.91	1.04	1.89	−1.56	0.862	7.82	9.27	
2H-6, 71	14.21	15.63	0.91350	17.8	0.91400	12.50	57.59	0.88	1.62	−1.40	0.855	7.27	12.30	
2H-6, 81	14.31	15.73	0.91933	17.1	0.92200	8.33	66.65	0.98	1.79	−1.43	0.855	7.73	8.70	
2H-6, 91	14.41	15.83	0.92517	17.1	0.93400	8.33	65.58	0.93	1.60	−1.54	0.826	8.01	8.50	
2H-6, 101	14.51	15.93	0.93100	17.1	0.94600	21.05	63.49	0.85	1.77	−1.58	0.784	12.95	7.40	
2H-6, 111	14.61	16.03	0.93683	17.1	0.95075	21.05	65.05	0.95	1.33	−1.59	0.848	14.78	5.40	
2H-6, 121	14.71	16.13	0.94267	17.1	0.95550	21.05	71.51	0.98	1.58	−1.29	0.798	10.49	4.47	
2H-6, 131	14.81	16.23	0.94850	17.1	0.96025	21.05	73.04	0.97	1.35	−1.13	0.777	11.45	3.87	
2H-6, 141	14.91	16.33	0.95433	17.1	0.96500	25.00	71.40	1.03	1.18	−1.25	0.841	13.66	4.00	
2H-7, 1	15.01	16.43	0.96017	17.1	0.96900	25.00	57.22	0.81	1.37	−1.31	0.826	8.81	8.13	
2H-7, 11	15.11	16.53	0.96600	17.1	0.97300	25.00	57.32	0.85	1.40	−1.46	0.869	7.39	11.67	

2H-7, 21	15.21	16.63	0.97183	17.1	0.97700	25.00	58.29	0.80	1.46	−1.69	0.798	7.10	8.60	
2H-7, 31	15.31	16.73	0.97767	17.1	0.98100	25.00	57.56	0.74	1.37	−1.66	0.755	8.54	9.77	
2H-7, 41	15.41	16.83	0.98361	16.8	0.98500	13.13	64.97	0.93	1.46	−1.51	0.855	14.65	6.67	
2H-7, 51	15.51	16.93	0.98963	16.6	0.99262	13.13	61.43	0.78	1.49	−1.62	0.762	11.46	6.40	
2H-7, 61	15.61	17.03	0.99565	16.6	1.00023	13.13	60.23	0.82	1.47	−1.62	0.819	11.95	7.50	
2H-7, 71	15.71	17.13	1.00166	16.6			63.41	0.83	1.48	−1.22	0.784	13.13	7.57	
2H-CC, 1	15.78	17.20	1.00588	16.6			65.96	0.89	1.77	−1.51	0.812	13.02	6.20	
121-758B-														
2H-5, 21	15.71	17.21	1.00648	16.7			63.96	0.84	1.34	−1.40	0.784	13.63	6.00	
2H-5, 31	15.81	17.31	1.01250	16.6			67.40	0.90	1.09	−1.35	0.805	18.57	6.07	
2H-5, 41	15.91	17.41	1.01851	16.6			54.76	0.73	1.25	−1.15	0.798	13.03	9.77	
2H-5, 51	16.01	17.51	1.02453	16.6			59.97	0.78	1.19	−1.44	0.784	12.42	9.00	
2H-5, 61	16.11	17.61	1.03055	16.6			57.46	0.80	1.58	−1.34	0.841	9.49	9.40	
2H-5, 71	16.21	17.71	1.03657	16.6			65.09	0.86	1.39	−1.32	0.798	9.45	5.37	
121-758A-														
3H-1, 21	15.81	17.72	1.03717	16.7			62.43	0.84	1.41	−1.40	0.812	8.13	5.00	
3H-1, 31	15.91	17.82	1.04319	16.6			57.61	0.74	1.66	−1.55	0.777	9.17	4.50	
3H-1, 41	16.01	17.92	1.04920	16.6			62.07	0.78	1.26	−1.51	0.755	13.10	3.67	
3H-1, 51	16.11	18.02	1.05522	16.6			64.56	0.87	1.51	−1.45	0.812	14.85	4.50	
3H-1, 61	16.21	18.12	1.06124	16.6			55.09	0.70	1.37	−1.55	0.769	15.89	10.97	
3H-1, 71	16.31	18.22	1.06726	16.6			63.84	0.79	1.51	−1.15	0.741	18.95	5.20	
3H-1, 81	16.41	18.32	1.07327	16.6			64.24	0.84	1.44	−1.14	0.784	18.13	4.60	
3H-1, 91	16.51	18.42	1.07929	16.6			58.08	0.81	1.54	−1.37	0.841	15.85	6.13	
3H-1, 101	16.61	18.52	1.08531	16.6			59.86	0.79	1.61	−1.29	0.798	14.46	5.93	
3H-1, 111	16.71	18.62	1.09133	16.6			58.53	0.78	1.39	−1.25	0.798	7.86	5.90	
3H-1, 121	16.81	18.72	1.09735	16.6			60.29	0.81	1.41	−1.65	0.812	10.66	4.23	
3H-1, 131	16.91	18.82	1.10336	16.6			65.42	0.85	1.46	−1.36	0.777	13.73	2.33	
3H-1, 141	17.01	18.92	1.10938	16.6			58.57	0.71	1.18	−1.21	0.734	17.46	4.60	
3H-2, 1	17.11	19.02	1.11540	16.6			51.56	0.68	1.23	−0.88	0.791	10.35	7.03	
3H-2, 11	17.21	19.12	1.12142	16.6			53.66	0.72	1.39	−0.73	0.805	10.97	9.97	
3H-2, 21	17.31	19.22	1.12743	16.6			56.82	0.82	1.46	−1.32	0.869	11.97	9.50	
3H-2, 31	17.41	19.32	1.13345	16.6			59.69	0.80	1.57	−1.26	0.805	10.24	9.03	
3H-2, 41	17.51	19.42	1.13947	16.6			63.90	0.83	1.68	−1.37	0.784	11.56	8.57	
3H-2, 51	17.61	19.52	1.14549	16.6			61.54	0.79	1.76	−1.84	0.777	14.29	8.20	
3H-2, 61	17.71	19.62	1.15150	16.6			60.12	0.83	1.39	−1.12	0.826	12.16	8.07	
3H-2, 71	17.81	19.72	1.15752	16.6			58.51	0.76	1.43	−1.07	0.784	16.05	9.37	
3H-2, 81	17.91	19.82	1.16354	16.6			49.49	0.70	1.51	−1.04	0.848	11.49	11.20	
3H-2, 91	18.01	19.92	1.16956	16.6			61.82	0.83	1.72	−1.21	0.812	7.19	7.63	
3H-2, 101	18.11	20.02	1.17558	16.6			61.92	0.84	1.79	−1.64	0.812	11.00	7.37	
3H-2, 111	18.21	20.12	1.18159	16.6			65.22	0.82	1.44	−1.64	0.755	14.72	4.30	
3H-2, 121	18.31	20.22	1.18761	16.6			64.48	0.85	1.39	−1.32	0.798	15.65	4.17	
3H-2, 131	18.41	20.32	1.19363	16.6			62.36	0.83	1.50	−1.50	0.798	12.69	4.43	
3H-2, 141	18.51	20.42	1.19965	16.6			57.17	0.81	1.54	−1.47	0.855	8.04	8.20	
3H-3, 1	18.61	20.52	1.20566	16.6			60.22	0.84	1.83	−1.07	0.838	5.82	7.20	
3H-3, 11	18.71	20.62	1.21168	16.6			56.85	0.77	1.90	−1.59	0.819	5.73	10.80	
3H-3, 21	18.81	20.72	1.21770	16.6			60.19	0.84	1.56	−1.82	0.841	9.11	9.40	
3H-3, 31	18.91	20.82	1.22372	16.6			64.99	0.88	1.56	−1.36	0.819	9.54	7.23	
3H-3, 41	19.01	20.92	1.22973	16.6			66.84	0.87	1.57	−1.39	0.784	8.81	6.97	
3H-3, 51	19.11	21.02	1.23575	16.6			61.05	0.80	1.54	−1.30	0.784	10.82	8.00	
3H-3, 61	19.21	21.12	1.24177	16.6			60.66	0.77	1.68	−1.27	0.762	6.24	9.83	
3H-3, 71	19.31	21.22	1.24779	16.6			60.20	0.80	1.79	−1.45	0.798	9.64	7.60	
3H-3, 81	19.41	21.32	1.25381	16.6			63.63	0.86	1.75	−1.41	0.812	8.90	8.20	
3H-3, 91	19.51	21.42	1.25982	16.6			62.33	0.81	1.81	−1.70	0.784	9.25	9.37	
3H-3, 101	19.61	21.52	1.26584	16.6			59.22	0.77	1.61	−1.50	0.784	8.88	9.20	
3H-3, 111	19.71	21.62	1.27186	16.6			56.15	0.70	1.25	−1.61	0.748	11.17	6.60	
3H-3, 121	19.81	21.72	1.27788	16.6			31.20	0.41	1.33	−1.44	0.784	5.64	12.40	Ash F, and below
3H-3, 131	19.91	21.82	1.28389	16.6			56.60	0.79	1.20	−1.59	0.841	10.16	12.73	
3H-3, 141	20.01	21.92	1.28991	16.6			61.11	0.80	1.41	−1.27	0.784	8.17	8.40	
3H-4, 1	20.11	22.02	1.29593	16.6			58.22	0.83	1.78	−1.60	0.855	9.05	8.87	
3H-4, 11	20.21	22.12	1.30195	16.6			61.41	0.88	1.81	−2.17	0.862	9.87	9.20	

Appendix F (continued).

Core, section, interval (cm)	ODP depth (mbsf)	Composite depth (m)	Magnetic age (m.y.)	Magnetic sedimentation rate (m/m.y.)	$\delta^{18}O$ age (m.y.)	$\delta^{18}O$ sedimentation rate (m/m.y.)	Mean (wt% $CaCO_3$)	Magnetic $CaCO_3$ MAR ($g/cm^2/k.y.$)	$\delta^{13}C$ ‰ to (PDB)	$\delta^{18}O$ ‰ to (PDB)	Dry-bulk density (g/cm^3)	Coarse fraction (wt% >150 μm)	Interpolated MS K (10-6) (cgs)	Comment
121-758A-(Cont.)														
3H-4, 21	20.31	22.22	1.30796	16.6			67.38	0.89	1.55	−1.82	0.798	10.32	5.60	
3H-4, 31	20.41	22.32	1.31398	16.6			58.06	0.78	1.26	−1.89	0.805	11.63	5.37	
3H-4, 41	20.51	22.42	1.32000	16.6			55.77	0.70	1.19	−1.46	0.755	14.56	5.63	
3H-4, 51	20.61	22.52	1.32602	16.6			61.14	0.90	1.63	−1.15	0.883	9.52	6.20	
3H-4, 61	20.71	22.62	1.33204	16.6			57.12	0.77	1.83	−1.38	0.812	9.41	6.87	
3H-4, 71	20.81	22.72	1.33805	16.6			62.18	0.94	1.79	−1.55	0.912	7.61	7.03	
3H-4, 81	20.91	22.82	1.34407	16.6			63.64	0.90	1.97	−2.18	0.855	8.59	7.10	
3H-4, 91	21.01	22.92	1.35009	16.6			68.93	0.96	1.74	−1.68	0.841	9.57	7.10	
3H-4, 101	21.11	23.02	1.35611	16.6			61.21	0.84	1.78	−1.63	0.826	12.23	8.47	
3H-4, 111	21.21	23.12	1.36212	16.6			62.70	0.85	1.68	−1.30	0.812	11.61	7.60	
3H-4, 121	21.31	23.22	1.36814	16.6			64.15	0.85	1.76	−1.22	0.798	10.67	6.27	
3H-4, 131	21.41	23.32	1.37416	16.6			63.22	0.88	1.80	−1.52	0.834	9.70	6.30	
3H-4, 141	21.51	23.42	1.38018	16.6			59.85	0.82	2.09	−1.61	0.826	11.97	8.50	
3H-5, 1	21.61	23.52	1.38619	16.6			66.09	0.93	1.96	−1.79	0.849	16.10	4.17	
3H-5, 11	21.71	23.62	1.39221	16.6			65.05	0.87	1.47	−1.64	0.805	14.72	6.37	
3H-5, 21	21.81	23.72	1.39823	16.6			58.88	0.79	1.32	−1.47	0.812	16.03	7.10	
3H-5, 31	21.91	23.82	1.40425	16.6			60.36	0.84	1.68	−1.30	0.841	11.58	7.07	
3H-5, 41	22.01	23.92	1.41027	16.6			61.87	0.89	1.84	−1.35	0.869	10.37	9.07	
3H-5, 51	22.11	24.02	1.41628	16.6			61.10	0.87	1.95	−1.59	0.855	7.10	8.80	
3H-5, 61	22.21	24.12	1.42230	16.6			65.16	0.91	1.90	−1.47	0.841	8.38	6.43	
3H-5, 71	22.31	24.22	1.42832	16.6			64.04	0.94	1.82	−1.68	0.883	10.62	6.77	
3H-5, 81	22.41	24.32	1.43434	16.6			61.29	0.87	1.82	−1.84	0.855	12.02	5.60	
3H-5, 91	22.51	24.42	1.44035	16.6			62.85	0.89	1.77	−1.41	0.855	12.71	4.20	
3H-5, 101	22.61	24.52	1.44637	16.6			63.81	0.89	1.73	−1.28	0.841	9.37	4.77	
3H-5, 111	22.71	24.62	1.45239	16.6			63.85	0.94	1.80	−1.52	0.883	9.07	5.40	
3H-5, 121	22.81	24.72	1.45841	16.6			62.62	0.83	1.72	−1.67	0.798	9.14	6.21	
3H-6, 1	23.11	25.02	1.47646	16.6			65.69	0.91	2.01	−1.79	0.831	11.85	6.39	
3H-6, 11	23.21	25.12	1.48248	16.6			64.11	0.93	1.81	−1.45	0.869	8.30	7.00	
3H-6, 21	23.31	25.22	1.48850	16.6			63.98	0.91	1.85	−1.60	0.855	12.31	7.60	
3H-6, 31	23.41	25.32	1.49451	16.6			58.15	0.85	2.08	−1.88	0.876	12.39	8.43	
3H-6, 41	23.51	25.42	1.50053	16.6			66.40	0.91	2.08	−1.31	0.826	9.94	7.20	
3H-6, 51	23.61	25.52	1.50655	16.6			63.71	0.89	1.98	−1.69	0.841	11.07	8.50	
3H-6, 61	23.71	25.62	1.51257	16.6			61.54	0.83	1.94	−1.75	0.812	14.12	6.70	
3H-6, 71	23.81	25.72	1.51858	16.6			59.44	0.83	1.65	−1.30	0.841	9.51	7.70	
3H-6, 81	23.91	25.82	1.52460	16.6			60.69	0.86	1.79	−1.25	0.855	12.72	5.20	
3H-6, 91	24.01	25.92	1.53062	16.6			62.78	0.89	1.74	−1.32	0.855	12.49	4.30	
3H-6, 101	24.11	26.02	1.53664	16.6			49.17	0.67	1.50	−1.39	0.826	7.33	7.37	
3H-6, 111	24.21	26.12	1.54265	16.6			59.04	0.85	1.72	−1.50	0.869	8.03	7.50	
3H-6, 121	24.31	26.22	1.54867	16.6			67.30	1.02	1.49	−1.62	0.912	10.50	6.50	
3H-6, 131	24.41	26.32	1.55469	16.6			67.68	0.85	1.54	−1.73	0.755	12.40	6.43	
3H-6, 141	24.51	26.42	1.56071	16.6			62.31	0.84	1.35	−1.62	0.812	13.76	11.00	
3H-7, 1	24.61	26.52	1.56673	16.6			61.32	0.85	1.42	−1.43	0.834	13.58	6.87	
3H-7, 11	24.71	26.62	1.57274	16.6			56.60	0.76	1.06	−1.41	0.812	11.63	7.57	
3H-7, 21	24.81	26.72	1.57876	16.6			61.51	0.88	1.45	−1.36	0.862	11.56	6.20	
3H-7, 31	24.91	26.82	1.58478	16.6			61.69	0.84	1.41	−1.41	0.819	12.13	7.30	
3H-7, 41	25.01	26.92	1.59080	16.6			66.43	0.87	1.45	−1.74	0.784	14.07	6.93	
3H-7, 51	25.11	27.02	1.59681	16.6			63.49	0.87	1.42	−1.39	0.826	9.60	7.20	
3H-7, 61	25.21	27.12	1.60283	16.6			64.24	0.97	1.77	−1.47	0.912	8.73	6.25	
121-758B-														
3H-3, 141	23.31	27.13	1.60343	16.7			64.63	0.91	1.62	−1.36	0.841	9.11	5.90	
3H-4, 1	23.41	27.23	1.60945	16.6			61.54	0.93	1.62	−1.50	0.912	10.60	6.40	
3H-4, 11	23.51	27.33	1.61547	16.6			60.24	0.82	1.30	−1.73	0.819	13.16	7.93	
3H-4, 21	23.61	27.43	1.62149	16.6			59.22	0.84	1.41	−1.15	0.855	8.06	9.40	

3H-4, 31	23.71	27.53	1.62750	16.6	60.81	0.79	1.29	−1.45	0.784	7.84	9.27	
3H-4, 41	23.81	27.63	1.63352	16.6	53.93	0.74	1.47	−1.28	0.826	6.12	12.23	
3H-4, 51	23.91	27.73	1.63954	16.6	55.08	0.74	1.80	−1.34	0.812	8.49	12.10	Ash G, and below
3H-4, 73	24.13	27.95	1.65278	16.6	66.21	0.92	1.57	−1.29	0.841	8.75	38.40	
3H-4, 81	24.21	28.03	1.65759	16.6	62.79	0.92	1.37	−1.45	0.883	10.73	10.80	
3H-4, 91	24.31	28.13	1.66584	12.1	62.44	0.69	1.44	−1.65	0.912	10.44	8.13	
3H-4, 101	24.41	28.23	1.67558	10.3	64.18	0.54	1.51	−1.66	0.812	14.27	6.93	
3H-4, 111	24.51	28.33	1.68531	10.3	61.37	0.53	1.54	−1.22	0.841	10.88	6.80	
3H-4, 121	24.61	28.43	1.69504	10.3	65.67	0.64	1.49	−1.38	0.955	8.76	8.00	
3H-4, 131	24.71	28.53	1.70478	10.3	60.71	0.54	1.61	−1.49	0.869	6.21	10.60	
3H-4, 141	24.81	28.63	1.71451	10.3	64.96	0.62	1.65	−1.38	0.926	9.25	8.40	
3H-5, 1	24.91	28.73	1.72425	10.3	61.92	0.55	1.59	−1.62	0.872	10.04	6.87	
3H-5, 11	25.01	28.83	1.73398	10.3	57.02	0.52	1.45	−1.07	0.883	6.95	8.10	
3H-5, 21	25.11	28.93	1.74372	10.3	58.70	0.54	1.62	−1.38	0.898	6.62	8.30	
3H-5, 31	25.21	29.03	1.75345	10.3	59.82	0.56	1.55	−1.77	0.905	7.99	8.87	
3H-5, 41	25.31	29.13	1.76319	10.3	59.51	0.53	1.55	−1.32	0.869	6.21	8.50	
3H-5, 51	25.41	29.23	1.77292	10.3	56.86	0.51	1.58	−1.47	0.869	6.29	9.60	
3H-5, 61	25.51	29.33	1.78265	10.3	57.48	0.50	1.31	−1.82	0.841	10.50	19.27	
3H-5, 71	25.61	29.43	1.79239	10.3	60.25	0.52	1.40	−1.89	0.841	11.55	10.73	
3H-5, 81	25.71	29.53	1.80212	10.3	62.31	0.55	1.51	−1.68	0.855	13.46	6.10	
121-758A-												
4H-1, 1	25.21	29.54	1.80310	10.2	62.51	0.49	1.64	−1.67	0.771	10.35	5.73	
4H-1, 11	25.31	29.64	1.81283	10.3	58.52	0.47	1.62	−1.39	0.784	10.48	6.00	
4H-1, 21	25.41	29.74	1.82257	10.3	57.88	0.47	1.10	−1.48	0.784	9.62	5.00	
4H-1, 31	25.51	29.84	1.83230	10.3	59.82	0.48	1.93	−1.52	0.784	8.32	6.03	
4H-1, 41	25.61	29.94	1.84204	10.3	66.20	0.59	1.70	−1.50	0.869	8.91	4.20	
4H-1, 51	25.71	30.04	1.85177	10.3	68.42	0.66	1.47	−1.32	0.940	11.26	4.70	
4H-1, 61	25.81	30.14	1.86150	10.3	67.20	0.58	1.54	−1.33	0.834	8.14	7.53	
4H-1, 71	25.91	30.24	1.87124	10.3	59.82	0.56	1.76	−1.85	0.912	11.33	10.73	
4H-1, 81	26.01	30.34	1.88072	10.5	57.80	0.52	1.37	−1.46	0.855	8.36	5.20	
4H-1, 91	26.11	30.44	1.88791	13.9	59.81	0.71	1.63	−1.49	0.855	8.21	5.37	
4H-1, 101	26.21	30.54	1.89511	13.9	66.98	0.80	1.65	−1.88	0.855	10.92	4.10	
4H-1, 111	26.31	30.64	1.90230	13.9	62.89	0.79	1.46	−1.40	0.898	8.23	3.90	
4H-1, 121	26.41	30.74	1.90950	13.9	63.77	0.81	1.60	−1.55	0.912	11.29	3.73	
4H-1, 131	26.51	30.84	1.91670	13.9	68.64	0.85	2.01	−1.44	0.890	7.44	2.13	
4H-1, 141	26.61	30.94	1.92389	13.9	66.08	0.80	1.92	−1.92	0.869	8.36	1.70	
4H-2, 1	26.71	31.04	1.93109	13.9	66.19	0.80	1.81	−1.68	0.865	12.01	3.23	
4H-2, 11	26.81	31.14	1.93828	13.9	64.74	0.78	1.85	−1.65	0.869	12.17	4.73	
4H-2, 21	26.91	31.24	1.94548	13.9	65.11	0.77	1.80	−1.63	0.855	9.88	3.60	
4H-2, 31	27.01	31.34	1.95267	13.9	66.19	0.81	1.72	−1.37	0.883	12.52	3.73	
4H-2, 41	27.11	31.44	1.95987	13.9	67.37	0.79	1.55	−1.42	0.841	12.20	3.17	
4H-2, 51	27.21	31.54	1.96706	13.9	61.02	0.71	1.40	−1.12	0.834	10.09	4.30	
4H-2, 61	27.31	31.64	1.97426	13.9	63.82	0.80	1.60	−1.48	0.898	13.88	4.60	
4H-2, 71	27.41	31.74	1.98145	13.9	63.68	0.71	1.65	−1.32	0.798	12.01	5.20	
4H-2, 81	27.51	31.84	1.98865	13.9	63.62	0.76	1.58	−1.48	0.855	7.56	5.10	
4H-2, 91	27.61	31.94	1.99584	13.9	64.25	0.81	1.81	−1.53	0.912	9.45	3.97	
4H-2, 101	27.71	32.04	2.00304	13.9	63.60	0.77	1.60	−1.53	0.869	7.65	3.47	
4H-2, 111	27.81	32.14	2.01023	13.9	62.81	0.77	1.64	−1.58	0.876	6.18	4.60	
4H-2, 121	27.91	32.24	2.01743	13.9	62.10	0.74	1.64	−1.38	0.855	8.35	3.30	
4H-2, 131	28.01	32.34	2.02462	13.9	60.82	0.81	1.65	−1.22	0.955	5.31	3.47	
4H-2, 141	28.11	32.44	2.03182	13.9	63.39	0.78	1.53	−1.66	0.883	10.95	3.00	
4H-3, 1	28.21	32.54	2.03901	13.9	66.84	0.86	1.56	−0.99	0.926	8.74	3.70	
4H-3, 11	28.31	32.64	2.04621	13.9	68.26	0.85	1.57	−1.19	0.898	8.67	4.07	
4H-3, 21	28.41	32.74	2.05340	13.9	64.84	0.82	1.50	−1.23	0.912	8.52	4.00	
4H-3, 31	28.51	32.84	2.06060	13.9	65.47	0.88	1.66	−1.36	0.969	11.09	4.50	
4H-3, 41	28.61	32.94	2.06779	13.9	68.96	0.85	1.80	−1.45	0.883	9.80	4.50	
4H-3, 51	28.71	33.04	2.07499	13.9	71.76	0.92	1.73	−1.59	0.926	8.11	3.90	
4H-3, 61	28.81	33.14	2.08218	13.9	71.24	0.88	1.73	−1.90	0.890	10.87	3.97	
4H-3, 71	28.91	33.24	2.08938	13.9	71.02	0.90	1.87	−2.21	0.912	7.49	3.33	
4H-3, 81	29.01	33.34	2.09657	13.9	70.38	0.91	1.69	−1.39	0.926	9.30	3.90	
4H-3, 91	29.11	33.44	2.10377	13.9	69.93	0.91	1.76	−1.42	0.940	7.11	3.80	
4H-3, 101	29.21	33.54	2.11096	13.9	62.53	0.81	1.68	−1.52	0.926	5.12	4.17	

Appendix F (continued).

Core, section, interval (cm)	ODP depth (mbsf)	Composite depth (m)	Magnetic age (m.y.)	Magnetic sedimentation rate (m/m.y.)	$\delta^{18}O$ age (m.y.)	$\delta^{18}O$ sedimentation rate (m/m.y.)	Mean (wt% $CaCO_3$)	Magnetic $CaCO_3$ MAR ($g/cm^2/k.y.$)	$\delta^{13}C$ ‰ to (PDB)	$\delta^{18}O$ ‰ to (PDB)	Dry-bulk density (g/cm^3)	Coarse fraction (wt% >150 μm)	Interpolated MS K (10-6) (cgs)	Comment
121-758A-(Cont.)														
4H-3, 111	29.31	33.64	2.11816	13.9			65.27	0.82	1.61	−1.97	0.905	8.86	4.70	
4H-3, 121	29.41	33.74	2.12535	13.9			67.12	0.86	1.81	−1.62	0.926	6.41	4.63	
4H-3, 131	29.51	33.84	2.13255	13.9			68.03	0.83	1.59	−1.67	0.883	8.45	4.83	
4H-3, 141	29.61	33.94	2.13974	13.9			70.92	0.97	1.32	−1.42	0.983	9.73	3.80	
4H-4, 1	29.71	34.04	2.14694	13.9			69.07	0.97	1.60	−1.32	1.016	4.62	3.93	
4H-4, 11	29.81	34.14	2.15413	13.9			67.63	0.88	1.94	−2.14	0.933	7.04	4.80	
4H-4, 21	29.91	34.24	2.16133	13.9			69.54	0.88	1.81	−1.75	0.912	10.11	4.50	
4H-4, 31	30.01	34.34	2.16852	13.9			65.05	0.76	1.55	−1.82	0.841	8.78	5.73	
4H-4, 41	30.11	34.44	2.17572	13.9			61.45	0.77	1.58	−1.57	0.898	10.11	5.53	
4H-4, 51	30.21	34.54	2.18291	13.9			63.42	0.87	1.64	−1.54	0.983	5.59	5.00	
4H-4, 61	30.31	34.64	2.19011	13.9			61.75	0.80	1.76	−1.67	0.933	5.14	5.47	
4H-4, 71	30.41	34.74	2.19730	13.9			59.18	0.77	1.54	−1.79	0.940	4.85	4.60	
4H-4, 81	30.51	34.84	2.20450	13.9			58.94	0.78	1.78	−1.66	0.955	6.86	4.50	
4H-4, 91	30.61	34.94	2.21170	13.9			68.12	0.90	1.57	−1.69	0.955	7.75	5.63	
4H-4, 101	30.71	35.04	2.21889	13.9			67.23	0.91	1.58	−1.66	0.969	4.77	6.33	
4H-4, 111	30.81	35.14	2.22609	13.9			67.03	0.87	1.69	−1.88	0.933	5.87	6.80	
4H-4, 121	30.91	35.24	2.23328	13.9			65.68	0.86	1.60	−1.53	0.940	6.39	6.27	
4H-4, 131	31.01	35.34	2.24048	13.9			67.01	0.84	1.63	−1.28	0.905	6.91	4.57	
4H-4, 141	31.11	35.44	2.24767	13.9			57.04	0.72	1.76	−1.31	0.912	7.29	4.50	Ash H, and below
4H-5, 7	31.27	35.60	2.25918	13.9			61.74	0.83	1.85	−1.56	0.969	5.93	16.83	
4H-5, 11	31.31	35.64	2.26206	13.9			56.65	0.76	1.85	−1.71	0.962	4.09	8.10	
4H-5, 21	31.41	35.74	2.26926	13.9			67.51	0.86	1.83	−1.84	0.912	6.54	5.30	
4H-5, 31	31.51	35.84	2.27645	13.9			67.66	0.87	1.91	−1.72	0.926	6.18	4.63	
4H-5, 41	31.61	35.94	2.28365	13.9			70.18	0.93	2.18	−1.61	0.955	6.40	4.03	
4H-5, 51	31.71	36.04	2.29084	13.9			72.06	0.93	1.94	−1.50	0.926	10.87	3.70	
4H-5, 61	31.81	36.14	2.29804	13.9			75.28	0.94	1.84	−1.84	0.898	14.40	3.63	
4H-5, 71	31.91	36.24	2.30523	13.9			70.74	0.85	1.79	−1.62	0.869	15.03	3.53	
4H-5, 81	32.01	36.34	2.31243	13.9			70.82	0.93	1.63	−1.47	0.947	13.92	4.10	
4H-5, 91	32.11	36.44	2.31962	13.9			71.96	0.91	1.75	−1.39	0.912	12.89	3.47	
4H-5, 101	32.21	36.54	2.32682	13.9			69.39	0.85	1.61	−1.50	0.883	11.76	4.43	
4H-5, 111	32.31	36.64	2.33401	13.9			67.54	0.86	1.54	−1.49	0.912	10.24	4.40	
4H-5, 121	32.41	36.74	2.34121	13.9			71.91	0.81	1.72	−1.62	0.812	11.23	3.60	
4H-5, 131	32.51	36.84	2.34840	13.9			74.68	0.92	1.82	−1.85	0.890	14.76	3.30	
4H-5, 141	32.61	36.94	2.35560	13.9			71.04	0.81	1.63	−1.94	0.826	15.54	3.30	
4H-6, 1	32.71	37.04	2.36279	13.9			64.54	0.79	1.40	−1.61	0.876	13.92	3.33	
4H-6, 11	32.81	37.14	2.36999	13.9			65.13	0.82	1.55	−1.03	0.905	8.48	4.40	
4H-6, 21	32.91	37.24	2.37718	13.9			64.24	0.84	1.58	−1.49	0.940	9.94	4.10	
4H-6, 31	33.01	37.34	2.38438	13.9			67.08	0.78	1.74	−1.88	0.834	14.22	4.03	
4H-6, 41	33.11	37.44	2.39157	13.9			65.60	0.79	1.30	−1.39	0.869	12.58	4.10	
4H-6, 51	33.21	37.54	2.39877	13.9			63.69	0.78	1.26	−1.16	0.883	12.34	4.30	
4H-6, 61	33.31	37.64	2.40596	13.9			60.45	0.76	1.39	−1.46	0.905	9.12	5.37	
4H-6, 71	33.41	37.74	2.41316	13.9			59.99	0.81	1.35	−1.25	0.969	6.98	4.90	
4H-6, 81	33.51	37.84	2.42035	13.9			59.48	0.79	1.30	−1.87	0.955	2.41	6.40	
4H-6, 91	33.61	37.94	2.42755	13.9			60.41	0.77	1.75	−1.74	0.912	5.82	4.03	
4H-6, 101	33.71	38.04	2.43474	13.9			64.54	0.79	1.69	−1.59	0.883	5.24	4.17	
4H-6, 111	33.81	38.14	2.44194	13.9			60.71	0.79	1.45	−1.65	0.940	3.26	5.50	
4H-6, 121	33.91	38.24	2.44913	13.9			66.59	0.87	1.73	−1.87	0.940	4.47	4.27	
4H-6, 131	34.01	38.34	2.45633	13.9			67.24	0.86	1.58	−1.67	0.919	4.60	3.63	
4H-6, 141	34.11	38.44	2.46352	13.9			66.84	0.81	1.73	−2.16	0.869	9.99	3.60	
4H-7, 1	34.21	38.54	2.47074	13.9			69.73	0.87	1.33	−1.70	0.898	12.74	3.07	
4H-7, 11	34.31	38.64	2.47809	13.6			68.39	0.87	1.45	−1.49	0.940	9.08	4.27	
4H-7, 21	34.41	38.74	2.48544	13.6			61.47	0.80	1.48	−1.33	0.955	2.29	5.20	
4H-7, 31	34.51	38.84	2.49279	13.6			68.01	0.84	1.78	−1.68	0.912	4.52	3.83	
4H-7, 41	34.61	38.94	2.50015	13.6			67.28	0.82	1.57	−1.54	0.898	5.33	3.53	

4H-7, 51	34.71	39.04	2.50750	13.6	67.72	0.87	1.60	−1.97	0.940	5.83	3.50
4H-7, 61	34.81	39.14	2.51485	13.6	64.80	0.80	1.76	−2.05	0.912	8.26	3.57
4H-7, 71	34.91	39.24	2.52221	13.6	68.05	0.92	1.64	−1.62	0.997	4.96	3.85
121-758B-											
4H-5, 101	35.41	39.25	2.52294	13.7	64.06	0.83			0.940	5.30	3.98
4H-5, 111	35.51	39.35	2.53029	13.6	61.53	0.81			0.969	2.52	5.20
4H-5, 121	35.61	39.45	2.53765	13.6	61.04	0.72			0.869	3.73	4.17
4H-5, 131	35.71	39.55	2.54500	13.6	67.95	0.80			0.869	5.40	3.23
4H-5, 141	35.81	39.65	2.55235	13.6	64.71	0.79			0.898	5.56	3.60
4H-6, 1	35.91	39.75	2.55971	13.6	68.03	0.81			0.876	8.28	3.60
4H-6, 11	36.01	39.85	2.56706	13.6	66.15	0.83			0.926	5.31	4.20
4H-6, 21	36.11	39.95	2.57441	13.6	67.84	0.89			0.969	4.34	4.30
4H-6, 31	36.21	40.05	2.58176	13.6	71.13	0.92			0.947	8.40	3.63
4H-6, 41	36.31	40.15	2.58912	13.6	70.62	0.85			0.883	8.83	3.40
121-758A-											
5H-1, 21	35.01	40.16	2.58985	13.7	71.26	0.88			0.898	9.65	3.40
5H-1, 31	35.11	40.26	2.59721	13.6	66.28	0.80			0.890	5.77	4.73
5H-1, 41	35.21	40.36	2.60456	13.6	68.42	0.85			0.912	5.20	4.50
5H-1, 51	35.31	40.46	2.61191	13.6	71.88	0.91			0.926	4.60	4.30
5H-1, 61	35.41	40.56	2.61926	13.6	70.53	0.90			0.933	5.62	3.77
5H-1, 71	35.51	40.66	2.62662	13.6	70.13	0.90			0.940	6.27	3.63
5H-1, 81	35.61	40.76	2.63397	13.6	72.51	0.93			0.940	7.88	4.00
5H-1, 91	35.71	40.86	2.64132	13.6	68.43	0.73			0.784	5.12	4.27
5H-1, 101	35.81	40.96	2.64868	13.6	68.20	0.83			0.898	4.47	4.33
5H-1, 111	35.91	41.06	2.65603	13.6	71.99	0.87			0.890	6.71	3.80
5H-1, 121	36.01	41.16	2.66338	13.6	69.32	0.83			0.883	8.12	3.63
5H-1, 131	36.11	41.26	2.67074	13.6	71.25	0.82			0.848	7.85	3.70
5H-1, 141	36.21	41.36	2.67809	13.6	69.99	0.83			0.869	5.98	3.80
5H-2, 1	36.31	41.46	2.68544	13.6	70.82	0.81			0.841	6.30	4.20
5H-2, 11	36.41	41.56	2.69279	13.6	69.58	0.86			0.912	4.74	5.23
5H-2, 21	36.51	41.66	2.70015	13.6	67.60	0.82			0.898	5.42	5.80
5H-2, 31	36.61	41.76	2.70750	13.6	67.44	0.82			0.898	6.53	5.47
5H-2, 41	36.71	41.86	2.71485	13.6	66.33	0.84			0.926	5.22	5.03
5H-2, 51	36.81	41.96	2.72221	13.6	67.86	0.81			0.883	3.95	5.70
5H-2, 61	36.91	42.06	2.72956	13.6	63.67	0.74			0.855	5.50	6.70
5H-2, 71	37.01	42.16	2.73691	13.6	56.05	0.65			0.855	4.66	10.57
5H-2, 81	37.11	42.26	2.74426	13.6	64.13	0.73			0.834	5.42	8.00
5H-2, 91	37.21	42.36	2.75162	13.6	64.11	0.76			0.869	4.56	7.37
5H-2, 101	37.31	42.46	2.75897	13.6	63.93	0.74			0.855	6.57	7.37
5H-2, 111	37.41	42.56	2.76632	13.6	63.30	0.77			0.890	4.84	7.60
5H-2, 121	37.51	42.66	2.77368	13.6	65.71	0.74			0.826	5.70	10.23
5H-2, 131	37.61	42.76	2.78103	13.6	67.55	0.79			0.862	9.09	8.80
5H-2, 141	37.71	42.86	2.78838	13.6	65.96	0.77			0.855	5.67	7.20
5H-3, 1	37.81	42.96	2.79574	13.6	67.83	0.78			0.848	7.73	6.77
5H-3, 11	37.91	43.06	2.80309	13.6	65.51	0.80			0.898	4.03	7.50
5H-3, 21	38.01	43.16	2.81044	13.6	62.09	0.77			0.912	2.91	7.30
5H-3, 31	38.11	43.26	2.81779	13.6	66.01	0.81			0.898	8.28	6.30
5H-3, 41	38.21	43.36	2.82515	13.6	68.02	0.79			0.855	7.44	5.47
5H-3, 51	38.31	43.46	2.83250	13.6	64.79	0.78			0.883	7.44	5.60
5H-3, 61	38.41	43.56	2.83985	13.6	68.93	0.86			0.919	6.59	6.03
5H-3, 71	38.51	43.66	2.84721	13.6	66.86	0.79			0.869	7.28	5.53
5H-3, 81	38.61	43.76	2.85456	13.6	65.95	0.79			0.883	5.37	6.10
5H-3, 91	38.71	43.86	2.86191	13.6	61.91	0.72			0.855	6.98	5.67
5H-3, 101	38.81	43.96	2.86926	13.6	61.81	0.73			0.869	10.86	5.90
5H-3, 111	38.91	44.06	2.87662	13.6	70.72	0.81			0.848	9.34	5.70
5H-3, 121	39.01	44.16	2.88397	13.6	69.31	0.82			0.869	9.03	5.17
5H-3, 131	39.11	44.26	2.89132	13.6	68.33	0.83			0.898	4.82	6.13
5H-3, 141	39.21	44.36	2.89868	13.6	67.73	0.83			0.898	4.68	6.00
5H-4, 1	39.31	44.46	2.90603	13.6	67.75	0.84			0.912	3.89	7.03
5H-4, 11	39.41	44.56	2.91338	13.6	66.85	0.85			0.933	3.67	7.50

Appendix F (continued).

Core, section, interval (cm)	ODP depth (mbsf)	Composite depth (m)	Magnetic age (m.y.)	Magnetic sedimentation rate (m/m.y.)	$\delta^{18}O$ age (m.y.)	$\delta^{18}O$ sedimentation rate (m/m.y.)	Mean (wt% $CaCO_3$)	Magnetic $CaCO_3$ MAR (g/cm²/k.y.)	$\delta^{13}C$ ‰ to (PDB)	$\delta^{18}O$ ‰ to (PDB)	Dry-bulk density (g/cm³)	Coarse fraction (wt% >150 μm)	Interpolated MS K (10-6) (cgs)	Comment
121-758A-(Cont.)														
5H-4, 21	39.51	44.66	2.92070	13.7			66.59	0.78			0.855	4.77	8.00	
5H-4, 31	39.61	44.76	2.92770	14.3			63.97	0.83			0.912	1.88	9.57	
5H-4, 41	39.71	44.86	2.93470	14.3			68.06	0.86			0.883	3.71	8.33	
5H-4, 51	39.81	44.96	2.94170	14.3			70.89	0.97			0.955	3.03	7.00	
5H-4, 61	39.91	45.06	2.94870	14.3			71.42	0.92			0.905	3.93	6.50	
5H-4, 71	40.01	45.16	2.95570	14.3			72.22	0.97			0.940	5.70	5.83	
5H-4, 81	40.11	45.26	2.96270	14.3			69.90	0.92			0.926	9.53	5.40	
5H-4, 91	40.21	45.36	2.96970	14.3			72.28	0.93			0.898	6.93	6.07	
5H-4, 101	40.31	45.46	2.97670	14.3			72.16	0.93			0.898	8.06	6.00	
5H-4, 111	40.41	45.56	2.98370	14.3			73.17	0.88			0.841	9.51	6.00	
5H-4, 121	40.51	45.66	2.99064	14.4			74.92	0.91			0.841	10.68	5.40	
5H-4, 131	40.61	45.76	2.99707	15.6			70.46	0.95			0.869	8.59	6.50	
5H-4, 141	40.71	45.86	3.00350	15.6			71.56	1.03			0.926	9.71	6.70	
5H-5, 1	40.81	45.96	3.00993	15.6			68.93	1.05			0.983	7.88	6.50	
5H-5, 11	40.91	46.06	3.01636	15.6			66.28	0.93			0.902	4.45	8.23	
5H-5, 21	41.01	46.16	3.02279	15.6			65.96	0.95			0.926	4.61	8.00	
5H-5, 31	41.11	46.26	3.02921	15.6			70.61	0.97			0.883	7.20	7.53	
5H-5, 41	41.21	46.36	3.03564	15.6			66.31	0.95			0.926	4.93	7.83	
5H-5, 51	41.31	46.46	3.04207	15.6			66.44	0.93			0.898	5.77	8.00	
5H-5, 61	41.41	46.56	3.04850	15.6			68.33	0.94			0.883	5.71	7.27	
5H-5, 71	41.51	46.66	3.05493	15.6			64.60	0.93			0.926	6.76	8.40	
5H-5, 81	41.61	46.76	3.06136	15.6			67.03	1.05			1.004	10.57	8.80	
5H-5, 91	41.71	46.86	3.06779	15.6			64.66	0.86			0.855	5.63	7.60	
5H-5, 101	41.81	46.96	3.07421	15.6			64.39	0.90			0.898	5.59	7.00	
5H-5, 111	41.91	47.06	3.08095	14.8			63.21	0.83			0.883	4.50	7.80	
5H-5, 121	42.01	47.16	3.09048	10.5			69.16	0.63			0.869	6.30	7.03	
5H-5, 131	42.11	47.26	3.10000	10.5			69.96	0.63			0.862	8.55	6.30	
5H-6, 1	42.31	47.46	3.11905	10.5			66.71	0.63			0.896	8.52	5.96	
5H-6, 11	42.41	47.56	3.12857	10.5			69.16	0.66			0.905	10.65	4.53	
5H-6, 21	42.51	47.66	3.13810	10.5			67.20	0.70			0.997	8.65	4.60	
5H-6, 31	42.61	47.76	3.14762	10.5			62.96	0.62			0.933	6.70	5.60	
5H-6, 41	42.71	47.86	3.15714	10.5			59.83	0.55			0.883	3.61	8.23	
5H-6, 51	42.81	47.96	3.16667	10.5			63.57	0.73			1.097	2.32	10.00	
5H-6, 61	42.91	48.06	3.17619	10.5			63.30	0.64			0.969	3.78	7.77	
5H-6, 71	43.01	48.16	3.18411	12.6			63.69	0.71			0.883	4.77	7.23	
5H-6, 81	43.11	48.26	3.19097	14.6			65.04	0.89			0.940	5.66	8.70	
5H-6, 91	43.21	48.36	3.19782	14.6			62.77	0.86			0.940	4.85	9.07	
5H-6, 101	43.31	48.46	3.20467	14.6			60.40	0.82			0.926	6.83	8.70	
5H-6, 111	43.41	48.56	3.21153	14.6			62.46	0.83			0.912	6.08	8.20	
5H-6, 121	43.51	48.66	3.21838	14.6			64.17	0.84			0.898	7.81	5.57	
5H-6, 131	43.61	48.76	3.22523	14.6			64.98	0.84			0.883	6.03	6.70	
5H-6, 141	43.71	48.86	3.23209	14.6			70.36	0.92			0.898	4.50	8.10	
5H-7, 1	43.81	48.96	3.23894	14.6			68.75	0.92			0.919	5.97	6.60	
5H-7, 11	43.91	49.06	3.24579	14.6			67.94	0.90			0.912	4.48	6.40	
5H-7, 21	44.01	49.16	3.25265	14.6			63.94	0.81			0.869	3.81	7.50	
5H-7, 31	44.11	49.26	3.25950	14.6			63.28	0.84			0.905	4.13	8.00	
5H-7, 41	44.21	49.36	3.26636	14.6			63.88	0.81			0.869	5.43	8.63	
5H-7, 51	44.31	49.46	3.27321	14.6			56.38	0.71			0.862	4.47	11.50	
121-758B-														
5H-4, 131	43.81	49.47	3.27389	14.7			55.90	0.71			0.862	3.07	10.65	
5H-4, 141	43.91	49.57	3.28075	14.6			62.48	0.84			0.919	4.08	8.30	
5H-5, 1	44.01	49.67	3.28760	14.6			64.95	0.89			0.940	3.72	6.53	
5H-5, 11	44.11	49.77	3.29446	14.6			64.87	0.87			0.919	4.11	7.10	

5H-5, 21	44.21	49.87	3.30131	14.6	66.68	0.93	0.955	3.63	7.50
5H-5, 31	44.31	49.97	3.30816	14.6	67.88	0.92	0.926	3.54	7.67
5H-5, 41	44.41	50.07	3.31502	14.6	67.80	0.87	0.883	5.37	7.13
5H-5, 51	44.51	50.17	3.32187	14.6	69.19	0.99	0.983	5.76	8.10
5H-5, 61	44.61	50.27	3.32872	14.6	68.94	0.95	0.940	4.08	8.07
5H-5, 71	44.71	50.37	3.33558	14.6	69.79	0.93	0.912	4.78	7.80
5H-5, 81	44.81	50.47	3.34243	14.6	68.70	0.94	0.940	3.95	8.50
5H-5, 91	44.91	50.57	3.34928	14.6	67.36	0.91	0.926	4.04	8.53
5H-5, 101	45.01	50.67	3.35614	14.6	67.43	0.90	0.912	3.11	8.73
5H-5, 111	45.11	50.77	3.36299	14.6	61.32	0.84	0.933	2.09	10.70
5H-5, 121	45.21	50.87	3.36984	14.6	69.18	0.92	0.912	3.39	9.00
5H-5, 131	45.31	50.97	3.37670	14.6	69.05	0.89	0.883	3.60	11.10
5H-5, 141	45.41	51.07	3.38355	14.6	67.93	0.86	0.865	3.30	9.70
5H-6, 1	45.51	51.17	3.39041	14.6	69.99	0.97	0.955	4.16	4.83
5H-6, 21	45.71	51.37	3.40279	16.2	73.35	1.01	0.855	8.30	6.60
5H-6, 30	45.80	51.46	3.40698	21.5	71.68	1.40	0.912	6.30	6.90
5H-6, 41	45.91	51.57	3.41209	21.5	74.09	1.52	0.955	6.75	9.63
5H-6, 51	46.01	51.67	3.41674	21.5	68.75	1.33	0.898	3.91	21.00
5H-6, 61	46.11	51.77	3.42140	21.5	66.34	1.34	0.940	2.75	27.70
5H-6, 71	46.21	51.87	3.42605	21.5	69.05	1.38	0.926	2.89	12.73
5H-6, 81	46.31	51.97	3.43070	21.5	68.31	1.40	0.955	2.86	11.50
5H-6, 91	46.41	52.07	3.43535	21.5	70.24	1.40	0.926	4.49	9.83
121-758A-									
6H-1, 31	44.71	52.08	3.43581	21.7	69.24	1.34	0.890	6.55	9.75
6H-1, 41	44.81	52.18	3.44047	21.5	64.19	1.20	0.869	4.52	12.40
6H-1, 51	44.91	52.28	3.44512	21.5	63.74	1.21	0.883	3.18	18.60
6H-1, 61	45.01	52.38	3.44977	21.5	64.19	1.27	0.919	4.00	29.87
6H-1, 71	45.11	52.48	3.45442	21.5	69.40	1.30	0.869	6.10	36.90
6H-1, 81	45.21	52.58	3.45907	21.5	74.29	1.35	0.848	11.66	9.90
6H-1, 91	45.31	52.68	3.46372	21.5	68.68	1.33	0.898	10.41	6.17
6H-1, 101	45.41	52.78	3.46837	21.5	70.50	1.30	0.855	9.56	7.00
6H-1, 111	45.51	52.88	3.47302	21.5	66.70	1.29	0.898	5.34	7.10
6H-1, 121	45.61	52.98	3.47767	21.5	66.23	1.52	1.068	3.11	9.10
6H-1, 131	45.71	53.08	3.48233	21.5	65.80	1.25	0.883	3.55	8.67
6H-1, 141	45.81	53.18	3.48698	21.5	68.25	1.38	0.940	4.73	8.50
6H-2, 1	45.91	53.28	3.49163	21.5	67.30	1.28	0.883	4.73	7.20
6H-2, 11	46.01	53.38	3.49628	21.5	65.22	1.17	0.834	3.25	9.13
6H-2, 21	46.11	53.48	3.50093	21.5	64.37	1.09	0.784	3.19	7.90
6H-2, 31	46.21	53.58	3.50558	21.5	65.06	1.10	0.784	3.45	8.03
6H-2, 41	46.31	53.68	3.51023	21.5	63.97	1.08	0.784	3.36	6.23
6H-2, 51	46.41	53.78	3.51488	21.5	66.74	1.13	0.784	3.35	6.00
6H-2, 61	46.51	53.88	3.51954	21.5	66.17	1.11	0.784	2.72	7.87
6H-2, 71	46.61	53.98	3.52419	21.5	65.48	1.18	0.841	3.02	9.23
6H-2, 81	46.71	54.08	3.52884	21.5	69.76	1.31	0.876	3.62	7.50
6H-2, 91	46.81	54.18	3.53349	21.5	72.10	1.41	0.912	5.47	6.23
6H-2, 101	46.91	54.28	3.53814	21.5	73.23	1.30	0.826	6.83	6.00
6H-2, 111	47.01	54.38	3.54279	21.5	70.68	1.27	0.834	6.74	5.80
6H-2, 121	47.11	54.48	3.54744	21.5	74.27	1.34	0.841	8.53	7.53
6H-2, 131	47.21	54.58	3.55209	21.5	68.85	1.31	0.883	4.41	12.20
6H-2, 141	47.31	54.68	3.55674	21.5	67.23	1.40	0.969	3.11	22.70
6H-3, 1	47.41	54.78	3.56140	21.5	76.34	1.37	0.834	11.00	10.80
6H-3, 11	47.51	54.88	3.56605	21.5	67.91	1.28	0.876	5.52	11.93
6H-3, 21	47.61	54.98	3.57070	21.5	71.13	1.44	0.940	5.43	19.10
6H-3, 31	47.71	55.08	3.57535	21.5	70.55	1.40	0.926	3.83	16.37
6H-3, 41	47.81	55.18	3.58000	21.5	70.98	1.39	0.912	4.18	19.17
6H-3, 51	47.91	55.28	3.58465	21.5	72.63	1.49	0.955	5.35	29.30
6H-3, 61	48.01	55.38	3.58930	21.5	73.93	1.37	0.862	5.53	11.60
6H-3, 71	48.11	55.48	3.59395	21.5	72.83	1.38	0.883	6.89	9.67
6H-3, 81	48.21	55.58	3.59860	21.5	75.88	1.48	0.905	7.32	8.37
6H-3, 91	48.31	55.68	3.60326	21.5	74.07	1.47	0.926	5.06	7.07
6H-3, 101	48.41	55.78	3.60791	21.5	71.96	1.39	0.898	5.05	6.03
6H-3, 111	48.51	55.88	3.61256	21.5	72.18	1.42	0.912	8.29	6.20

Appendix F (continued).

Core, section, interval (cm)	ODP depth (mbsf)	Composite depth (m)	Magnetic age (m.y.)	Magnetic sedimentation rate (m/m.y.)	$\delta^{18}O$ age (m.y.)	$\delta^{18}O$ sedimentation rate (m/m.y.)	Mean (wt% $CaCO_3$)	Magnetic $CaCO_3$ MAR ($g/cm^2/k.y.$)	$\delta^{13}C$ ‰ to (PDB)	$\delta^{18}O$ ‰ to (PDB)	Dry-bulk density (g/cm^3)	Coarse fraction (wt% >150 μm)	Interpolated MS K (10-6) (cgs)	Comment
121-758A-(Cont.)														
6H-3, 121	48.61	55.98	3.61721	21.5			71.68	1.45			0.940	7.26	7.87	
6H-3, 131	48.71	56.08	3.62186	21.5			72.45	1.42			0.912	5.08	10.60	
6H-3, 141	48.81	56.18	3.62651	21.5			74.14	1.45			0.912	5.84	6.10	
6H-4, 1	48.91	56.28	3.63116	21.5			67.60	1.26			0.869	4.14	6.77	
6H-4, 11	49.01	56.38	3.63581	21.5			69.34	1.39			0.933	4.71	6.80	
6H-4, 21	49.11	56.48	3.64047	21.5			68.69	1.39			0.940	3.81	7.80	
6H-4, 31	49.21	56.58	3.64512	21.5			66.87	1.36			0.947	5.25	6.93	
6H-4, 41	49.31	56.68	3.64977	21.5			72.30	1.44			0.926	6.69	5.93	
6H-4, 51	49.41	56.78	3.65442	21.5			73.36	1.60			1.012	10.89	5.40	
6H-4, 61	49.51	56.88	3.65907	21.5			73.49	1.52			0.962	5.69	5.57	
6H-4, 71	49.61	56.98	3.66372	21.5			69.43	1.40			0.940	7.25	5.97	
6H-4, 81	49.71	57.08	3.66837	21.5			69.08	1.40			0.940	6.34	5.50	
6H-4, 91	49.81	57.18	3.67302	21.5			67.22	1.48			1.026	4.58	6.20	
6H-4, 101	49.91	57.28	3.67767	21.5			71.79	1.32			0.855	7.13	5.33	
6H-4, 111	50.01	57.38	3.68233	21.5			75.31	1.59			0.983	9.16	4.70	
6H-4, 121	50.11	57.48	3.68698	21.5			75.56	1.46			0.898	11.35	4.70	
6H-4, 131	50.21	57.58	3.69163	21.5			73.78	1.40			0.883	11.62	5.10	
6H-4, 141	50.31	57.68	3.69628	21.5			72.23	1.42			0.912	8.39	6.00	
6H-5, 1	50.41	57.78	3.70093	21.5			70.10	1.51			1.004	7.39	6.43	
6H-5, 11	50.51	57.88	3.70558	21.5			67.66	1.43			0.983	5.87	6.37	
6H-5, 21	50.61	57.98	3.71023	21.5			70.70	1.28			0.841	7.32	5.40	
6H-5, 31	50.71	58.08	3.71488	21.5			66.58	1.27			0.890	6.96	4.80	
6H-5, 41	50.81	58.18	3.71954	21.5			67.10	1.23			0.855	5.73	6.50	
6H-5, 51	50.91	58.28	3.72419	21.5			44.09	0.92			0.969	5.30	3.80	Ash blebs
6H-5, 61	51.01	58.38	3.72884	21.5			67.55	1.31			0.905	8.31	4.67	
6H-5, 71	51.11	58.48	3.73349	21.5			72.83	1.45			0.926	6.93	4.10	
6H-5, 81	51.21	58.58	3.73814	21.5			70.21	1.39			0.919	6.64	4.90	
6H-5, 91	51.31	58.68	3.74279	21.5			70.65	1.32			0.869	8.40	3.50	
6H-5, 101	51.41	58.78	3.74744	21.5			71.80	1.39			0.898	6.34	3.57	
6H-5, 111	51.51	58.88	3.75209	21.5			70.51	1.41			0.933	5.63	3.80	
6H-5, 121	51.61	58.98	3.75674	21.5			69.46	1.40			0.940	4.86	4.10	
6H-6, 1	51.91	59.28	3.77070	21.5			68.13	1.36			0.929	7.24	5.78	
6H-6, 11	52.01	59.38	3.77535	21.5			60.26	1.26			0.969	4.97	8.00	
6H-6, 21	52.11	59.48	3.78000	21.5			61.28	1.22			0.926	3.25	10.00	
6H-6, 31	52.21	59.58	3.78465	21.5			56.66	1.11			0.912	4.42	12.33	
6H-6, 41	52.31	59.68	3.78930	21.5			57.25	1.14			0.926	3.85	10.97	
6H-6, 51	52.41	59.78	3.79395	21.5			72.23	1.46			0.940	6.89	5.70	
6H-6, 61	52.51	59.88	3.79860	21.5			71.35	1.41			0.919	7.76	6.70	
6H-6, 71	52.61	59.98	3.80326	21.5			68.13	1.40			0.955	4.95	6.40	
6H-6, 81	52.71	60.08	3.80791	21.5			68.62	1.30			0.883	5.10	6.30	
6H-6, 91	52.81	60.18	3.81256	21.5			68.90	1.35			0.912	4.74	8.03	
6H-6, 101	52.91	60.28	3.81721	21.5			67.26	1.19			0.826	5.01	11.90	
6H-6, 111	53.01	60.38	3.82186	21.5			58.28	1.12			0.890	3.48	27.90	
6H-6, 121	53.11	60.48	3.82651	21.5			63.56	1.36			0.997	4.60	17.33	
6H-6, 131	53.21	60.58	3.83116	21.5			65.87	1.31			0.926	5.21	7.00	
6H-6, 141	53.31	60.68	3.83581	21.5			55.85	1.16			0.969	4.93	10.50	
6H-7, 1	53.41	60.78	3.84047	21.5			69.54	1.45			0.969	5.71	5.67	
6H-7, 11	53.51	60.88	3.84512	21.5			72.81	1.29			0.826	6.61	5.40	
6H-7, 21	53.61	60.98	3.84977	21.5			71.48	1.39			0.905	6.55	7.00	
6H-7, 31	53.71	61.08	3.85442	21.5			73.40	1.44			0.912	7.07	7.37	
6H-7, 41	53.81	61.18	3.85907	21.5			71.60	1.46			0.947	6.31	6.30	
6H-7, 51	53.91	61.28	3.86372	21.5			70.96	1.41			0.926	5.71	6.00	
6H-7, 61	54.01	61.38	3.86837	21.5			71.57	1.39			0.905	5.73	6.03	
6H-7, 71	54.11	61.48	3.87302	21.5			25.13	0.51			0.940	2.37	6.40	

121-758B-										
6H-4, 61	52.81	61.49	3.87349	21.3	66.31	1.33	0.940	7.72	6.80	
6H-4, 71	52.91	61.59	3.87814	21.5	68.83	1.39	0.940	8.29	6.17	
6H-4, 81	53.01	61.69	3.88335	19.2	72.27	1.28	0.926	9.10	4.60	
6H-4, 91	53.11	61.79	3.88894	17.9	71.66	1.11	0.869	7.10	4.87	
6H-4, 101	53.21	61.89	3.89453	17.9	73.83	1.19	0.898	6.42	4.60	
6H-4, 111	53.31	61.99	3.90012	17.9	76.58	1.27	0.926	6.71	3.80	
6H-4, 121	53.41	62.09	3.90571	17.9	75.71	1.29	0.955	3.47	5.70	
6H-4, 131	53.51	62.19	3.91130	17.9	71.46	1.15	0.898	3.80	6.40	
6H-4, 141	53.61	62.29	3.91689	17.9	71.40	1.10	0.862	4.83	6.40	
6H-5, 1	53.71	62.39	3.92248	17.9	71.52	1.18	0.922	5.40	6.33	
6H-5, 11	53.81	62.49	3.92807	17.9	71.29	1.14	0.898	6.16	7.03	
6H-5, 21	53.91	62.59	3.93366	17.9	68.38	1.10	0.898	2.76	8.60	
6H-5, 31	54.01	62.69	3.93925	17.9	67.59	1.11	0.919	2.57	8.63	
6H-5, 41	54.11	62.79	3.94484	17.9	69.46	1.12	0.898	4.38	7.00	
6H-5, 51	54.21	62.89	3.95043	17.9	71.26	1.14	0.898	6.25	6.60	
6H-5, 61	54.31	62.99	3.95602	17.9	72.05	1.19	0.926	5.52	8.03	
6H-5, 71	54.41	63.09	3.96162	17.9	69.91	1.14	0.912	5.69	7.50	
6H-5, 81	54.51	63.19	3.96721	17.9	69.13	1.16	0.940	3.83	9.70	
121-758A-										
7H-1, 1	54.01	63.20	3.96776	18.2	69.11	1.04	0.829	5.38	9.47	
7H-1, 11	54.11	63.30	3.97363	17.0	52.69	0.74	0.829	3.14	26.97	
7H-1, 21	54.21	63.40	3.97967	16.6	58.65	0.83	0.855	2.44	15.10	
7H-1, 31	54.31	63.50	3.98572	16.5	65.40	0.89	0.826	3.23	18.83	
7H-1, 41	54.41	63.60	3.99177	16.5	69.83	1.08	0.940	4.67	8.80	
7H-1, 51	54.51	63.70	3.99781	16.6	66.37	0.99	0.898	3.21	9.40	
7H-1, 61	54.61	63.80	4.00386	16.5	57.42	0.84	0.883	2.36	15.80	
7H-1, 71	54.71	63.90	4.00991	16.5	60.64	0.93	0.926	2.84	15.87	
7H-1, 81	54.81	64.00	4.01595	16.6	69.60	1.01	0.876	3.22	7.90	
7H-1, 91	54.91	64.10	4.02200	16.5	71.70	1.10	0.926	4.14	6.53	
7H-1, 101	55.01	64.20	4.02805	16.5	72.09	1.10	0.926	5.14	4.47	
7H-1, 111	55.11	64.30	4.03409	16.6	64.79	1.12	1.040	2.56	8.30	
7H-1, 121	55.21	64.40	4.04014	16.5	61.63	1.13	1.111	2.57	11.23	
7H-1, 131	55.31	64.50	4.04619	16.5	62.06	0.96	0.940	2.08	9.97	
7H-1, 141	55.41	64.60	4.05223	16.6	71.98	1.09	0.912	2.99	6.00	
7H-2, 1	55.51	64.70	4.05828	16.5	74.16	1.15	0.937	5.50	6.20	
7H-2, 11	55.61	64.80	4.06433	16.5	74.24	1.08	0.883	4.88	7.87	
7H-2, 21	55.71	64.90	4.07037	16.6	72.15	1.04	0.869	3.77	7.50	
7H-2, 31	55.81	65.00	4.07642	16.5	69.64	1.07	0.933	2.30	8.33	
7H-2, 41	55.91	65.10	4.08247	16.5	69.89	1.04	0.898	2.97	8.10	
7H-2, 51	56.01	65.20	4.08851	16.6	72.35	1.06	0.883	4.52	6.90	
7H-2, 61	56.11	65.30	4.09456	16.5	72.98	1.13	0.933	5.14	6.33	
7H-2, 71	56.21	65.40	4.10057	16.6	73.27	1.16	0.955	4.01	6.33	
7H-2, 81	56.31	65.50	4.10629	17.5	72.86	1.18	0.926	5.04	6.50	
7H-2, 91	56.41	65.60	4.11200	17.5	71.05	1.13	0.912	3.65	7.27	
7H-2, 101	56.51	65.70	4.11771	17.5	68.20	1.05	0.883	5.20	7.87	
7H-2, 111	56.61	65.80	4.12343	17.5	69.60	1.13	0.926	4.56	11.10	
7H-2, 121	56.71	65.90	4.12914	17.5	6.22	0.11	1.040		35.02	Ash I, not processed
7H-2, 131	56.81	66.00	4.13486	17.5	73.65	1.11	0.862	3.51	7.57	
7H-2, 141	56.91	66.10	4.14057	17.5	75.92	1.23	0.926	4.93	7.10	
7H-3, 1	57.01	66.20	4.14629	17.5	75.79	1.18	0.890	4.24	5.73	
7H-3, 11	57.11	66.30	4.15200	17.5	75.74	1.12	0.841	5.67	6.27	
7H-3, 21	57.21	66.40	4.15771	17.5	74.35	1.21	0.926	6.07	7.30	
7H-3, 31	57.31	66.50	4.16343	17.5	69.39	1.04	0.855	6.46	10.57	
7H-3, 41	57.41	66.60	4.16914	17.5	47.57	0.68	0.812	6.66	20.03	
7H-3, 51	57.51	66.70	4.17486	17.5	75.65	1.21	0.912	9.18	5.50	
7H-3, 61	57.61	66.80	4.18057	17.5	72.38	1.17	0.926	4.14	8.23	
7H-3, 71	57.71	66.90	4.18629	17.5	61.82	0.95	0.883	2.26	13.20	
7H-3, 81	57.81	67.00	4.19200	17.5	73.25	1.10	0.855	4.17	7.50	
7H-3, 91	57.91	67.10	4.19771	17.5	76.11	1.22	0.912	6.36	5.27	
7H-3, 101	58.01	67.20	4.20343	17.5	76.53	1.18	0.883	7.31	5.27	

Appendix F (continued).

Core, section, interval (cm)	ODP depth (mbsf)	Composite depth (m)	Magnetic age (m.y.)	Magnetic sedimentation rate (m/m.y.)	$\delta^{18}O$ age (m.y.)	$\delta^{18}O$ sedimentation rate (m/m.y.)	Mean (wt% $CaCO_3$)	Magnetic $CaCO_3$ MAR ($g/cm^2/k.y.$)	$\delta^{13}C$ ‰ to (PDB)	$\delta^{18}O$ ‰ to (PDB)	Dry-bulk density (g/cm^3)	Coarse fraction (wt% >150 μm)	Interpolated MS K (10-6) (cgs)	Comment
121-758A-(Cont.)														
7H-3, 111	58.11	67.30	4.20914	17.5			72.00	1.12			0.890	7.56	5.70	
7H-3, 121	58.21	67.40	4.21486	17.5			71.76	1.09			0.869	6.85	5.97	
7H-3, 131	58.31	67.50	4.22057	17.5			73.85	1.25			0.969	3.48	6.30	
7H-3, 141	58.41	67.60	4.22629	17.5			69.36	1.17			0.962	4.29	7.70	
7H-4, 1	58.51	67.70	4.23200	17.5			72.98	1.14			0.890	4.59	6.63	
7H-4, 11	58.61	67.80	4.23771	17.5			78.75	1.19			0.862	6.37	5.77	
7H-4, 21	58.71	67.90	4.24337	17.7			74.27	1.18			0.898	7.48	6.00	
7H-4, 31	58.81	68.00	4.24898	17.8			64.11	1.10			0.962	5.43	9.47	
7H-4, 41	58.91	68.10	4.25460	17.8			50.11	0.89			0.997	4.97	9.40	Ash
7H-4, 51	59.01	68.20	4.26021	17.8			79.30	1.33			0.940	4.67	5.30	
7H-4, 61	59.11	68.30	4.26582	17.8			79.65	1.40			0.983	3.14	5.03	
7H-4, 71	59.21	68.40	4.27144	17.8			77.34	1.27			0.926	1.40	5.93	
7H-4, 81	59.31	68.50	4.27705	17.8			73.26	1.20			0.919	2.08	6.20	
7H-4, 91	59.41	68.60	4.28267	17.8			76.42	1.26			0.926	3.61	5.83	
7H-4, 101	59.51	68.70	4.28828	17.8			79.74	1.28			0.898	5.16	4.50	
7H-4, 111	59.61	68.80	4.29389	17.8			76.51	1.24			0.912	4.05	4.00	
7H-4, 121	59.71	68.90	4.29951	17.8			73.02	1.22			0.940	2.81	6.43	
7H-4, 131	59.81	69.00	4.30512	17.8			71.29	1.13			0.890	2.34	7.63	
7H-4, 141	59.91	69.10	4.31074	17.8			73.66	1.20			0.912	2.61	7.00	
7H-5, 1	60.01	69.20	4.31635	17.8			73.42	1.29			0.983	2.69	6.73	
7H-5, 11	60.11	69.30	4.32197	17.8			74.83	1.26			0.947	4.12	6.33	
7H-5, 21	60.21	69.40	4.32758	17.8			77.45	1.34			0.969	3.73	5.30	
7H-5, 31	60.31	69.50	4.33319	17.8			75.27	1.25			0.933	2.71	7.07	
7H-5, 41	60.41	69.60	4.33881	17.8			71.48	1.14			0.898	1.35	10.27	
7H-5, 51	60.51	69.70	4.34442	17.8			71.20	1.27			0.997	1.96	12.60	
7H-5, 61	60.61	69.80	4.35004	17.8			69.91	1.24			0.997	2.55	9.63	
7H-5, 71	60.71	69.90	4.35565	17.8			71.27	1.21			0.955	3.77	10.13	
7H-5, 81	60.81	70.00	4.36126	17.8			76.81	1.23			0.898	4.67	9.00	
7H-5, 91	60.91	70.10	4.36688	17.8			75.97	1.29			0.955	4.33	5.10	
7H-5, 101	61.01	70.20	4.37249	17.8			77.33	1.28			0.926	4.28	4.03	
7H-5, 111	61.11	70.30	4.37811	17.8			73.79	1.26			0.962	1.59	5.70	
7H-5, 121	61.21	70.40	4.38372	17.8			76.57	1.34			0.983	1.97	5.97	
7H-5, 131	61.31	70.50	4.38933	17.8			76.67	1.25			0.912	3.39	4.53	
7H-5, 141	61.41	70.60	4.39495	17.8			77.77	1.24			0.898	4.04	4.60	
7H-6, 1	61.51	70.70	4.40045	18.2			77.31	1.18			0.841	3.20	6.27	
7H-6, 11	61.61	70.80	4.40497	22.1			78.03	1.65			0.955	2.96	6.57	
7H-6, 21	61.71	70.90	4.40948	22.2			74.71	1.58			0.955	2.43	6.80	
7H-6, 31	61.81	71.00	4.41400	22.1			79.61	1.69			0.962	3.73	6.20	
7H-6, 41	61.91	71.10	4.41852	22.1			80.90	1.63			0.912	3.92	5.33	
7H-6, 51	62.01	71.20	4.42303	22.2			80.33	1.75			0.983	4.23	4.70	
7H-6, 61	62.11	71.30	4.42755	22.1			77.98	1.65			0.955	3.53	6.10	
7H-6, 71	62.21	71.40	4.43206	22.2			76.94	1.58			0.926	2.17	7.77	
7H-6, 81	62.31	71.50	4.43658	22.1			74.70	1.60			0.969	1.94	9.10	
7H-6, 91	62.41	71.60	4.44110	22.1			75.90	1.72			1.026	2.31	7.33	
7H-6, 101	62.51	71.70	4.44561	22.2			78.81	1.77			1.012	2.73	5.03	
7H-6, 111	62.61	71.80	4.45013	22.1			79.75	1.63			0.926	3.44	4.60	
7H-6, 121	62.71	71.90	4.45465	22.1			76.16	1.71			1.012	2.88	4.73	
7H-6, 131	62.81	72.00	4.45916	22.2			77.65	1.69			0.983	2.80	4.30	
7H-6, 141	62.91	72.10	4.46368	22.1			74.94	1.56			0.940	2.68	4.80	
7H-7, 1	63.01	72.20	4.46819	22.2			73.28	1.61			0.990	2.62	5.60	
7H-7, 11	63.11	72.30	4.47790	10.3			70.83	0.73			0.997	1.80	6.43	
7H-7, 21	63.21	72.40	4.49105	7.6			77.00	0.59			1.012	2.60	5.50	
7H-7, 31	63.31	72.50	4.50421	7.6			80.49	0.60			0.983	3.47	4.60	
7H-7, 41	63.41	72.60	4.51737	7.6			75.99	0.55			0.955	2.20	5.30	

7H-7, 51	63.51	72.70	4.53053	7.6	73.97	0.53	0.940	1.75	5.30	
7H-7, 61	63.61	72.80	4.54368	7.6	74.46	0.55	0.969	2.78	6.65	
121-758B-										
7H-4, 121	63.01	72.81	4.54500	7.6	71.91	0.53	0.969	2.80	7.10	
7H-4, 131	63.11	72.91	4.55816	7.6	42.71	0.34	1.047	0.92	13.43	Ash J, and below
7H-4, 141	63.21	73.01	4.57049	8.1	77.08	0.58	0.926	1.70	5.10	
7H-5, 1	63.31	73.11	4.57535	20.6	75.12	1.56	1.012	2.37	4.00	
7H-5, 11	63.41	73.21	4.58022	20.5	78.35	1.55	0.962	3.79	4.83	
7H-5, 21	63.51	73.31	4.58508	20.6	75.11	1.50	0.969	1.67	5.80	
7H-5, 31	63.61	73.41	4.58995	20.5	75.37	1.49	0.962	1.18	5.07	
7H-5, 41	63.71	73.51	4.59482	20.5	78.58	1.54	0.955	2.54	5.17	
7H-5, 51	63.81	73.61	4.59968	20.6	80.91	1.61	0.969	3.78	4.30	
7H-5, 61	63.91	73.71	4.60455	20.5	79.64	1.58	0.969	4.54	3.43	
7H-5, 71	64.01	73.81	4.60942	20.5	78.25	1.44	0.898	4.42	5.07	
7H-5, 81	64.11	73.91	4.61428	20.6	77.91	1.53	0.955	4.17	5.10	
7H-5, 91	64.21	74.01	4.61915	20.5	74.12	1.52	0.997	2.49	5.65	
121-758A-										
8H-1, 1	63.71	74.02	4.61963	20.8	75.51	1.35	0.858	3.01	5.80	
8H-1, 11	63.81	74.12	4.62450	20.5	63.18	1.11	0.858	2.33	7.17	
8H-1, 21	63.91	74.22	4.62937	20.5	71.97	1.35	0.912	2.04	7.00	
8H-1, 31	64.01	74.32	4.63423	20.6	78.03	1.45	0.905	4.72	5.10	
8H-1, 41	64.11	74.42	4.63910	20.5	79.85	1.54	0.940	5.52	4.20	
8H-1, 51	64.21	74.52	4.64397	20.5	79.05	1.50	0.926	7.85	4.70	
8H-1, 61	64.31	74.62	4.64883	20.6	76.80	1.49	0.940	6.37	4.47	
8H-1, 71	64.41	74.72	4.65370	20.5	76.81	1.44	0.912	6.89	4.43	
8H-1, 81	64.51	74.82	4.65856	20.6	79.36	1.59	0.976	5.94	4.00	
8H-1, 91	64.61	74.92	4.66343	20.5	74.12	1.56	1.026	2.70	4.83	Ash K, and below
8H-1, 101	64.71	75.02	4.66830	20.5	73.17	1.47	0.976	1.99	5.77	
8H-1, 111	64.81	75.12	4.67316	20.6	76.04	1.52	0.969	2.58	5.40	
8H-1, 121	64.91	75.22	4.67803	20.5	78.53	1.52	0.940	6.66	4.07	
8H-1, 131	65.01	75.32	4.68290	20.5	77.14	1.43	0.905	6.33	4.20	
8H-1, 141	65.11	75.42	4.68776	20.6	74.92	1.47	0.955	5.74	5.40	
8H-2, 1	65.21	75.52	4.69263	20.5	74.67	1.52	0.993	4.13	5.97	
8H-2, 11	65.31	75.62	4.69749	20.6	73.98	1.39	0.912	2.03	7.33	
8H-2, 21	65.41	75.72	4.70236	20.5	75.87	1.51	0.969	3.43	6.90	
8H-2, 31	65.51	75.82	4.70723	20.5	78.00	1.46	0.912	4.73	5.73	
8H-2, 41	65.61	75.92	4.71209	20.6	76.77	1.46	0.926	4.55	4.13	
8H-2, 51	65.71	76.02	4.71696	20.5	73.48	1.50	0.997	3.14	6.20	
8H-2, 61	65.81	76.12	4.72182	20.6	77.51	1.52	0.955	3.30	6.60	
8H-2, 71	65.91	76.22	4.72669	20.5	77.62	1.50	0.940	3.74	6.37	
8H-2, 81	66.01	76.32	4.73156	20.5	73.45	1.44	0.955	4.19	7.60	
8H-2, 91	66.11	76.42	4.73642	20.6	71.50	1.43	0.969	3.98	11.53	
8H-2, 101	66.21	76.52	4.74129	20.5	71.13	1.46	0.997	2.99	19.50	
8H-2, 111	66.31	76.62	4.74616	20.5	60.85	1.18	0.947	1.63	40.10	
8H-2, 121	66.41	76.72	4.75102	20.6	66.56	1.33	0.969	2.43	20.40	Ash L, and below
8H-2, 131	66.51	76.82	4.75589	20.5	73.28	1.45	0.962	4.75	10.53	
8H-2, 141	66.61	76.92	4.76075	20.6	63.57	1.19	0.912	3.44	18.80	
8H-3, 1	66.71	77.02	4.76562	20.5	65.87	1.29	0.955	2.61	6.90	
8H-3, 11	66.81	77.12	4.77059	20.1	72.74	1.33	0.912	2.81	10.77	
8H-3, 21	66.91	77.22	4.77646	17.0	74.10	1.13	0.898	4.31	8.10	
8H-3, 31	67.01	77.32	4.78234	17.0	74.48	1.24	0.976	3.30	6.83	
8H-3, 41	67.11	77.42	4.78822	17.0	72.02	1.15	0.940	3.19	7.07	
8H-3, 51	67.21	77.52	4.79409	17.0	72.53	1.23	0.997	2.93	7.10	
8H-3, 61	67.31	77.62	4.79997	17.0	74.25	1.19	0.940	4.52	6.70	
8H-3, 71	67.41	77.72	4.80585	17.0	76.66	1.26	0.969	6.55	5.40	
8H-3, 81	67.51	77.82	4.81172	17.0	74.54	1.19	0.940	5.06	6.10	
8H-3, 91	67.61	77.92	4.81760	17.0	75.45	1.15	0.898	4.97	5.90	
8H-3, 101	67.71	78.02	4.82347	17.0	75.27	1.21	0.940	4.29	5.87	
8H-3, 111	67.81	78.12	4.82935	17.0	77.21	1.16	0.883	5.92	5.50	
8H-3, 121	67.91	78.22	4.83523	17.0	79.40	1.27	0.940	7.66	4.43	

Appendix F (continued).

Core, section, interval (cm)	ODP depth (mbsf)	Composite depth (m)	Magnetic age (m.y.)	Magnetic sedimentation rate (m/m.y.)	$\delta^{18}O$ age (m.y.)	$\delta^{18}O$ sedimentation rate (m/m.y.)	Mean (wt% $CaCO_3$)	Magnetic $CaCO_3$ MAR ($g/cm^2/k.y.$)	$\delta^{13}C$ ‰ to (PDB)	$\delta^{18}O$ ‰ to (PDB)	Dry-bulk density (g/cm^3)	Coarse fraction (wt% >150 μm)	Interpolated MS K (10-6) (cgs)	Comment
121-758A-(Cont.)														
8H-3, 131	68.01	78.32	4.84110	17.0			74.59	1.15			0.905	6.84	5.53	
8H-3, 141	68.11	78.42	4.84698	17.0			69.72	1.00			0.841	3.73	8.70	
8H-4, 1	68.21	78.52	4.85286	17.0			68.17	1.05			0.905	2.64	9.97	
8H-4, 11	68.31	78.62	4.85873	17.0			69.03	1.09			0.926	3.48	10.43	
8H-4, 21	68.41	78.72	4.86461	17.0			67.83	1.08			0.940	3.21	12.10	
8H-4, 31	68.51	78.82	4.87049	17.0			71.19	1.13			0.933	3.81	9.20	
8H-4, 41	68.61	78.92	4.87636	17.0			67.41	1.06			0.926	3.36	8.63	
8H-4, 51	68.71	79.02	4.88224	17.0			72.49	1.23			0.997	3.74	8.20	
8H-4, 61	68.81	79.12	4.88811	17.0			73.99	1.20			0.955	5.24	6.43	
8H-4, 71	68.91	79.22	4.89399	17.0			75.15	1.24			0.969	4.46	6.73	
8H-4, 81	69.01	79.32	4.89987	17.0			75.51	1.24			0.962	3.18	7.60	
8H-4, 91	69.11	79.42	4.90574	17.0			71.07	1.23			1.012	1.96	9.23	
8H-4, 101	69.21	79.52	4.91162	17.0			63.77	1.00			0.926	4.40	11.20	
8H-4, 111	69.31	79.62	4.91750	17.0			72.55	1.13			0.912	4.19	7.10	
8H-4, 121	69.41	79.72	4.92337	17.0			74.53	1.25			0.983	3.00	6.87	
8H-4, 131	69.51	79.82	4.92925	17.0			72.34	1.11			0.905	2.80	6.43	
8H-4, 141	69.61	79.92	4.93513	17.0			72.14	1.15			0.940	3.35	6.30	
8H-5, 1	69.71	80.02	4.94100	17.0			73.30	1.17			0.940	2.96	6.33	
8H-5, 11	69.81	80.12	4.94688	17.0			73.87	1.23			0.983	2.54	8.20	
8H-5, 21	69.91	80.22	4.95276	17.0			72.12	1.17			0.955	3.02	8.10	
8H-5, 31	70.01	80.32	4.95863	17.0			76.98	1.32			1.004	3.37	8.00	
8H-5, 41	70.11	80.42	4.96451	17.0			77.08	1.23			0.940	4.01	6.50	
8H-5, 51	70.21	80.52	4.97038	17.0			75.89	1.29			0.997	3.10	7.00	
8H-5, 61	70.31	80.62	4.97626	17.0			75.89	1.32			1.026	2.83	6.97	
8H-5, 71	70.41	80.72	4.98214	17.0			75.40	1.21			0.940	2.11	6.83	
8H-5, 81	70.51	80.82	4.98801	17.0			77.10	1.19			0.905	3.48	5.90	
8H-5, 91	70.61	80.92	4.99389	17.0			78.84	1.41			1.054	3.13	4.67	
8H-5, 101	70.71	81.02	4.99977	17.0			76.22	1.27			0.983	2.46	5.37	
8H-5, 111	70.81	81.12	5.00564	17.0			76.01	1.24			0.955	2.45	5.90	
8H-5, 121	70.91	81.22	5.01152	17.0			71.69	1.16			0.955	1.06	6.83	
8H-5, 131	71.01	81.32	5.01740	17.0			77.14	1.27			0.969	1.26	5.20	
8H-6, 1	71.21	81.52	5.02915	17.0			81.12	1.27			0.919	2.13	4.54	
8H-6, 11	71.31	81.62	5.03503	17.0			79.23	1.26			0.933	1.58	5.67	
8H-6, 21	71.41	81.72	5.04090	17.0			77.67	1.30			0.983	0.97	6.40	
8H-6, 31	71.51	81.82	5.04678	17.0			80.77	1.28			0.933	1.82	5.10	
8H-6, 41	71.61	81.92	5.05265	17.0			77.64	1.22			0.926	1.84	4.70	
8H-6, 51	71.71	82.02	5.05853	17.0			77.15	1.27			0.969	2.08	5.20	
8H-6, 61	71.81	82.12	5.06441	17.0			79.25	1.34			0.997	1.71	5.33	
8H-6, 71	71.91	82.22	5.07028	17.0			79.24	1.33			0.983	1.03	5.90	
8H-6, 81	72.01	82.32	5.07616	17.0			79.19	1.33			0.990	1.00	5.70	
8H-6, 91	72.11	82.42	5.08204	17.0			77.79	1.21			0.912	1.09	5.67	
8H-6, 101	72.21	82.52	5.08791	17.0			73.92	1.20			0.955	0.93	6.53	
8H-6, 111	72.31	82.62	5.09379	17.0			73.58	1.12			0.898	1.11	6.50	
8H-6, 121	72.41	82.72	5.09967	17.0			69.21	1.14			0.969	1.21	7.83	
8H-6, 131	72.51	82.82	5.10554	17.0			64.42	1.07			0.976	1.02	10.30	
8H-6, 141	72.61	82.92	5.11142	17.0			37.42	0.64			1.012	0.79	10.20	Ash
8H-7, 1	72.71	83.02	5.11729	17.0			71.23	1.13			0.933	1.98	6.77	
8H-7, 11	72.81	83.12	5.12317	17.0			75.18	1.15			0.898	2.36	6.93	
8H-7, 21	72.91	83.22	5.12905	17.0			72.41	1.13			0.919	2.31	6.60	
8H-7, 31	73.01	83.32	5.13492	17.0			65.99	1.11			0.983	1.16	7.10	
8H-7, 41	73.11	83.42	5.14080	17.0			64.57	1.01			0.919	1.63	8.00	

121-758B-

8H-5, 11	73.11	83.43	5.14139	16.9	70.06	1.13	0.947	2.18	7.80
8H-5, 21	73.21	83.53	5.14726	17.0	72.97	1.20	0.969	2.49	7.40
8H-5, 31	73.31	83.63	5.15314	17.0	72.85	1.17	0.947	3.47	7.43
8H-5, 41	73.41	83.73	5.15902	17.0	71.61	1.09	0.898	3.66	8.87
8H-5, 51	73.51	83.83	5.16489	17.0	62.22	1.04	0.983	1.62	12.10
8H-5, 61	73.61	83.93	5.17077	17.0	74.82	1.20	0.940	1.35	6.07
8H-5, 71	73.71	84.03	5.17665	17.0	79.03	1.34	0.997	2.84	5.53
8H-5, 81	73.81	84.13	5.18252	17.0	78.64	1.30	0.969	3.02	4.70

Note: Magnetic ages have been estimated to 5 decimal places to differentiate between closely spaced samples, not to reflect the accuracy of the age estimates.